NOVA SCHOOL OF SCIENCE & TECHNOLOGY

DEPARTAMENT OF CHEMISTRY

César Daniel Marques Duarte

BSc in Biochemistry

Topical eye drug delivery: hybrid nanoparticles with improved bioactivity and mucoadhesive properties

MASTER IN BIOCHEMISTRY

NOVA University of Lisbon

October 2022

NOVA SCHOOL OF SCIENCE & TECHNOLOGY

DEPARTAMENT OF CHEMISTRY

Topical eye drug delivery: hybrid nanoparticles with improved bioactivity and mucoadhesive properties

César Daniel Marques Duarte

BSc in Biochemistry

Adviser: Lídia M. D. Gonçalves
Principal Investigator, University of Lisbon

Examination Committee:

Chair: Mário Emanuel Campos de Sousa Diniz,
Assistant Professor, FCT-NOVA

Adviser: Lídia M. D. Gonçalves
Principal Investigator, University of Lisbon

Members: Liliana Aranha Caetano,
Researcher, Lisbon School of Health Technology (EsTESL)

MASTER IN BIOCHEMISTRY

NOVA University of Lisbon
October 2022

Topical eye drug delivery: hybrid nanoparticles with improved bioactivity and mucoadhesive properties

Copyright © César Daniel Marques Duarte, NOVA School of Science and Technology, NOVA University Lisbon. The NOVA School of Science and Technology and the NOVA University Lisbon have the right, perpetual and without geographical boundaries, to file and publish this dissertation through printed copies reproduced on paper or on digital form, or by any other means known or that may be invented, and to disseminate through scientific repositories and admit its copying and distribution for non-commercial, educational or research purposes, as long as credit is given

ACKNOWLEDGMENTS

Firstly, I would like to thank my advisor professor Lídia Gonçalves for accepting me and for giving me the opportunity to work with this investigation group and on this project and for all the advice and clarifications.

To the team of the advanced technologies for drug delivery laboratory from the research institute for medicines for the good spirits and help provided in the course of the experimental assays.

I would also like to thank my family for all the support during these years, especially my mother, father and stepfather who always pushed me to give my best. To Ana, my master's colleague with whom I shared good times and coffee, thank you and a thank you for all my friends for all the support they gave me throughout the years.

A special thanks to my girlfriend who was there for me in all the steps of my thesis, who supported me and endured all the difficult times with me.

In memory of my grandmother.

This work was supported by FCT (Fundação para a Ciência e Tecnologia) through iMed.ULisboa (UIDB/04138/2020, UIDP/04138/2020) and Principal Researcher grant CEECIND/03143/2017 (L.Gonçalves).

ABSTRACT

The eye topical drug delivery continues to be challenging due to the eye's biological mechanisms preventing the achievement of optimal drug concentration with therapeutic effect. Various strategies can be made to enhance the bioavailability, retention time, and penetration of the drug into the eye. In this work, it was developed the use of naturally available polymers like chitosan and hyaluronic acid (HA) with mucoadhesive and targeting properties in a hybrid nanoparticulated system with lipids (hyLNPs), taking advantage to deliver both lipophilic and hydrophilic drugs.

The hyLNPs were optimized by surface modulation properties and lipophilic drug (Curcumin-Curc) incorporation using the high shear homogenization technique. The HA and ceftazidime (CZ) were adsorbed to the LNPs' surface. The characterization was done in terms of size, polydispersity index (PDI) and ζ-potential, mucoadhesion and permeation properties, *in vitro* cell uptake, cell viability, the efficiency of drug encapsulation and loading (%EE, %DL), and drugs' bio-efficacy.

The optimized formulations comprising solid and liquid lipids, chitosan, and HA presents an average particle size of 256.2 ± 6.0 nm, PDI of 0.386 ± 0.013, and ζ-potential -33.3 ± 0.5 mV and mucoadhesive properties. The %EE was 86.5 ± 0.9 % and 48.4 ± 7.9 %, with a %DL of 0.135 ± 0.009 % and 2.0 ± 0.3 % for Curc and CZ, respectively. Both drugs were released from the nanoparticles and successfully permeated through membranes within 2 h after instillation. The empty and drug-loaded hyLNPs didn't present cytotoxicity in human retinal pigment epithelia cell line (ARPE-19). The drug-loaded hyLNPs reduced oxidative stress and were effective in inhibiting *P. aeruginosa* growth. CZ-Curc-hyLNPs are cell internalized being biocompatible which potentiates its application for the treatment of ocular pathologies.

Keywords: Eye, Mucoadhesive, Nanoparticles, Curcumin, Ceftazidime, ARPE-19

RESUMO

A administração tópica ocular de fármacos continua a ser um desafio devido aos mecanismos biológicos do olho, impedindo que se atinja uma concentração de fármacos com um efeito terapêutico eficaz. Várias estratégias podem ser usadas para aumentar a biodisponibilidade, tempo de retenção e permeação do fármaco no olho. Neste trabalho, desenvolveu-se o uso de polímeros naturalmente disponíveis como o quitosano e o ácido hialurónico (HA) com propriedades mucoadesivas e seletivas, num sistema híbrido de nanopartículas com lípidos (hyLNPs), com capacidade para a formulação de fármacos lipofílicos e hidrofílicos.

As hyLNPs foram otimizadas por modulação das propriedades da superfície e incorporação de fármacos lipofílicos (Curcumina-Curc) utilizando a técnica de homogeneização de alta velocidade. O HA e ceftazidima (CZ) foram adsorvidos á superfície das LNPs. A caracterização foi feita em termos do tamanho, índice de polidispersão (PDI), potenciais-ζ, propriedades de mucoadesão e permeação, internalização em células *in vitro*, viabilidade celular, eficiência de encapsulação e de carga (%EE, %DL) e bio-eficácia dos fármacos.

As formulações otimizadas compostas por lípidos sólidos e líquidos, quitosano e HA apresentaram um tamanho médio de 256,2 ± 6,0 nm, PDI 0,386 ± 0,013, potencial-ζ -33,3 ± 0,5 mV e propriedades mucoadesivas. A %EE foi de 86,5± 0,9 % e de 48,4 ± 7,9 %, com um %DL de 0,135 ± 0,009 % e 2,0 ± 0,3 % para a Curc e a CZ, respectivamente. Ambos fármacos libertaram-se das nanopartículas e permearam por membranas 2 h após instilação. HyLNPs vazios e CZ-Curc-hyLNPs não apresentaram citotoxicidade na linha celular do epitélio pigmentar da retina humana (ARPE-19). CZ-Curc-HyLNPs reduziram o stress oxidativo e foram efetivos na inibição do crescimento de *P. aeruginosa*. CZ-Curc-hyLNPs foram internalizadas e sendo biocompatíveis isto potencia a sua aplicação no tratamento de patologias oculares.

Palavras chave: Olho, Mucoadesivas, Nanopartículas, Curcumina, Ceftazidima, ARPE-19

INDEX

Figure index

Table index

Abreviations

%AE	Adsorption Efficiency
%DL	Drug Loading
%EE	Encapsulation Efficiency
ACN	Acetonitrile
ALG	Alginic Acid
ARPE-19	Human Retinal Pigment Epithelia Cell Line
CD44	Cluster-Determined 44 (Receptors)
CMC	Critical micelle concentration
CS	Chitosan
CS-HA-NP	Hyaluronic Acid modified Chitosan Nanoparticle
CTAB	Cetrimonium Bromide
CZ	Ceftazidime
Curc	Curcumin
DAPI	4'-6-diamidine-2'-phenylindole dihydrochloride
DLS	Dynamic Light Scattering
G	α-1,4-L-guluronic acid
HA/ HAEye	Hyaluronic Acid/ Eye Drop grade Hyaluronic Acid
HHSH	Hot High Shear Homogenization
ISO	International Organization for Standardization
LMW CS	Low Molecular weight Chitosan
M	β-1,4-D-mannuronic acid
MIC	Minimum Inhibitory Concentration
MTT	3-(4,5-dimethylthiazol-2-yl)-2,5-diphenyltetrazolium bromide
NLC	Nanostructured Lipid Carrier
NP	Nanoparticle
OD	Optical Density
PDI	Polydispersity Index
PE	Permeation Enhancer
PEG	Polyethylene Glycol
PF68	Pluronic™ F-68
PVDF	Polyvinylidene Difluoride
ROS	Reactive Oxygen Species
SC	Sodium Cholate
SD	Sodium Deoxycholate
SLN	Solid Lipid Nanoparticle
hyLNP	Lipid-polymer hybrid Nanoparticle
ζP	Zeta Potential

1. Introduction

1.1 Current Drug Delivery for Treatment of Ocular Diseases

1.1.1 State of Vision in Portugal

The sense of vision represents one of the fundamental means for communication and interpersonal relationships, as well as for professional activity. In Portugal, according to the Programa Nacional para a Saúde da Visão [1-2], it is estimated that about half of the population suffers from impaired vision, from decreased visual acuity to blindness, which about 20 % of children and half of the adult population suffers from refractive errors and that about half of the people with blindness are of working age, however, 75 % of severe disorders including blindness can be treated and prevented [3]. Therefore, the visual function must be preserved, and congenital or age-related pathologies must be diagnosed and treated in advance.

1.1.2 Anatomy of the Eye

The eye is a complex organ in both its anatomy and its physiology and as such the development and delivery of drug molecules to this organ is a challenging field of study. The eye is a specialized organ that focuses light and enables it to be processed and interpreted by the brain, it can be structured in two main segments, anterior (front of the eye) and posterior (back of the eye) [4,5] as illustrated in Figure 1.1. The anterior segment is a part of the eye that is anterior to the lens and includes tissues such as the cornea, pupil, conjunctiva, aqueous humour, lens, iris, and ciliary body [6, 7]. This segment is further divided into two chambers connected by the opening of the pupil, the anterior chamber which is composed of everything between the cornea and the iris, and the posterior chamber which contains the space immediately posterior to the iris composed of the lens, it's suspensory ligaments and the ciliary processes [7]. The posterior segment is composed of the optic nerve, neural retina, retinal pigment epithelium, vitreous humour, choroid, and sclera [6].

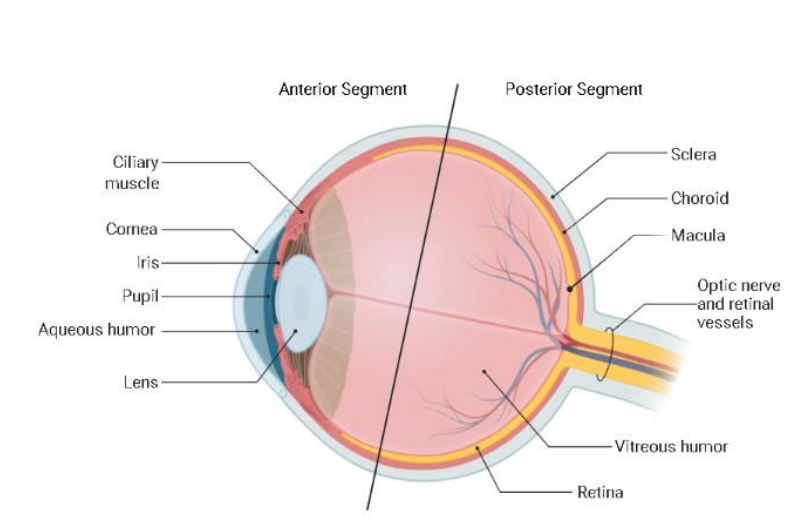

Figure 1.1: The anatomy of the eye. [8] (Created using BioRender).

1.1.3 Barriers and Protective Mechanisms of the Eye

Drug delivery to the eye is challenging due to the eye's multiple biological mechanisms that prevent therapeutic systems to achieve an optimal concentration of the drug during the appropriate amount of time to provide a therapeutic effect at the target site [4,6,9].

These mechanisms include lacrimation, tear dilution, tear turnover, nasolacrimal drainage, and the corneal epithelium, endothelium, and inner stroma [4,6,9] with the last trio being the main barriers that lower drug bioavailability. Such mechanisms help the organism to expel xenobiotics, however, those also include drugs and, as such, only 5 % of the drug applied in a topical therapy penetrates the corneal barrier due to it being relatively impermeable [7, 10-12]. Furthermore, after it reaches the ocular tissue, the drug molecule, can still spill onto the lacrimal sac and into the nasolacrimal drainage in which it is absorbed into the bloodstream [10] leading to the systemic circulation of the drug and the potential for systemic side effects, for example, timolol is a therapeutic molecule used in the treatment of ocular hypertension and glaucoma as an eye drop, however, being a β-blocker and due to its absorption by the conjunctiva, it can have a deleterious effect on the heart [10, 13].

There are two possible pathways that can be taken by drugs can still spill onto, either the corneal or the conjunctival routes, being the corneal route the dominant in the delivery of the majority of drugs [14,15]. The cornea is a transparent tissue of 0.5 – 0.7 mm of thickness that protects the inner tissues of the eye, it is made of 5 main different layers as illustrated in figure 1.2. Of its five layers, the corneal epithelium is the main barrier that restricts the absorption of small and lipophilic drugs into the eye [14,15].

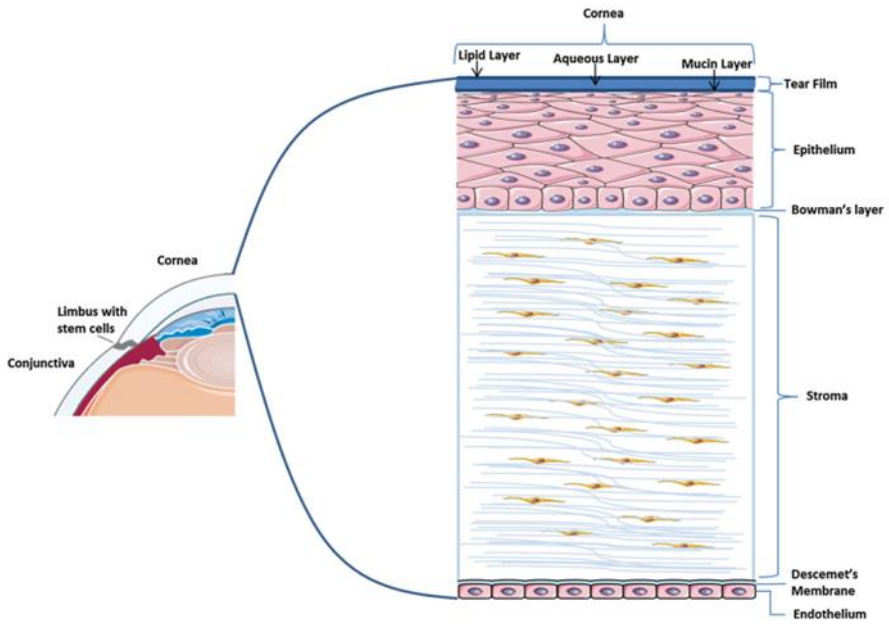

Figure 1.2: Illustration of the anatomy of the cornea. It is made of 5 main layers with each different characteristics: 1) Epithelium; 2) Bowman's membrane; 3) Stroma; 4) Descemet's membrane and 5) Endothelium. (Adapted from Rowsey and Karamichos 2017 [16]).

Thus, there is a need for novel drug delivery systems that can increase the residence time and bioavailability of drug molecules in the eye, eliminating the need for formulations with a high drug concentration and thereby reducing systemic and local side effects [10, 17].

1.1.4 Ocular Drug Delivery Methods

Drug bioavailability depends, among other factors, on the route of administration into the eye, as such, the anatomy and physiology of the eye must be considered when designing drug delivery systems. Among the many possible routes for ocular drug delivery, the three main administration routes are intravitreal, periocular, and topical administration [18].

Systemic administration, such as that of the ingestion of an oral formulation or intravenous injection, is also used due to its ease of compliance by the patients. However, the wide-body distribution of the drug, the gastrointestinal and the blood-retinal barriers, this last one selectively permeable to lipophilic molecules, often result in the need to administer large doses, a requirement to achieve a therapeutic effect which in turn leads to significant side effects [18,19]. As such a localized administration in the eye, such as that found in the three main routes, is preferred.

1.1.4.1 Intravitreal

The current treatment of pathologies in the posterior segment of the eye requires surgical procedures by intravitreal injection under topical anaesthesia. Therefore the presence of an ophthalmologist is needed to inject the drug formulation into the vitreous chamber, there is also the need to maintain sterility and proper storage conditions [20,21]. It is a route that allows for higher concentrations of drugs in the eye, diminishing side effects by systemic route, but it is not without barriers, with the inner limiting barrier, which separates the retina and the vitreous humour, being the primary limiting barrier to the diffusion of therapeutic drugs [19].

Patients suffering from chronic pathologies in the posterior segment require, therefore, frequent invasive dosing which can lead to several side effects, including, ocular infection and/or inflammation of the vitreous humour, retinal detachment and damage, cataracts, among others [9, 20,21].

Even with these side effects, being a direct administration route into the posterior segment of the eye and allowing higher bioavailability, the intravitreal route is a preferred delivery method into this segment [21].

1.1.4.2 Periocular

The periocular route involves the injection to the area immediately surrounding the eye to effectively bypass the barriers created by the tear film and conjunctiva for the delivery to the posterior segment, this allows to diminish the chances of the more severe side effects found in intravitreal injections [5,19]. This type of route consists of five subdivisions: subconjunctival, retrobulbar, peribulbar, sub-Tenon, and posterior juxtascleral routes, each with their advantages and disadvantages [5,19,21].

For example, in the subconjunctival injection, the formation of a small blister that slowly diffuses the drug directly to the sclera eliminates the need to transverse the conjunctival surface that limits the permeation of hydrophilic drugs and minimizes systemic side effects [5,22].

One of the many issues of the periocular route is the remaining physiological barriers needed to get an effective therapeutical concentration at the target site such as the sclera, choroid, retina, etc.. Moreover, injected therapeutical agents can still move via the anterior eye chamber to the vitreous humour, and from there, into systemic circulation albeit less so than the intravitreal injection [5,21].

1.1.4.3 Topical

Current conventional topical administration is done using eye drops, eye ointments, contact lenses, etc., which accounts for 90 % of the ophthalmic formulations in the market [11]. Pharmaceutical formulations in the form of eye drops mainly target pathologies in the anterior segment of the eye, has the precorneal barriers (lacrimation, tear dilution, tear turnover, nasolacrimal drainage, etc.) hinder the topical formulations' path through the cornea to the anterior chamber making so that only 5 % of the instilled dose reaches the target site and even less permeate to the posterior segment of the eye [11,22,23].

However, although their efficacy is low, due to the several barriers present in the eye, topical administration avoids several adverse ocular and systemic side effects that are present in most of the invasive techniques like intravitreal or intravenous injections used in the treatment of posterior segment disorders [7]. Furthermore, being applied on the surface of the cornea, topical administration bypasses the first passage metabolism of the drugs in the liver, and therefore, requiring less dosage than those applied in the systemic route [5]. Furthermore, these formulations have also the advantage of the ease of administration and compliance of the patient [21].

The lower permeation to the posterior segment has been addressed and novel drug delivery systems are in development, such as the use of polymers as permeation enhancers as a way to enhance the permeation of the drug into the posterior segment of the eye [21]. Such an example was demonstrated by Popov et al. 2016 [24] that made use of mucus-penetrating particles, coated with Pluronic™ F127 and Poly-(vinyl alcohol) partially hydrolysed to enhance these nanoparticle's mucus permeation ability showing that with certain grades of partially hydrolysed Poly-(vinyl alcohol) it can aid the particle's mobility in mucus and thus allowing access to the posterior segment to a drug molecule.

However, the fast clearance from the surface of the cornea still stands as a problem in topical administration even with the use of permeation enhancers. Thus, there is a need for novel drug delivery systems that can increase both the residence time and bioavailability of drug molecules in the eye, eliminating the need for formulations with a high concentration of active ingredients and thereby reducing side effects [10, 17].

1.2 Nanotechnology for the Delivery of Pharmaceutical Molecules

Nanoparticles (NPs) have shown potential to become these new delivery systems, being able to deliver a plethora of therapeutics, from small molecules to polypeptides and genes, as well as, improving both pharmacokinetics and the therapeutic index of drugs in a systemic context [17,25]. This is mainly due to their small size ranging from 10 to 1000 nm, high surface area to volume ratio and their capacity to conjugate with several molecules giving NPs functionality such as specific targeting or to deliver them as payloads which in turn makes these nanoscale structures a powerful tool in the field of medicine [12].

As a topical ophthalmic delivery system, nanoparticles, ranging in size from 50 to 400 nm, provide several advantages when compared with current topical administration technology, some of them include: 1) improvement of the overall pharmacokinetics and pharmacodynamic properties of the drug molecules; 2) mucoadhesive properties for sustained and prolonged drug residence in the eye; 3) ability to avoid several physical and chemical barriers due to their characteristics; 4) Passive or ligand-mediated targeted drug delivery by conjugating several molecules with the nanoparticles; 5) Minimal toxic damage to cell membranes and cellular environment [12,25-29]. A dispersion of drug-loaded nanoparticles also has the advantage of application in a liquid formulation, much like conventional eye drops which provides ease of application in the context of a topical administration as well as being patient-friendly [27]. They also avoid the discomfort associated with some preparations that lead to blurry vision when properly administered [27] further aiding in patient compliance.

In the last few decades, several colloidal carrier systems have been developed for ocular drug delivery such as liposomes [6,30-32], Solid lipid nanoparticles (SLNs) and nanostructured lipid carriers (NLCs) [33-35], polymeric nanoparticles [36-41] and lipid-polymer hybrid nanoparticles (hyLNPs) [42,43]. These carriers are oriented toward achieving an improved or enhanced absorption, retention time and stability of the drug molecules applied to the eye.

1.2.1 Liposomes

Liposomes are vesicles with sizes ranging between 10 - 100 nm, that are composed of one or more phospholipid molecules which can rearrange themselves in concentric bilayers when in an aqueous solution [11, 44]. This unique structure enables the liposome to be a carrier of both hydrophilic and hydrophobic drugs at the site of action and the presence of their surface charge gives the liposome the ability to adsorb to the corneal and conjunctival surfaces by weak electrostatic interactions making them a suitable drug delivery system with positively charged liposomes preferably captured at the negatively charged corneal surface [7,11,44,45]. Furthermore, being able to be prepared from natural and synthetic phospholipids, liposomes reveal to have biocompatibility and low cytotoxicity as they mimic biological membranes [36]. These characteristics attributed to the liposomes lead to an increase of the absorption and a possible controlled release of pharmaceutical formulations to the ocular surface [12].

Cationic liposomes in specific have shown improved efficiency in ophthalmic topical delivery when compared with anionic liposomes due to their electrostatic interactions with the negative charges on the corneal surface. Law, Huang, and Chiang 2000 [47] investigated the *in vivo* absorption of acyclovir-loaded cationic and anionic liposomes, incorporated with stearylamine and dicetylphosphate as the positive and negative charged lipids respectively. In rabbit eyes, and 2.5 h after the topical administration, the antiviral drug showed both greater absorption and greater concentration in the cornea when loaded into the cationic liposomes when compared with anionic liposomes and acyclovir in solution (1093.3 ± 279.7; 571.7 ± 105.3 and 253 ± 279.7 ng/g respectively). The proposed reason was the higher binding strength, by electrostatic interaction, of the positively charged liposomes to the negatively charged corneal surface which led to the increased in-residence time and acyclovir absorption [47].

However, these drug delivery systems have several drawbacks such as the tendency to form aggregates and for positively liposomal aggregates to completely disintegrate on the negatively charged mucin membrane which gives rise to a burst release of the drug molecules in the eye, and the difficult manufacturing processes, low loading efficiency for hydrophobic drugs and leakage of the entrapped drug during storage observed in the liposomes [11,46,48].

1.2.2 Solid Lipid Nanoparticles (SLNs) & Nanostructured Lipid Carriers (NLCs)

SLNs and NLCs are nanoparticles prepared using various lipids such as mono-, di-, and triglycerides, fatty acids, and steroids from both natural and synthetic origins, and usually have a size of 50 – 1000 nm remaining in a solid state at body temperature and are stabilized by emulsifiers [7]. These nanoparticles have the advantage of being able to incorporate both hydrophilic and lipophilic drugs, having a low cost for large-scale production and being bio-compatible, decreases the danger of acute and chronic toxicity.

SLNs allow for the controlled release of the pharmaceutical molecule by hindering its mobility due to the solid-state matrixes of the nanoparticles, thus elevating bioavailability, and retention time at the ocular site [44,49,50]. However, due to the same solid-state matrix, SLNs show some disadvantages such as a limited drug loading efficiency inherent in the crystalline structure and an initial burst release of the drug, which hinders a sustained release on the ocular surface [33,51,52].

NLCs, a second-generation SLNs, were introduced early this century to overcome these limitations. They are produced by the controlled addition of a liquid lipid, such as Labrasol®, Transcutol® P and Miglyol 812®, to the solid lipid component, to accommodate a larger quantity of the drug by forming imperfections on the solid lipid matrix but still produce a final product with a solid structure which in turn prevents the expulsion of the drug molecule during storage [53,54].

The use of NLCs for ocular drug delivery was first reported by J. Li et al. 2010 [55]. Fabricating NLCs from a combination of the solid lipids Compritol ATO®, Gelucire 44/14, and stearylamine and with the liquid lipids Miglyol 812®, Cremphor EL and Transcutol® P, they investigated the possible controlled release of ibuprofen loaded into these nanoparticles. The obtained NLCs proved to be well tolerated in rabbit eyes and it was observed an enhanced bioavailability of ibuprofen in the rabbit aqueous humour when compared with the drug in eye drops. This increase in bioavailability was concluded to the enhanced permeability provided by Gelucire 44/14 and Transcutol® P while stearylamine prolonged the pre-corneal retention of the drug [55]. Therefore, all these three components contributed to an optimized formulation of an NLC for ocular drug delivery.

1.2.3 Polymeric Nanoparticles

The formulation of biodegradable and mucoadhesive polymeric nanoparticles holds significant interest for ophthalmic drug delivery as the core-shell structure of these nanoparticles promotes the easy encapsulation and higher loading of lipophilic drugs than the liposomal systems and minimizes the drainage from the ocular surface by interacting with the mucin present in the ocular surface enhancing contact time and increasing the bioavailability of the drug [17,27,56]. This enhanced contact time is provided by the functional groups found in polysaccharides such as amino, carboxyl and hydroxyl groups that can form hydrogen bonds with the mucosa

in the eye as well as the combination of other weak bond interactions [17,27,56,57]. Without this mucoadhesive characteristic, nanoparticles are eliminated from the eye almost as quickly as an aqueous solution due to the tear turnover but by interacting with the mucosa the retention time of the nanoparticle is prolonged due to the slower mucus turnover [7,17,27,56,58]. Several polymers and biomaterials which are biodegradable and biocompatible such as poly-(lactide-co-glycolic acid), polysaccharides such as cellulose derivatives, chitosan (CS), and hyaluronic acid (HA), among others [7,27,58-63] are used to achieve a prolonged residence time of the drugs in the cornea's surface as well as provide active targeting by using polymer moieties to allow the NPs to bind to specific receptors found the cells of the ocular tissue [57,64].

1.2.3.1 Chitosan

Chitosan (CS), a derivative of the naturally occurring polysaccharide chitin composed of randomly distributed monomers of D-glucosamine and N-acetyl-D-glucosamine linked by a β-(1→4) glycosidic bond, is an emerging biodegradable polymer for ocular drug delivery due to it being hydrolysed by lysozyme found in the eye [65] with several chitosan formulations being investigated [37,39,66] to overcome the rapid elimination of the instilled solutions and to enhance the permeation through the corneal epithelium.

The mucoadhesive property of the CS is made possible through the presence of positive charges at physiological pH due to the amine groups present in its structure, this cationic nature, helps the CS to enhance the precorneal contact time of the drug through interaction with negatively charged molecules found in the mucosal surface thereby prolonging residence time of the applied nanoparticles [18,66,67].

Chitosan is also known to, transiently, open the thigh junctions between epithelial cells found in the cornea, providing an enhanced permeation of hydrophilic molecules through the paracellular pathway, this opening is reversible with a complete recovery of the barrier function of the tight junctions without any detectable change in morphology of the epithelium [68-71].

1.2.3.2 Hyaluronic Acid

Hyaluronic Acid (HA) is a long, linear polysaccharide composed of alternating D-glucuronic acid and N-Acetyl-glucosamine units linked by β-(1→4) and β-(1→3) glycosidic bonds [72]. Being endogenously synthesised in the eye, HA is widely distributed in several ophthalmic tissues including the cornea, aqueous humour, iris, lens, and retinal pigment epithelial cells participating in the recovery of the cornea and maintenance of intraocular pressure [18,72,64].

The advantageous characteristics of HA are: first a non-covalent binding to the mucin layer of the cornea in which the acid groups of the polymer interact with the sialic acid present in this layer; secondly, HA interacts with cells and tissues through recognition of HA receptors, the most studied being the cluster-determined 44 (CD44) receptors that are found distributed in the corneal epithelium and endothelium, this recognition is followed by receptor-mediated endocytosis of the HA into the cells. This endocytosis can increase the uptake of ophthalmologic nano-formulations using HA as a carrier bulk while increasing the precorneal residence time with its bio-adhesion [43,64,72]. As such, and due to its bioadhesion, biocompatibility and receptor recognition characteristics, HA has been found to be a suitable polymer for ocular drug delivery.

Wadhwa et al. 2009 [37] developed HA modified CS nanoparticles (CS-HA-NPs) loaded with timolol maleate and dorzolamide hydrochloride for the treatment of glaucoma, these nanoparticles showed enhanced mucoadhesive strength when compared with CS nanoparticles due to the interaction of HA with the CD44 receptors present in the mucosal linings [37,73] which favours the retention of CS-HA-NPs in the ocular epithelium. Furthermore, they showed an effective control on the release rate of the drugs and no signs of discomfort after 24 h on *in vivo* ocular irritation assays [37]. Silva et al. 2020 [36] successfully encapsulated the glycoprotein erythropoietin in CS- HA-NPs using a low molecular weight CS and eye drop grade quality HA of 300 kDa which showed favourable physicochemical properties for ocular delivery of the hormone including a strong mucoadhesive strength provided by the HA polymer of 300 kDa.

1.2.3.3 Sodium Alginate

Alginic acid (ALG) is a biocompatible, linear, and anionic polysaccharide and a co-polymer of α-1, 4-L-guluronic acid (G) and β-1, 4- D-mannuronic acid (M), presenting different G/M ratio that determines its structure and degree of polymerization [18,38,39,74] which can affect NPs physicochemical characteristics. For example, it is known that a high percentage of G content results in particles with larger diameters and polydispersity. As such the physical properties of ALG are affected by its composition, percentage of guluronic acid in its polymeric chain and its molecular weight [38,74].

The polymer is chemically versatile, varying its viscosity according to the pH values. The viscosity increases as the pH decreases, i.e., carboxylate groups in the alginate backbone get protonated and form hydrogen bonds, reaching a maximum range of pH 3 – 3.5 [74]. The salt sodium alginate shows bio-adhesive properties that offer a prolonged release of drugs at the target site due to the biding of its G residues to the divalent calcium ions present in the tears forming an *in-situ* gel in the cul-de-sac of the eye [75]. Due to its biocompatibility, recognized lack of toxicity and relatively low cost, it has wide potential both as a traditional excipient and more specifically as a tool in controlled drug delivery applications [38].

Costa et al. 2015 [39] aimed to develop an alternative carrier system of an antibiotic and to enhance its permeation, across ocular epithelia, using the favourable biological properties of alginate and chitosan. They were able to produce CS-ALG nanoparticles by ionotropic gelation [76] with a drug-loaded particle size range of 382.8 ± 7.5 to 421.2 ± 55.1 nm, well within the particle size for ophthalmologic applications, and a negative zeta potential generated by the sodium alginate. Furthermore, with a drug concentration of 10 µg/mL, a high encapsulation was obtained (91.45 ± 0.69 %). The CS-ALG nanoparticles efficiently encapsulated an antibiotic and preserved its antimicrobial activity against several major pathogens.

1.2.4 Lipid-Polymer Hybrid Nanoparticles (hyLNPs)

To explore the increased absorption observed in lipidic nanoparticles and the mucoadhesive characteristics of certain polymers and to overcome the disadvantages already presented, lipid-polymer hybrid nanoparticles (hyLNPs) have been developed.

The LPNs are normally comprised of two to three components illustrated in figure 1.3, which are (i) A lipophilic polymer core with the active agent incorporated in it with high loading yields, and (ii) a lipid layer that envelopes the polymer core which provides biocompatibility to the nanoparticle system and limits the degradation of the polymer core by reducing the diffusion of water to the core, and (iii) a hydrophilic polymer outer shell commonly of polyethylene glycol (PEG) that confers some degree of stealth and prolongs the LPNs lifetime in a systemic environment [46,56,77]. In addition, the lipid layer also acts to minimize leakage of the encapsulated drug and slows down the polymer degradation rate by limiting water diffusion inside the polymer core enabling a sustained release of the content [46].

On the other hand, lipid core/polymer-shell hybrid nanoparticles have not been as extensively investigated [78-80]. These hyLNPs merge the advantages of a lipidic core and polymeric shell, being able to encapsulate hydrophobic drugs with a high encapsulation efficiency and the low biotoxicity provided by the lipids and the bioadhesion properties of polymers such as polymers of chitosan.

Furthermore, these hyLNPs can be prepared by various techniques such as the high shear homogenization method wherein the lipid is first melted above its melting point and combined with an aqueous phase with surfactants pre-heated in the same water bath and at the same temperature as the lipid phase [81]. Afterwards, a high-shear mixer homogenises the dispersion which is subsequently cooled in a cold-water bath [81]. Methods such as this can produce a stable colloidal solution, without using toxic organic solvents and enables large-scale production of hyLNPs [81].

With these favourable characteristics, hyLNPs and have the potential to become a preferable drug delivery system of genetic material [82], tumour growth inhibitors [83], and diagnostic imaging agents [84], for both systemic and topical applications.

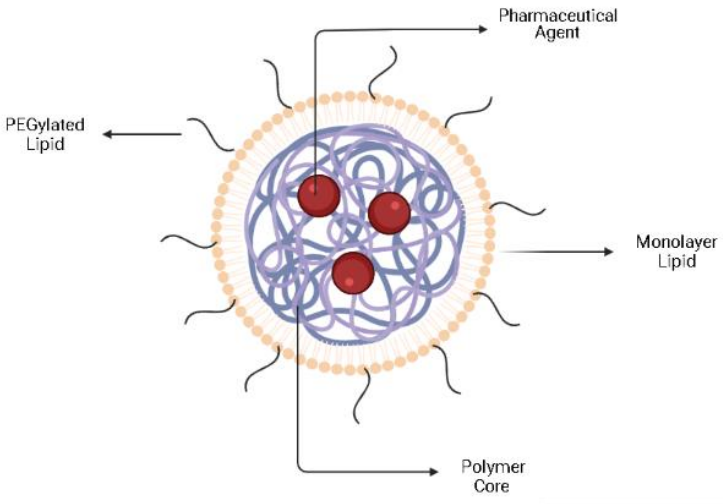

Figure 1.3: Illustration of the structure of a lipid-polymer hybrid nanoparticle with PEGylated lipids (Created using BioRender).

Several types of polymers, methods of preparation and compositions allow hyLNPs to respond to the need for a non-irritating, stable and effective ocular formulation that presents long-lasting action through the mucoadhesion capacity of the polymer which in turn, depends on the shape and size of its chains [85-87].

1.3 Action of Permeation Enhancers

Even though the mucoadhesive characteristics of the hyLNPs increase the bioavailability of drug molecules in the mucin of the eye, when used for topical administration these nanoparticles do not cross the corneal epithelium, the main barrier restricting drug absorption, even with a size as small as 21 nm [14,88].

Therefore, to further improve the therapeutic capabilities of the drug molecules, molecules that enhance drug permeation can be added which increase the transcorneal passage of drugs and as such, increase the amount of drug that reaches its action site, some examples of these molecules are shown in Table 1.1.

Table 1.1: List of several molecules with permeation enhancement properties.

Family of Agents	Name of the agent	Model Drug	Main Results	Reference
Ciclodextrins	Hydroxypropyl β-Cyclodextrin	Pilocarpine nitrate	*In Vitro* permeabilization assays demonstrated four times increase in the permeabilization coefficient when compared with the free-drug solution	89
Chelating Agents	Ethylenediaminetetraacetic acid	Riboflavin / Vitamin B2 & Atenolol; Timolol; Levobunolol and Betaxolol	An increase in the penetration of riboflavin into bovine eye tissues was observed due to the sequestration of Ca^{2+} by all three tested polyamine carboxylic acids, when compared to the free-drug solution. However, Ethylenediaminetetraacetic acid showed to reduce the permeability coefficient on lipophilic drugs such as β-blockers.	90 - 94
	Ethylenediamine-N, N'-disuccinic acid			
	Ethylene glycol-bis (β-aminoethyl ether) -N, N, N′, N′-tetraacetic acid			
Bile Salts	Sodium Glycocholate; Sodium Taurocholate; Sodium Deoxycholate (SD); Sodium Taurodeoxycholate; Sodium Ursodeoxycholate; Sodium Tauroursodeoxycholate	Atenolol; Timolol; Levobunolol and Betaxolol	It was observed that the bioavailability of polycaprolactone-pluronic™ F-68 NPs increased only in the anterior segment tissues of the eye (cornea, conjunctiva, iris, and lenses) with the bile salts sodium glycocholate, and taurocholate associated with NPs increasing the bioavailability in the cornea, iris, and ciliary body. For the permeation of β-blockers, atenolol permeation is enhanced using Taurodeoxycholate (0.05%) by 5.8-fold that of the permeation coefficient of the free drug solution. Deoxycholate (0.05%) and Ursodeoxycholate (0.05%) enhanced timolol permeation by 5.2 and 2.1-fold respectively. For the more lipophilic β-blocker betaxolol it was observed a slight increase in permeation using Deoxycholate (2.3-fold) and Ursodeoxycholate (1.6-fold).	92 - 94
Crown Ethers	12C4	Riboflavin / Vitamin B2	It has been shown, in *in vitro* studies, that crown ethers improve the permeability of riboflavin moderately when combined at a concentration of 1 mg mL^{-1}.	91
	15C5			
	18C6			

Non-ionic Surfactants	DL-9; Brij® 35; Brij® 78; Brij® 98	Atenolol; Levobunolol Betaxolol and Timolol;	For these non-ionic surfactants the permeation of drugs, both hydrophilic and lipophilic, increased even if slightly for the latter. Significantly, the permeabilization of Atenolol increased by 10.5x for Brij® 35, for Timolol its permeabilization increased by 4.2x and 3.9x for BL-9 and Brij® 78. In the case of Betaxolol the permeabilization increased by 2x for Brij ® 98.	93, 94
Surfactants	Benzalkonium chloride	Atenolol; Timolol; Levobunolol and Betaxolol	Benzalkonium chloride at a concentration of 0.02% (w/w) has been shown to significantly increase the permeability of β-blockers, with greater permeability for the more hydrophilic than the lipophilic ones. For the former, the permeability coefficient increased about 5.2x the value obtained in solutions with only buffer. It has also been shown to increase permeability of PCLPF68 nanoparticles in the anterior segment of the eye.	91 - 95
	Cetylpyridinium chloride	Penicillin	Cetylpyridinium chloride, at 0.02%, demonstrated to increase the penicillin flux rate across corneas with an intact epithelial layer in a manner similar to that found for benzalkonium chloride. However, it is known that this reagent is highly cytotoxic causing severe irritancy in a dose-dependent response.	96, 97
	Vitamin E TPGS Riboflavin / Vitamin B2	-	The amount of riboflavin extracted from corneal tissue increased with the concentration of VE-TPGS until reaching the critical micelle concentration (CMC). Accumulation assays in corneas with and without the epithelium demonstrate that the presence of VE-TPGS led to a greater accumulation of riboflavin in the corneal epithelium.	98
	Digitonin; Saponin; Aescin/Escin	Atenolol; Timolol; Levobunolol and Betaxolol	For the more hydrophilic β-blockers such as atenolol and timolol, the most significant increases in permeability were verified with saponin and aescin, with an increase of more than 10x than those observed in the buffer solution. In the case of Betaxolol only aescin produced a slight increase in permeability (1.5x). For Levobunolol both digitonin and saponin produced a permeability increase of 1.3x and 2x.	93, 94

Saturated Fatty acids	Decanoic Acid/ Capric Acid	-	The bioavailability of PCLPF68 nanoparticles increased in the conjunctiva when functionalized with capric acid due to the binding of polar groups to phospholipids found in the plasma membrane, thus increasing the permeability of drug carriers.	92
Polyethylene glycol ethers	Polyethoxylated Castor Oil / Cremophor® EL	Cyclosporin A & Timolol maleate	For the concentrations of 10% and 20% of Cremophor® EL that were studied, flux values of cyclosporin A across the cornea were significantly higher for the first 16 hours of the permeability experience. At a higher concentration of 0.023% (w/v) it showed high toxicity with cell-viability of the controls lower than 50% and causing the detachment of the membrane of the artificial rabbit corneal epithelium and in a lower concentration, 0.01% (w/v), no permeation enhancement was observed.	94, 95, 99
Cell-Penetrating Peptides	Penetratin; Transactivating transcriptional activator; Low molecular weight protamine; Poly(arginine)8	-	The apparent permeation coefficients of penetratin, Transactivating transcriptional activator, protamine, and Poly(arginine)8 were of 87.5x,31.8x,17.6x,16.3x respectively comparing to the negative control of poly(serine)8-Lys-FAM. The fluorophore labelled cell-penetrating peptides permitted to follow their distribution in frozen sections of rabbit cornea. Intense and non-specifically distributed green fluorescence was densely localized in the cornea's epithelium and sparsely so in the corneal stroma. The penetratin group showed a stronger fluorescence signal followed by Transactivating transcriptional activator, protamine, and Poly(arginine)8. Hydration values obtained from ex vivo rabbit cornea of all of the cell-penetrating peptides tested, showed that there is almost no cytotoxicity in ex vivo rabbit's corneal tissue.	100

This enhanced permeation is obtained through the modification of the corneal epithelium integrity, such as the sequestering of Ca^{2+} caused by chelating agents like EDTA [90-94] and cyclodextrins [89], that lead to the loosening of the thigh junctions between the cells that keep corneal epithelium integrity and promotes the paracellular transport of drugs through the cornea. As such, the presence of the polymer in hyLNPs in conjunction with the permeation enhancing molecules, such as, the ones presented in table 1.1 can overcome the ocular barriers and improve bioavailability in the several segments of the eye.

1.4 Objectives

The present work aimed at the development of an innovative hybrid nanoparticulate system composed of a lipid core/polymer shell that could take advantage of the high encapsulation efficiency and stability presented by NLCs and the enhanced permeation and residence time in the cornea and active targeting provided by polymers such as CS and HA respectively, to encapsulate and adsorb two drug molecules, curcumin, and ceftazidime respectively.

Curcumin (Curc) is isolated from the rhizome of *Curcuma longa*. It is a low-molecular-weight polyphenol and being a lipophilic molecule, it can pass through the cellular membrane easily [101,102]. It has been found to attenuate pathways related to the pathology of several ophthalmic disorders [103,104], such as the scavenging of ROS created by mitochondrial-mediated oxidative stress [105,106] and the downregulation of several enzymes responsible for inflammatory responses such as COX-2 and LOX [107] and the suppression of TNF-α

synthesis and several other proinflammatory cytokines such as interleukins released during the process of inflammation [108]. However, despite the therapeutic potential of Curc, several challenges have limited its clinical applications, including a fast metabolism in the body and rapid degradation in solution [101], but mainly its poor solubility in aqueous buffers at neutral pH [109] and therefore low bioavailability when applied in topical administration to the eye. To improve such characteristics the hybrid nanoparticles developed in this work present cores composed of either solid lipid matrixes such as SLNs or liquid lipid matrixes such as NLCs, which can be used to provide a hydrophobic pocket for the poorly soluble drug allowing it to persist in a stable colloidal solution and enhance transport across biological barriers.

Ceftazidime (CZ) is a third-generation cephalosporin that, due to the presence of a β-lactam ring, inhibits penicillin-binding proteins preventing the synthesis of a cell wall on the part of gram-positive and gram-negative bacteria [110-112]. However, CZ quickly degrades in aqueous solutions resulting in the opening of the β-lactam ring, and so, commercially manufactured eye drops containing CZ are not available which makes the intravenous or intramuscular delivery methods the only available for the treatment of pathologies with bacterial origin such as infectious keratitis provoked by the gram-negative bacillus *Pseudomonas aeruginosa* [110,113].

The key points of this project were:

1. Production of different formulations of hyLNPs with NLCs as the core and a polymer shell.
2. Physicochemical characterization of the hyLNPs.
3. Stability assays under storage conditions.
4. Evaluation of encapsulation and adsorption efficiency of Curc and CZ respectively.
5. Evaluation of hyLNPs' cytotoxicity.
6. Evaluation of Curc-loaded hyLNPs anti-oxidation properties.
7. Mucoadhesive properties of CS and HA in the context of hyLNPs.
8. HyLNPs Uptake (quantitative and qualitative) in ARPE-19 cells.
9. Evaluation of drug release by the hyLNPs.
10. Evaluation of the antibiotic activity of CZ-loaded hyLNPs.

2. Experimental Section

2.1 Materials

Pluronic™ F-68 non-ionic surfactant, low molecular weight chitosan (LMW CS, 100 kDa, 92 % deacetylation)and stearylamine/octadecylamine (> 99 %) were obtained from Sigma-Aldrich Inc. (U.K), Glyceryl distearate/Precirol® Ato 5 was a kind offer from Gattefossé company (France), laboratory grade sodium hyaluronate from the brand PrimalHyal™ with an average molecular weight of 50 kDa and 300 kDa from Soliance and an eye drop grade Hyaluronic Acid with an average molecular weight of 300 kDa from Shandong Topscience Biotech co. ltd, were a kind offer from Inquiaroma (Barcelona, Spain). Code names were attributed to the hyaluronic acids: HA50 = 50 kDa, HA300 = 300 kDa, HAEye = 300 kDa eye grade, low viscosity sodium alginate at 37%M|63%G and 60%M|40%G were purchased from IMCD, Ltd. and sodium alginate copolymer (laboratory grade reagent) was purchased from Sigma-Aldrich, Inc. (U.K). Cetrimonium Bromide (CTAB) cationic surfactant was purchased from Alfa Aesar, the bile salt sodium deoxycholate (SD) was purchased from PanReac AppliChem, and sodium cholate (SC) was purchased from Sigma-Aldrich, Inc. (U.K). The solid lipids Compritol® 888 Ato, Geleol®, Cetyl Palmitate and Gelucire® 48/16 were a kind gift from Gattefossé, Tripalmitin was obtained from Sigma-Aldrich Inc. (U.K) and Imwitor® 491 and 988 were purchased from IOI Oleo GmbH. The liquid lipids Labrafac™ lipophile WL 1349, Labrasol® and Labrasol® ALF, Transcutol® HP and P were a kind gift from Gattefossé, Miglyol 810N® and Miglyol 812® were purchased from IOI Oleo GmbH. Curcumin from *Curcuma longa* (Turmeric) was purchased from Sigma-Aldrich, Inc. (U.K.) and Ceftazidime was offered by Combino Pharm Portugal, mucin type II from porcine stomach was purchased from Sigma-Aldrich, Inc (U.K.). Tryptic soy broth and tryptic soy agar were obtained from Biokar (Panti, France). *Pseudomonas aeruginosa* (ATCC® 9027), and ARPE-19 (ATCC® CRL-2302™) cells were obtained from the American Type Cell Culture collection (Manassas, VA, USA). Cell culture media and supplements were from Gibco (ThermoFisher Scientific, Paisley, UK). Purified water was of Milli-Rx quality (Merck Millipore, Germany). All other reagents and solvents were of the purest grade available and generally were used without further treatment.

2.2 Methods

2.2.1 Formulation and Characterization of Lipid-polymer Hybrid Nanoparticles

2.2.1.1 Hot High Shear Homogenization (HHSH)

The formulation of solid lipid nanoparticles was made using glyceryl distearate/Precirol® Ato 5 at 0.05 % (w/v) as the lipid phase and Pluronic™ F-68 (PF68) as a non-ionic surfactant (aqueous phase) at 0.1% (w/v), for the nanostructured lipid carriers, these were produced similar to SLNs with the liquid lipid, Transcutol® P, being added to the lipid phase to create empty nanoparticles. Additionally, curcumin, at concentrations of 10, 25, 50 and 100 µg/mL, was loaded in conjunction with the lipid phase from a stock solution of 20 mg/mL of Curc in Transcutol® P.

To produce the hybrid nanoparticles, Low molecular weight CS in different concentrations (0.5, 0.2, 0.1, 0.05 and 0.01 mg/mL) was added to the aqueous phase. Furthermore, three different permeation enhancers were also separately added to the aqueous phase in conjunction with the LMW CS, namely, CTAB at 0.01% (w/v) and 0.005% (w/v), SD at 0.5 % (w/v) and SC at 1.0, 0.5 and 0.05 % (w/v).

Table 2.1: Tested conditions for the formulation of SLNs and NLCs using the HHSH technique.

Lipid Phase	PF68 (% w/v)	CS LMW (mg/mL)	Curcumin (µg/mL)	CTAB (% w/v)	SD (% w/v)	SC (% w/v)
Precirol® Ato 5	**0.0**	**-**	**-**	**-**	**0.5**	**0.5, 1.0**
	0.1	**0.5, 0.2, 0.1, 0.05, 0.01**	**-**	**0.01, 0.005**	**0.5**	**0.5, 1.0**
Precirol® Ato 5 + Transcutol® P	**0.1**	**0.05**	**-**	**-**	**-**	**0.5**
	0.1	**0.05**	**0.0, 10, 25, 50, 100**	**-**	**-**	**-**

All formulations were produced via the HHSH technique as previously described by Gaspar et al. 2016 [114]. Briefly, the lipid phase was melted in a hot bath (Avantor® VWB series), at a temperature 10 ºC above the melting point of the solid lipid, and the pre-prepared surfactant solution was heated to the same temperature. Homogenization was performed for 5 min using a Silverson L5M high-shear homogenizer equipped with the all-purpose disintegrating head (Silverson Machines, UK) at the nominal maximum speed of 8000 rpm (Figure 2.1). The hyLNPs containing the cationic polymer CS were obtained after cooling the emulsion, in an ice bath.

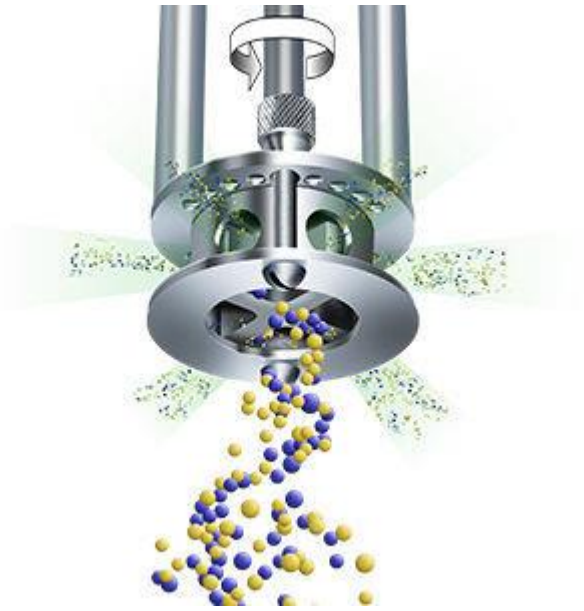

Figure 2.1: Representation of the shearing action by the Silverson L5M. (Adapted from https://www.silverson.com/us/products/laboratory-mixers/, consulted on July 1 of 2022).

2.2.1.2 Surface Modification

HyLNPs containing the anionic polymers HA and ALG and the antibiotic CZ were produced via adsorption. Briefly, to a previously produced hyLNP suspension, either HA or ALG is incorporated into the hyLNPs surface alongside CZ at 5.0 or 2.5 mg/mL under magnetic stirring. The polymers differ in molecular weight and ratio of the residues, respectively for HA and ALG, and at two different concentrations, each, 0.1 and 0.04 % (w/v). Each formulation, with differing parameters, was produced in triplicate for further characterization and testing.

2.2.1.3 Physicochemical Characterization

2.2.1.3.1 Particle Size

The mean hydrodynamic diameter of the hyLNP suspension [115] was measured by Dynamic Light Scattering (DLS) on the day after its production using a Zetasizer Nano S (Malvern Instruments, UK). For each formulation produced three measurements were performed with the results expressed as the mean ± standard deviation (SD) nm and polydispersity index (PDI) as mean ± SD.

2.2.1.3.2 Zeta Potential

Zeta potential (ζP) was determined by the electrophoretic mobility of the nanoparticles in an electrophoretic cell [115] (Figure 2.2). using Zetasizer Nano Z (Malvern Instruments, UK). For each formulation produced three measurements were performed with the results expressed in millivolts (mean ± SD mV). As with the particle size and (PDI), ζP was measured on the day after the nanoparticles' production and after 1 month as part of the stability assays.

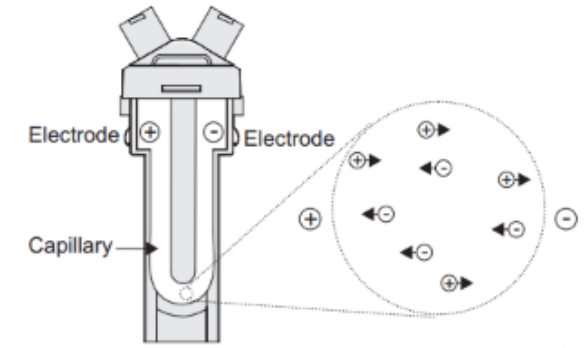

Figure 2.2: Schematic representation of the electrophoretic cell. Adapted from Zetasizer Nano Series User (2013) [115].

2.2.1.3.3 Stability Assays

The stability of the hyLNPs in suspension was studied after 1 month of their production in terms of their mean hydrodynamic diameter, PDI and ζP. All formulations were kept in storage under 4 ºC and protected from light.

2.2.2 Encapsulation/Adsorption Efficiency and Drug Loading

The encapsulation efficiency (%EE) and drug loading (%DL) of Curc inside the lipid core were determined by an indirect and direct ultracentrifugation method [116, 117]. Firstly, for the indirect method, 1mL of Curc-loaded NLCs in suspension was ultracentrifuged for 1 h at 30000 xg at 4 ºC in an Allegra 64R Benchtop Centrifuge (Beckman Coulter), 200 µL of the supernatant was then collected and placed in a 96 well microplate for the determination of %EE and %DL of Curc by fluorescence ($\lambda_{excitation}$ = 485 nm; $\lambda_{emission}$= 520 nm) using a microplate reader (FLUOstar Omega, BMG LabTech, Germany) all assessments were made in triplicate at. For the direct method, the resulting pellet of the indirect method was resuspended in 500 µL of acetonitrile (ACN) and centrifuged for 5 min at 13500 rpm after vortex mixing. Similarly, 200 µL of the resulting supernatant was then collected and placed in a 96-well microplate for the determination of %EE and %DL of the lipophilic drug. For every formulation, three samples were produced, and every sample was measured in triplicate.

The adsorption efficiency (%AE) and %DL of CZ adsorbed to the hyLNPs were determined by the indirect method using an ultra-filtration technique [116]. Briefly, solutions containing CZ-loaded hyLNPs were dosed up to centricons with a cut-off of 300 kDa and ultra-filtered at 15 000 xg for 15 min after which any aggregate found was resuspended and the sample was again ultra-filtered at 15 000 xg for 15 min. The resulting filtrated solution was then collected and placed in a 96-well microplate in triplicate for the determination of %AE and %DL of the hydrophilic drug using UV-Vis at λ_{CZ}=310 nm.

The %EE (for the direct and indirect methods respectively) as well as the %AE and %DL were calculated using the following equations:

$$EE/AE(\%) = \frac{(W_t - W_f)}{W_t} \times 100 \quad \text{..... (1)}$$

$$DL\ (\%) = \frac{(W_t - W_f)}{W_{np}} \times 100 \quad \text{..... (2)}$$

Where W_t is the total amount of the drug used, W_f is the amount of free drug detected in the supernatant after ultra-filtration or ultracentrifugation and W_{np} is the weight of the nanoparticles.

2.2.3 *In Vitro* Studies

2.2.3.1 Mucoadhesion Studies

The interaction between mucin type II from porcine stomach and hyLNPs was measured using zeta potential measurements as described previously by B. Silva et al. 2020 [17]. Briefly, several samples with mucin (2 mg/mL) in a 1:1 ratio with different formulations were tested for their electrophoretic mobility after the incubation with mucin, in addition, the mucin dispersion in water was also measured.

2.2.3.2 Drug Permeation Studies

Drug permeation was investigated using Franz-type diffusion cells with polyvinylidene difluoride (PVDF) membranes separating the donor and receptor phases. The receptor phase was filled with approximately 4 mL of 10 mM phosphate buffer at pH 7.4 (PBS) in a 1:1 ratio with ethanol (EtOH). The donor phase was filled with 1 mL of each of the following formulations: Empty hyNPs (n=1) and Curc-CZ loaded hyLNPs (Curc-CZ-hyLNPs) (n=8).

Franz cells were incubated at 36 ºC with magnetic stirring at 300 rpm. At the predefined time, intervals, throughout 6 h, a 200 µL sample of the receptor solution was collected for the determination of the drug released by the hyLNPs through the donor phase and it was replaced by an equal volume of fresh buffer solution at the same temperature.

All permeation studies were done using four Franz diffusion cells per formulation and were performed under sink conditions. Samples were analysed in a microplate reader by UV-spectrophotometry (λ_{CZ}= 310 nm) and fluorescence ($\lambda_{excitation}$= 485 nm; $\lambda_{emission}$= 520 nm) for the determination of CZ and Curc's permeation respectively.

The percentage of the cumulative amount of the drugs permeated through the membrane (%µg/cm^2) was determined using equation (3):

$$\%Q_t = \frac{V_r \times C_t + \sum_{t=0}^{t-1} V_s \times C_i}{S} \times \frac{100}{m_{CZ}} \quad \text{..... (3)}$$

where V_r is the volume of the receptor solution, C_t is the CZ concentration in the receptor solution at any given sampling time (t), V_s is the volume of the sample and C_i is the concentration at each sampling time. The S value is the membrane area, 1 cm^2. m_{CZ} corresponds to the weight of CZ (µg) for a 200 µL sample.

2.2.3.3 Cell Uptake of HyLNP

2.2.3.3.1 Quantitative Uptake Assessment

To assess the association between drug-loaded hyLNPs and cells, the curcumin encapsulated into the lipidic core was used as the fluorophore. Firstly, on the day prior to the experiment, ARPE-19 (human retinal pigment epithelia cell line, ATCC® CRL-2302TM) cells were seeded in a sterile flat bottom 96-well tissue culture plates (Greiner, Germany), in RPMI 1640 culture medium, supplemented with 10% foetal bovine serum, 100 U/mL of penicillin G, 100 µg/mL of streptomycin sulphate and 2 mM of L-glutamine (Gibco, Thermo Fisher, UK), at a cell density of 2 $\times 10^5$ cells/mL and 10 µL per well. The cells were incubated overnight at 37 ºC and 5 % CO2.

On the next day, the culture medium was removed and replaced with a medium containing different amounts of Curc-loaded NLCs (Curc-NLCs), Curc-loaded hybrid nanoparticles (Curc-hyLNPs) and CZ-Curc-loaded hybrid nanoparticles (Curc-CZ-hyLNPs) (n=8) to a final nanoparticle concentration of 100, 50, 25 and 12.5 µg/mL.

Fluorescence measurements for Curc were performed for the 96-well plate immediately after the addition of the samples. After a 2 h incubation, the 96 well plate was washed in 2 washing steps with 250 µL of 10 mM PBS + 20 mM glycerine at pH 7.4. Afterwards, the PBS solution was removed, and cells were lysed with 100 µL of 1 % Triton X-100 and fluorescence measurements were made to determine the amount of cell-associated hyLNPs.

2.2.3.3.2 Fluorescence Microscopy

ARPE-19 cell cultures were performed at the same conditions as described in the quantitative uptake assessment. Cells were grown on the surface of sterile glass slides (Greiner, Germany) on a 24-well plate. After a 2 h incubation with hyLNPs, cells were rinsed 3 times with 10 mM PBS + 20 mM glycerine at pH 7.4. Afterwards, the cells were fixed for 15 min at room temperature and protected from light with 4 % (w/v) paraformaldehyde (Sigma-Aldrich, UK).

The cells were then rinsed 3 times with 10 mM PBS + 20 mM glycerine at pH 7.4 and permeabilized with 0.1 % Triton X-100 for 4 min and rinsed again. Afterwards, a 6.6 µM phalloidin-TRITC solution (Life Technologies) in PBS was added to the cells for 30 min at room temperature. After the cells were newly rinsed with 10 mM PBS + 20 mM glycerine at pH 7.4, air dried and the cell slides mounted in fluorescent mounting medium ProLong® Gold antifade reagent with 4'-6-diamidine-2'-phenylindole dihydrochloride (DAPI) (Life Technologies, UK).

Fluorescence was observed and recorded on an Axioscop 40 fluorescence microscope (Carl Zeiss, Germany), equipped with an Axiocam HRc camera (Carl Zeiss, Germany). The AxioVision Rel. 4.8.1 software (Carl Zeiss, Germany) was used to process the images.

2.2.3.4 Cell Viability Studies

Cytotoxicity of the different formulations was assessed using an ARPE-19 cell line, using a 3-(4,5-dimethylthiazol-2-yl)-2,5-diphenyltetrazolium bromide (MTT) reduction assay to evaluate cell viability [118] after 24 h of incubation of the cell line with the different tested formulations of hyLNPs.

Firstly, on the day prior to the experiment, ARPE-19 cells were grown in a 96-well plate at the same density as in the quantitative cell uptake assessment and incubated in the same conditions. On the experiment day, the culture medium was replaced by fresh medium and hyLNPs were added to a final concentration of 500 µg/mL with each sample tested in 8 wells per plate. Additionally, cells were also incubated with PF68 and culture medium (negative controls), and as the positive control, sodium dodecyl sulphate (SDS) at 0.1 mg/mL and free curcumin at 50 µg/mL were added. Afterwards, an MTT reduction assay was performed, by replacing the medium with one containing 0.25 mg/mL of MTT and incubating the cells for 3 h. To solubilize the intracellular formazan crystals formed, the medium was carefully removed and 100 µL of DMSO was added, and after 15 min the absorbance at 570 nm was measured in the microplate reader (FLUOstar Omega, BMG LabTech, Germany). Cell viability (%) relative to the culture medium was calculated using equation 4:

$$Cell\ Viability\ (\%) = \frac{Sample_{Abs}}{Control_{Abs}} \times 100 \quad (4)$$

Where $Sample_{Abs}$ is the observed absorbance obtained for the cells incubated with hyLNPs and $Control_{Abs}$ is the observed absorbance for cells incubated in culture medium.

2.2.3.5 Activity Assays

2.2.3.5.1 Antioxidant Activity of Curc-Loaded NPs

The intracellular reactive oxygen species (ROS) production by chemical induction was used to evaluate the antioxidant effect of curcumin-loaded hyLNPs according to a previously published procedure [17]. Briefly, the same treatment as the one in the *in vitro* cell viability studies was given to the ARPE-19 cell culture on the day prior to the experiment.

After 24h incubation the culture medium was replaced by fresh medium and the fluorescence probe 2',7' dicholorofluoresceindiacetate (H2DCFDA, ThermoFisher Scientific, Paisley, UK) was added to the wells to a final concentration of 20 µM followed by incubation for 1h. Afterwards, the fresh culture medium was added alongside the formulations of NLCs with different Curc concentrations (10, 25, 50 and 100 µg/mL) and empty NLCs (negative control) were added in six replicates (10 µL/well) with the wells incubated with H_2O_2 and culture medium being a positive control.

After the cells were incubated for 1h with the samples tested, hydrogen peroxide (H_2O_2) was added to a final concentration of 500µM to generate reactive oxygen species and after a 2 h incubation period, fluorescence was measured at $\lambda_{excitation}$=485 nm and $\lambda_{emission}$=520 nm, using a microplate reader (FLUOstar Omega, BMG LabTech, Germany). Data collected is expressed as a percentage of reduction of ROS using the following equation:

$$ROS\ reduction\ (\%) = 100 - (\frac{Sample\_Fluorescence}{Control\_Fluorescence} \times 100) \quad \text{.....(5)}$$

2.2.3.5.2 Determination of Antimicrobial Activity of CZ

The antimicrobial activity of CZ-loaded hyLNPs against CZ in solution was assessed by the microtiter plate antibacterial assay adapted from a method previously described [119] and according to the guidelines of Clinical and Laboratory Standards Institute by broth microdilution method [120]. Briefly, a bacterial culture of *P. aeruginosa* was prepared in a tryptic-casein soy broth (TBS). After 24h of incubation, the optical density (OD) of *P. aeruginosa* was recorded at 600 nm, and various dilutions were made with aseptic techniques until the OD was between 0.5 and 1.0. The dilution factor was obtained after the dilution was carried out to achieve a 5×10^5 CFU/mL concentration.

In this study, the antimicrobial effect of hyLNPs with two differing loaded concentrations of CZ, 2.5 and 5 mg/mL, and loaded with Curc, were tested alongside free CZ.

A sterile 96-well plate was prepared under aseptic conditions. The last column was filled with 100 µL of TBS as the negative control. All the other wells were filled with 50 µL of TBS, as well as the second to last column which was filled with 50 µL *P. aeruginosa* as the positive control. Afterwards, the samples were loaded in the wells and subjected to serial dilutions. Finally, the bacterial suspension was added to each well to achieve the concentration previously mentioned. The plate was then incubated at 37 ± 1 ºC overnight.

A vital dye Alamar Blue was added to all wells in the plate and incubated for 3 h. The visual colour change from blue to pink was assessed as positive for bacterial growth and the first concentration with no detectable growth was taken as the minimum inhibitory concentration (MIC) value. To confirm the visual results, the wells' fluorescence intensity was measured in a microplate spectrophotometer reader (FLUOstar Omega. BMGLabtech, Ortenberg, Germany).

2.2.4 Statistical Data Analysis

The data were expressed as the mean and standard deviation (mean ± SD) of each experiment. Statistical analysis of the experimental data was performed using a one-way analysis of the variance (one-way ANOVA) and the significance of the differences between groups was assessed by Kruskal-Wallis multiple comparison test (GraphPad PRISM 9 software, La Jolla, CA, USA) assuming $p < 0.05$.

3. Results

3.1 Formulation and Physicochemical Characterization of HyLNPs

3.1.1 Formulation of HyLNPs

In the present work, all hyLNPs formulations were prepared by HHSH using the solid lipid Precirol® Ato 5 at 0.05 % (w/v) as the lipid phase and the surfactant PF68 at 0.1 % (w/v) as the aqueous phase in which the polymers were dissolved. This simple, rapid method of nanoparticle production makes use of the high-speed rotation of a stationary rotor to shear the melted lipid solution into the aqueous surfactant solution. As such, this method does not require the use of organic solvents to dissolve the lipid phase found in other methods such as the solvent evaporation technique.

3.1.1.1 Effects of Different Polymers in HyLNPs' Characteristics

3.1.1.1.1 Chitosan

The incorporation of a low molecular weight CS (LMW CS), in hyLNP was studied by adsorption to the surface of the lipid cores and by incorporation of CS into the aqueous surfactant solution at 0.01, 0.05, 0.1, 0.2 and 0.5 mg/mL.

The results obtained with the CS incorporated into the surfactant solution are presented in figure 3.1. An expected increase in size was observed as the concentration of CS increased for all concentrations except 0.01 mg/mL which showed to produce nanoparticles with a higher mean size of 478.2 ± 18.3 nm, this increase ($0.01 < p < 0.05$) could be attributed to insufficient amount of the cationic polymer to coat the anionic lipidic core as justified by the low anionic charge found in this formulation of -13.8 ± 0.3 mV. At the concentration of 0.01 mg/mL, LMW CS does not provide that stabilization leading to the formation of nanoparticles with increased size.

The wide values of PDI for 0.5CS ($0.001< p < 0.01$) corroborate with the higher-sized SLN observed in these formulations most likely indicating an ongoing aggregation.

The concentration of 0.05 mg/mL of CS incorporated showed no significant changes ($p \geq 0.05$) to both size and PDI when compared to the control formulation with a mean size of 178.8 ± 1.9 nm.

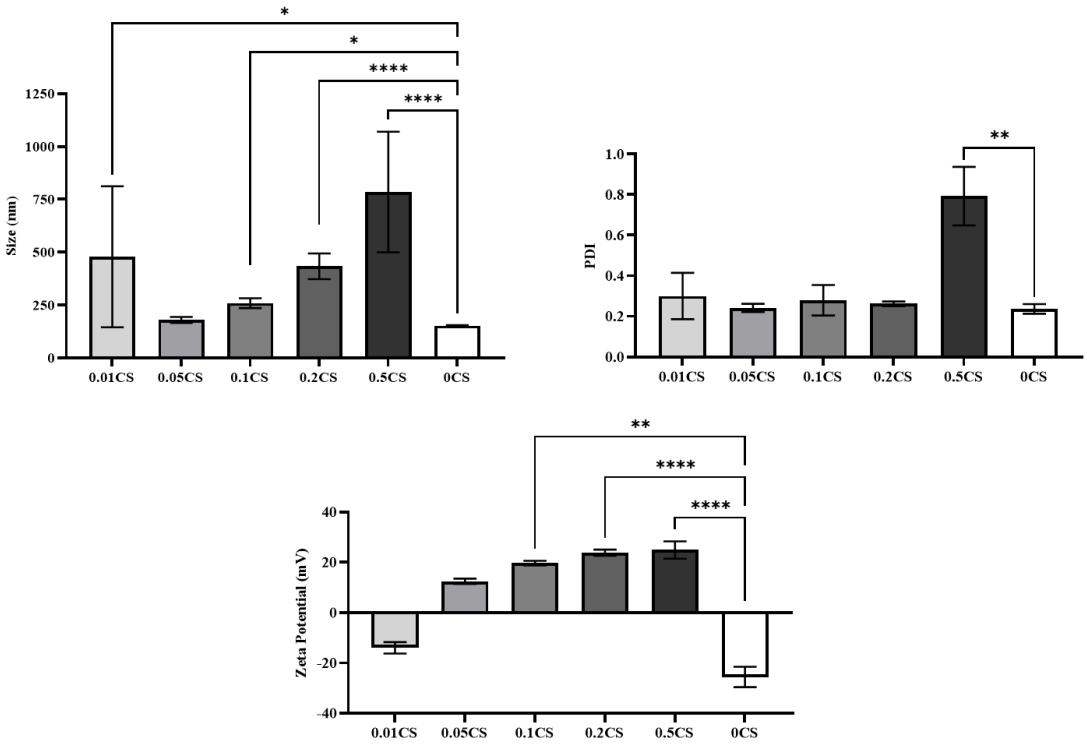

Figure 3.1: Influence of LMW CS concentration on SLNs' physicochemical properties, produced by HHSH. Results in terms of size (nm), PDI and ζP (mV) (mean ±SD, n=9), (* $0.01 < p < 0.05$, ** $0.001 < p < 0.01$, *** $0.0001 < p < 0.001$, **** $p < 0.0001$).

As expected, the ζP values increase with CS concentration, however, no significant ($p \geq 0.05$) changes were found between the two lowest concentrations of polymer, with the lowest ζP observed in 0.05CS formulations, however even with the smaller ζP of + 12.5 ± 0.5 mV it was observed that this concentration of LMW CS was enough to overcome the aggregation of the SLNs resulting in smaller nanoparticles of 178.8 ± 1.9 nm and a small PDI value 0.242 ± 0.007.

The results referring to LMW CS's adsorption onto the SLNs' surface (according to section 2.2.1.2) are represented in Figure 3.2. Similarly, to CS incorporated into the surfactant solution, higher concentrations of the polymer adsorbed in the surface lead to bigger sizes of nanoparticles with SLNs at 0.05 mg/mL CS showing to produce the smallest size of 198.9 ± 3.5 nm with no significant changes ($p \geq 0.05$) of PDI compared to the lipidic cores (0CS).

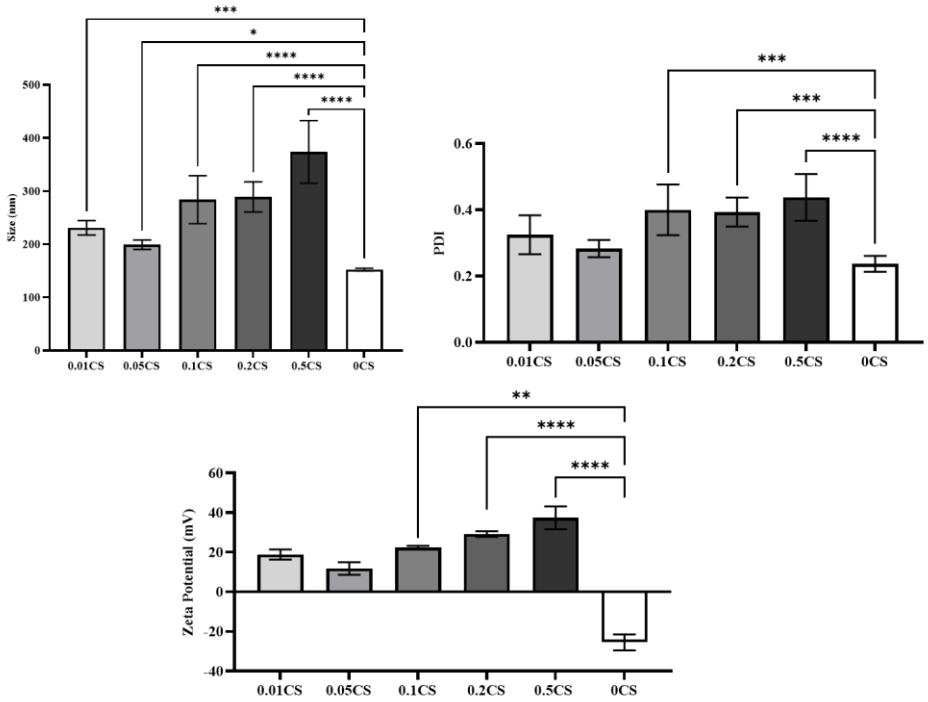

Figure 3.2: Influence of LMW CS's concentration adsorbed on to SLNs' surface on their physicochemical properties, produced by HHSH. Results in terms of size (nm), PDI and ζP (mV) (mean ±SD, n=9), (* 0.01 < p < 0.05, ** 0.001 < p < 0.01, *** 0.0001 < p < 0.001, **** p < 0.0001).

It was observed that in all formulations the ζP was positive, indicating a successful adsorption of the cationic polymer onto SLNs' surface.

Considering the results presented for both LMW CS incorporated or adsorbed, the polymer at 0.05 mg/mL showed the most promise, presenting smaller size nanoparticles when incorporated into the surfactant solution or adsorbed. The use of LMW CS incorporated in the surfactant solution was chosen for further studies allowing the adsorption of a secondary, anionic polymer with compelling characteristics for ocular drug delivery such as HA and ALG.

3.1.1.1.2 Hyaluronic Acid

In this work HA of molecular weights of 50 and 300 kDa (HA50, HA300 and HAEye) at the concentrations of 0.04 % (w/v) and 0.1 % (w/v) were firstly adsorbed onto the surface of SLNs made up of the solid lipid Precirol®, surfactant PF68 and the cationic lipid stearylamine (according to section 2.2.1.2), this last one added to allow the adsorption of the anionic polymer (0HA). The results for the influence of HA on the NPs' physicochemical characteristics are presented in figure 3.3.

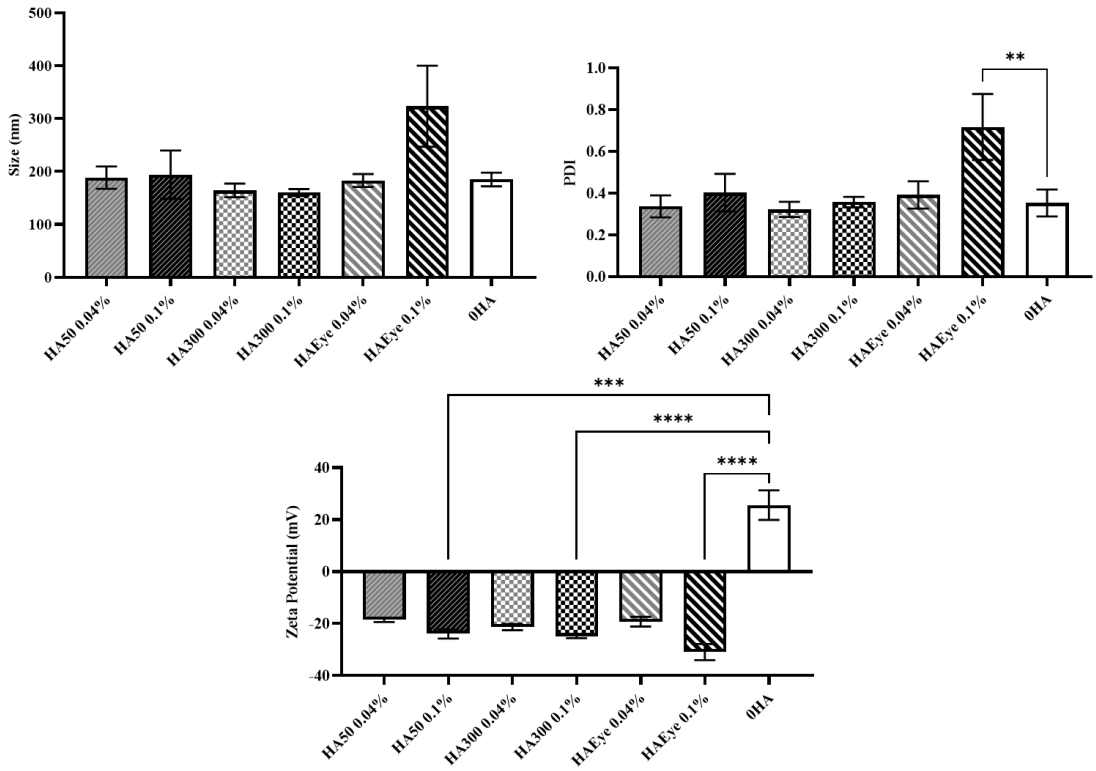

Figure 3.3: Influence of HA's concentration and molecular weight adsorbed on to SLNs' surface on their physicochemical properties. Results in terms of size (nm), PDI and ζP (mV) (mean ±SD, n=9), (* $0.01 < p < 0.05$, ** $0.001 < p < 0.01$, *** $0.0001 < p < 0.001$, **** $p < 0.0001$). SLNs with the added stearylamine were made the control.

It was observed no significant ($p \geq 0.05$) difference in the sizes of the nanoparticles due to the absorption of hyaluronic acid when compared with the control nanoparticles to any of the formulations tested except the formulation made up of eye drop grade hyaluronic acid (HAEye) at 0.1% (w/v) which presented higher sized nanoparticles at 323.5 ± 15.9 nm with a high polydispersity index of 0.760 ± 0.077. Furthermore, through the changes in ζP of the positive surface charge, of the control nanoparticles to a negative surface charge it was observed that in all formulations HA was able to be adsorbed.

With these results it was decided that eye drop grade HA at 0.04 % (w/v) could integrate the final, optimized formulation of the hyLNPs system as it showed to produce nanoparticles with small sizes of 183.0 ± 3.0 nm and PDI of 0.390 ± 0.028 and a ζP of – 19.2 ± 0.9 mV.

3.1.1.1.3 Sodium Alginate

Another polymer studied was Alginate of three different types at two concentrations [0.1 % (w/v) and 0.04 % (w/v)] differing from each other on the ratio of the monomers that constitute them, 37%M|63%G, 60%M|40%G and Low viscosity ALG (LV) due to their anionic nature, these polymers were adsorbed on to the surface of SLN (precirol®, surfactant PF68 and stearylamine). The results of nanoparticles properties in terms of size, PDI and zeta ζP obtained in the assays of adsorption of ALG are shown in Figure 3.4

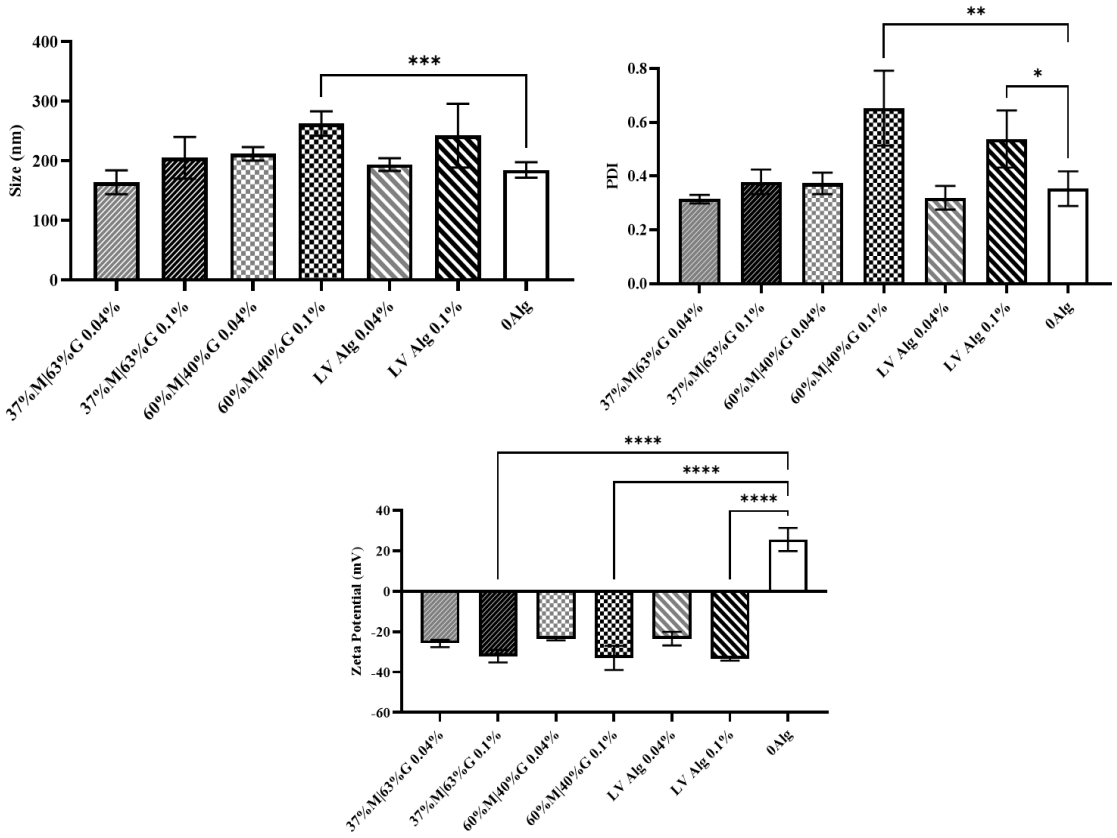

Figure 3.4: Influence of ALG's concentration and monomer ratios composition adsorbed on to SLNs' surface on their physicochemical properties. Results in terms of size (nm), PDI and ζP (mV) (mean ±SD, n=9), (* 0.01 < p < 0.05, ** 0.001 < p < 0.01, *** 0.0001 < p < 0.001, **** p < 0.0001). SLNs with stearylamine were used as control.

Through the ζP, it can be concluded that in all formulations the polymer is present at the SLN's surface as it is observed a predominantly net negative surface charge when compared to the SLN's positive surface charge with no polymer adsorbed (0Alg).

At the lower concentrations, the ratio of M/G residues that compose ALG showed to produce no significant ($p \geq 0.05$) changes in the SLN's size as well as the formulation of 37%M|63%G at 0.1% (w/v) when compared with the stearylamime-SLNs. On the other hand, the formulation with ALG 60%M|40%G at 0.1 % (w/v) showed to produce nanoparticles with bigger sizes ($0.0001 < p < 0.001$) and PDI ($0.001 < p < 0.01$).

The formulation with ALG composition of 37%M|63%G at 0.04 % (w/v) showed to result in a small size NPs of 164.3 ± 3.1 nm and a small polydispersity index of 0.314 ± 0.011 with a ζP suitable for ocular delivery of - 26.2 ± 1.2 mV, however, and although sodium alginate formulations presented good characteristics similar to those of the hyaluronic acid, they showed low stability at 4 ºC and where therefore discarded from further studies.

3.1.1.2 Effects of Permeation Enhancers in SLNs' Characteristics

In this work, the chosen permeation enhancers (PE) were the bile salts sodium deoxycholate (SD) and sodium cholate (SC). SD was tested both alone and being a co-surfactant of PF68 at a concentration of 0.5 % (w/v) and SC was tested in the same conditions with two concentrations of 1.0 % (w/v) and 0.5 % (w/v). The results of nanoparticles properties in terms of size, PDI and zeta potential obtained are shown in Figure 3.5.

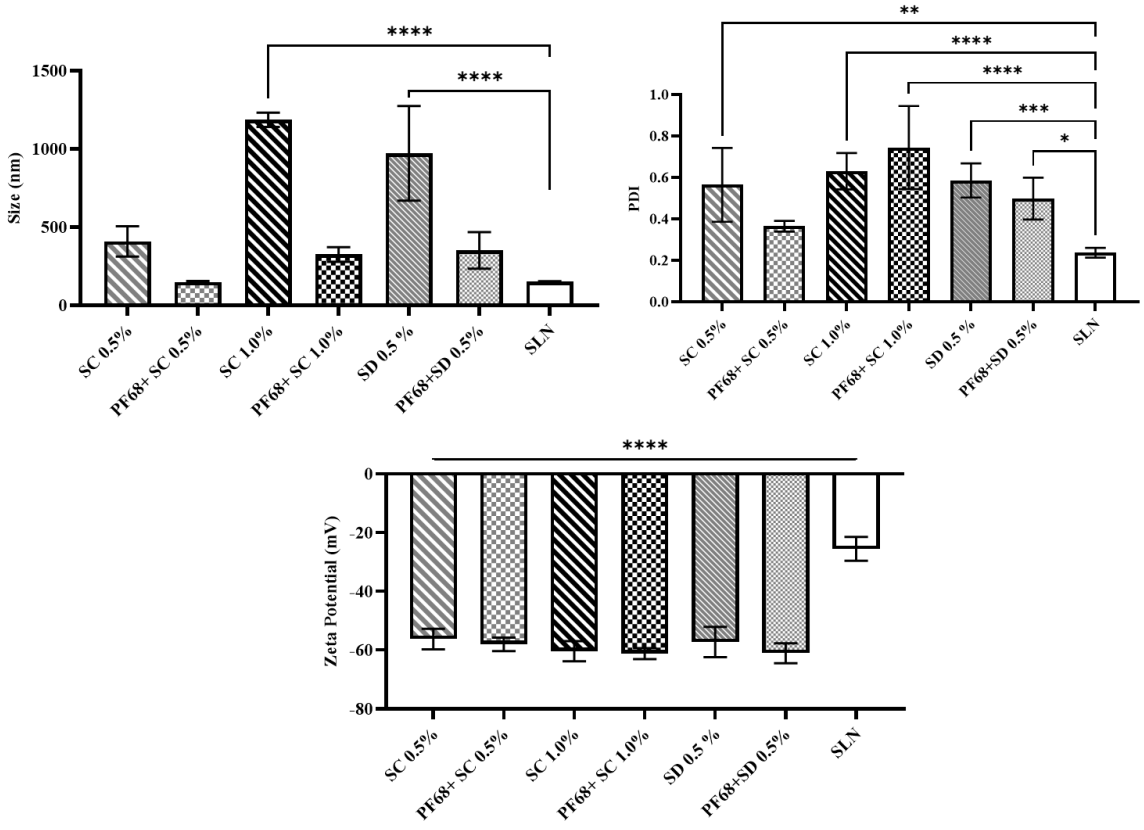

Figure 3.5: Influence of the bile salts sodium deoxycholate and sodium cholate as surfactant or as a co-surfactant in SLNs' physicochemical properties. Results in terms of size (nm), PDI and ζP (mV) (mean ±SD, n=9), (* $0.01 < p < 0.05$, ** $0.001 < p < 0.01$, *** $0.0001 < p < 0.001$, **** $p < 0.0001$). Control formulations were produced using PF68 as the surfactant and precirol® as the lipidic phase (SLN).

It was observed, extremely significant changes in ζP ($p < 0.0001$) in all formulations with surface charges between – 62.0 and – 54.0 mV among the tested formulations produced with both SC and SD (Figure 3.6).

The nanoparticles produced with SC 0.5% (w/v) as surfactant resulted in no significant differences ($p \geq 0.05$) in terms of the SLNs' size and PDI (408.8 ± 20.6 nm, 0.535 ± 0.054) when compared with those produced with PF68 (SLN).

All other formulations with the PEs as surfactants produced nanoparticles with significantly higher sizes than the control formulations, exceeding 1000 nm as observed in the formulation of SC 1.0 % (w/v) and SD 0.5 % (w/v) ($p < 0.0001$) in Figure 3.5.

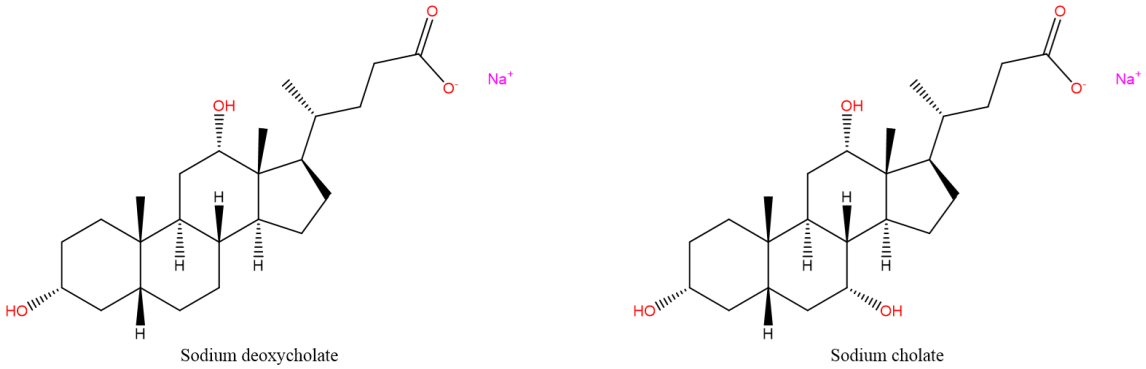

Figure 3.6: Chemical structure of the bile salts used as co-surfactants.

On the other hand, as a co-surfactant with PF68, bile salts show to be effective in stabilizing the lipidic phase with the best results shown in the formulation with SC at 0.5 % (w/v) as the co-surfactant, producing nanoparticles of 149.7 ± 4.3 nm, and PDI of 0.367 ± 0.014. This formulation was chosen for further studies, with SC as the permeation enhancer for the SLNs produced in this work.

3.1.2 Formulation Optimization

With all the components tested for their individual influence on SLNs' physicochemical characteristics the next step was to optimize the formulations to be able to efficiently encapsulate the hydrophobic antioxidant Curcumin (Curc) inside the lipidic matrix of the SLN core and the adsorption of a hydrophilic antibiotic, Ceftazidime (CZ), on to the polymeric shell, while maintaining the hyLNPs, physicochemical, mucoadhesive and permeation enhancing properties.

3.1.2.1 Curcumin Solubilization

The solubility of Curc was studied in different solid and liquid lipids and the results are presented in table 3.1. Curc demonstrates low solubility in all the different solid lipids tested except Imwitor® 988, however, the high amount of lipid required to solubilize Curc, led to it being discarded alongside all solid lipids as lone solubilizers. For liquid lipids, both Trascutol® P and HP showed to be good solubilizers for Curc at a lower needed volume.

Table 3.1: Solubility of Curcumin in different lipidic phases.

Lipid	Final Amount of Lipid (g)	Curc weighted (g)	Precipitate (Yes/No)
Precirol® Ato 5	0.300	0.0104	Y
Compritol® 888 Ato	0.300	0.0100	Y
Geleol®	0.300	0.0101	Y
Cetyl Palmitate	0.300	0.0103	Y
Tripalmitin	0.300	0.0104	Y
Imwitor® 491	0.300	0.0101	Y
Imwitor® 988	0.800	0.0108	N
Gelucire® 48/16	0.300	0.0105	N
	Final Volume added (µL)	**(g)**	
Labafrac™ WL1349	300	0.0103	Y
Labrasol®	300	0.0108	N
Larasol® ALF	300	0.0106	N
Transcutol® HP	200	0.0210	N
Transcutol® P	200	0.0208	N
Miglyol 810N®	300	0.0106	Y
Miglyol 812®	300	0.0104	Y

From this data the nanoparticles need to incorporate a liquid lipid to efficiently carry out the Curc molecule, thus the new hyLNPs comprise two lipids, Precirol® and Transcutol® P at 0.05 % (w/v). Therefore, it was necessary to assess the physicochemical characteristics of the new NLCs produced using the same methods as described in section 2.2.1. The results presented in table 3.2 showed no significant differences in terms of ($p \geq 0.05$) size, PDI and ζP between both types of lipidic nanoparticles.

Table 3.2: Physicochemical characteristics of nanostructured lipid carriers (NLCs) in comparison with solid lipid nanoparticles (SLNs). Results in terms of size (nm), PDI and ζP (mV) (mean ±SD, n=9).

Formulation	Size (nm)	PDI	ζP (mV)
SLN + 0.5%SC	149.7 ± 4.3	0.367 ± 0.014	-58.2± 1.0
NLC + 0.5%SC	152.1 ± 1.4	0.344 ± 0.007	-51.8±1.4

As such NLCs made up of Precirol® and Transcutol® P were used in further testing as the liquid lipid proved to solubilize Curc.

3.1.2.2 Sodium Cholate & Chitosan Interaction

The incorporation of CS at 0.05 mg/mL to the NLCs core with two concentrations of the permeation enhancer SC were tested, 0.05 % (w/v) and 0.5 % (w/v). Production and testing of the physicochemical characteristics of the resulting formulations were done as previously described in section 2.2.1 with both SC and CS in the aqueous surfactant solution. The results of the formed nanoparticles are shown in figure 3.7.

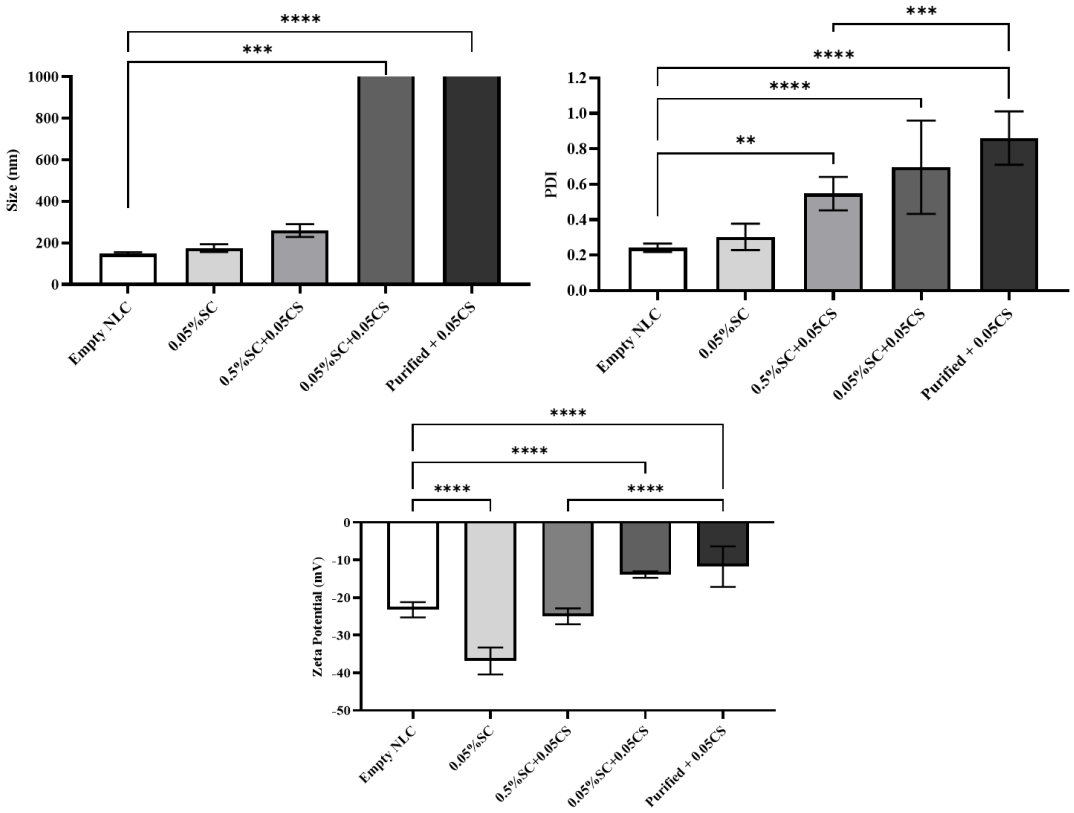

Figure 3.7: Influence of SC and CS on NLCs' on size (nm), PDI and ζP (mV) of NLCs (mean ±SD, n=9), (* $0.01 < p < 0.05$, ** $0.001 < p < 0.01$, *** $0.0001 < p < 0.001$, **** $p < 0.0001$).

At first observation, the addition of 0.5 % (w/v) of SC showed no significant changes ($p \geq 0.05$) to the nanoparticles' size and ζP with a very significant change ($0.001 < p < 0.01$) in PDI when compared to the control formulations (Empty NLC), however, at this concentration of bile salt all formulations exhibited low stability at 4 ºC thus, another concentration of SC was tested. At a concentration of 0.05 % (w/v) it was observed the aggregation of the nanoparticles.

As such, new formulations were produced as described in section 2.2.1 with SC at the initial concentration of 0.5 % (w/v) in the aqueous solution, followed by the removal of excess SC done using disposable PD-10 desalting columns (GE Healthcare, US) containing Sephadex ™ G-25 Medium and following a gravity protocol [121] and followed by the adsorption of CS at 0.05 mg/mL on to NLC's surface (Purified + 0.05CS). It was observed that the removal of the excess in the bile salt from the aqueous solution and posterior adsorption of the polymer did not prevent nanoparticles' aggregation.

Thus, the addition of bile salts as PE for topical ocular delivery was not considered for further studies.

3.1.2.3 Optimized Carrier of HyLNPs

Discarding the use of bile salts as permeation enhancers, the final formulation chosen to be the carrier of both Curc and CZ was composed of the solid lipid Precirol® and the liquid lipid Transcutol® P as the lipidic phase and the surfactant PF68 as the aqueous solution with a low molecular weight chitosan 0.05 mg/mL followed by the adsorption of an eye grade hyaluronic acid (300 kDa) on to the NLCs' surface at a concentration of 0.04 % (w/v) forming the empty Lipid-Polymer Hybrid Nanoparticles.

Table 3.3: Physicochemical characteristics of the lipidic core (Empty NLC), with CS incorporated in the aqueous solution (NLC + 0.05CS) and the final optimized formulation of the empty hyLNPs with HAEye at 0.04% adsorbed at the surface (hyLNPs). Results in terms of size (nm), PDI and ζP (mV) (mean ±SD, n = 9).

Formulation	Size (nm)	PDI	ζP (mV)
Empty NLC	148.3 ± 2.3	0.239 ± 0.015	- 23.2 ± 1.8
NLC + 0.05CS	217.8 ± 5.4	0.251 ± 0.014	+ 17.1 ± 0.4
hyLNP	241.4 ± 3.3	0.282 ± 0.006	- 26.6 ± 1.2

3.2 Encapsulation/Adsorption Efficiency and Drug Loading

The next step was the encapsulation of Curc inside the lipidic core and the adsorption of CZ onto the surface of the hyLNPs and the determination of the %EE and %AE respectively and %DL for both drugs.

3.2.1 Curcumin Encapsulation

3.2.1.1 Characterization of Curc-loaded NLC

The encapsulation of Curcumin (0, 10, 25, 50, and 100 µg/mL) was tested, by its addition to the lipidic phase. After the production of the Curc-loaded NLCs with CS incorporated the characteristics of the nanoparticles were assessed as previously described. The results are shown in figure 3.8.

It was observed that the presence of encapsulated Curc have no significant ($p \geq 0.05$) impact on the nanoparticles' size in all concentrations except 100 µg/mL which produced slightly bigger ($0.0001 < p$) nanoparticles (270.2 ± 8.0 nm), the lowest size recorded was of 205.0 ± 3.1 nm for $[Curc]_{Total}$ = 25 µg/mL.

The surface of the nanoparticles with Curc were all positively charged being the values significantly different from empty nanoparticles with the exception of the lowest tested concentration of curcumin.

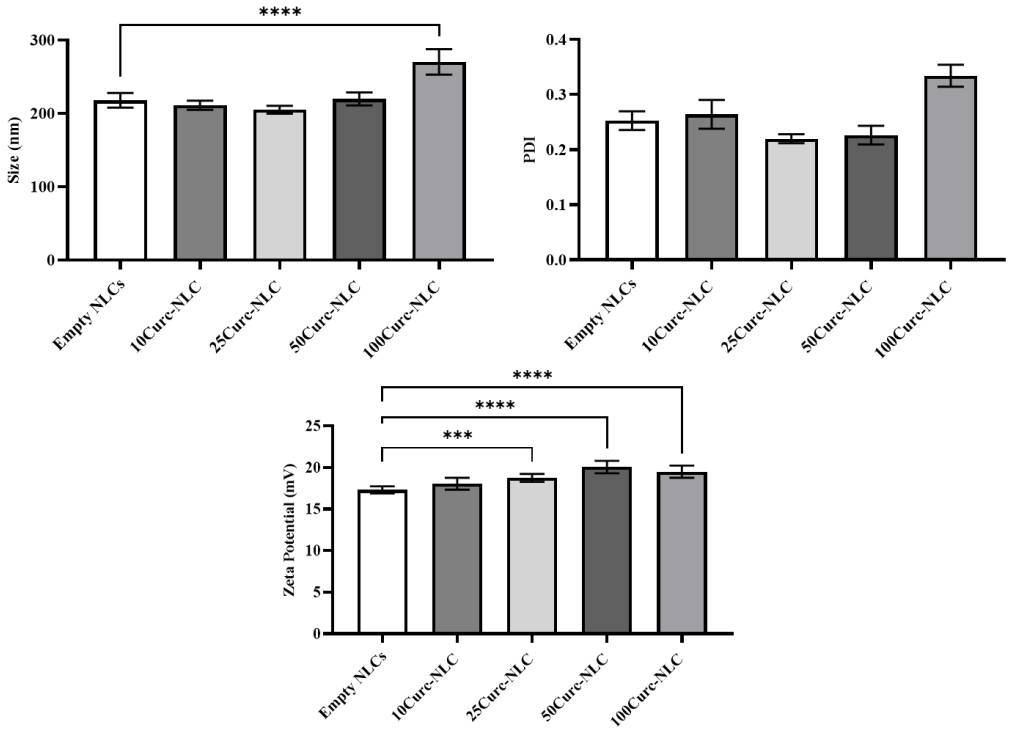

Figure 3.8: Effect of Curc encapsulation at different concentrations in the physicochemical characteristics of the lipidic core with CS incorporated in the aqueous solution. Results in terms of size (nm), PDI and ζP (mV) (mean ±SD, n = 9), (* 0.01 < p < 0.05, ** 0.001 < p < 0.01, *** 0.0001 < p < 0.001, **** p < 0.0001).

3.2.1.2 Encapsulation Efficiency and Drug Loading of Curc

To determine the %EE and %DL of Curc in the different formulations, a calibration curve (Figure 3.10) for the Cur dissolved in dimethyl sulfoxide (DMSO) was obtained measuring the fluorescence at the wavelengths $\lambda_{excitation}$ =485 nm; $\lambda_{emission}$=520 nm using Curc concentrations between 31.3 and 1 µg/mL. The UV-Vis spectrum of Curc is shown in figure 3.9.

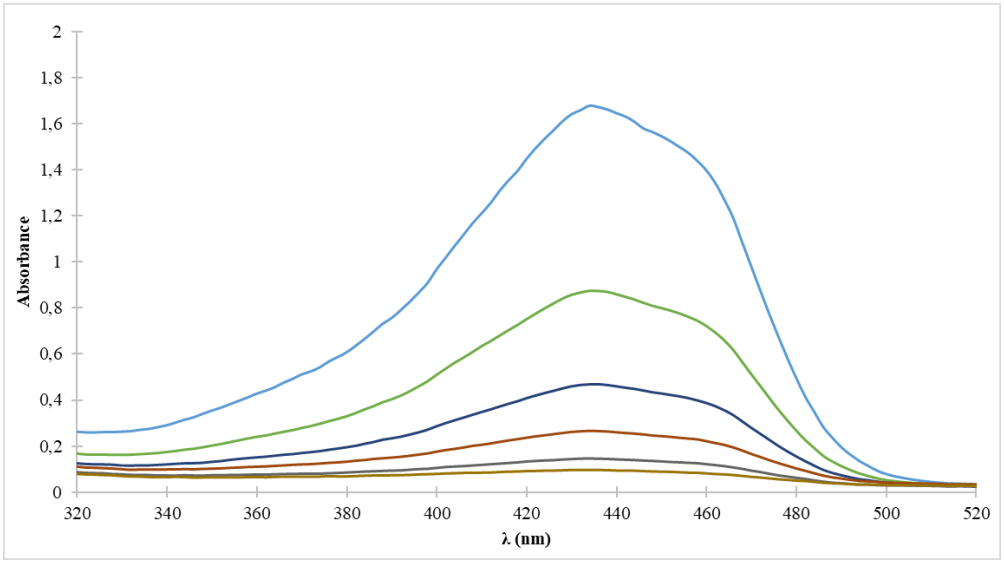

Figure 3.9: Curcumin in DMSO UV-Vis spectrum, in descending concentrations of 31.3, 15.6, 7.8, 3.9, 2.0 and 1.0 µg/mL. When dissolved in DMSO Curc presents an absorbance peak at 435 nm.

Both fluorescence and UV-Vis measurements were tested to determine Curc %EE and %DL in two ultracentrifugation methods indirect and direct and using the calibration curve presented in Figure 3.10 to determine the amount of Curc encapsulated in the lipidic matrixes.

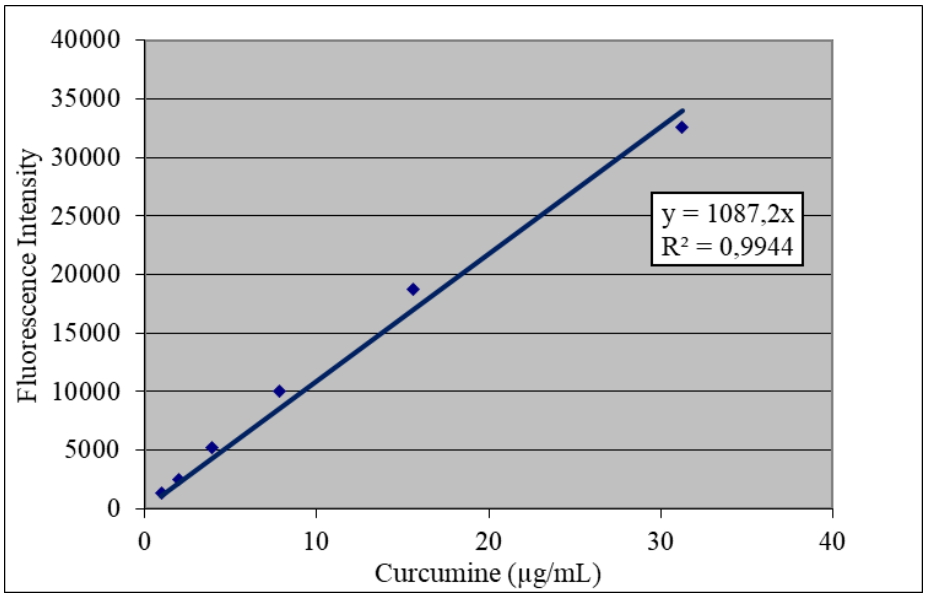

Figure 3.10: Calibration curve of Curcumin in DMSO through fluorescence measurements.

The concentration encapsulated, the encapsulation efficiency (%EE) and drug loading (%DL) of Curc in the lipidic matrix are presented in table 3.4.

Table 3.4: Amount of Curc encapsulated at different concentrations and the encapsulation efficiency and drug loading in the NLCs (mean ±SD, n = 3). Due to the high coefficient of variation (CV ≥ 20 %) found in the measurements for the formulation 25Curc its results were discarded.

$[Curc]_{Total}$ (µg/mL)	$[Curc]_{Encapsulated}$ (µg/mL)	$\%EE_{Curc}$	$\%DL_{Curc}$
100	27.52 ± 2.76	86.2 ± 1.4	0.275 ± 0.028
50	**13.54 ± 0.89**	**86.5 ± 0.9**	**0.135 ± 0.009**
10	2.87 ± 0.15	85.7 ± 0.8	0.029 ± 0.002
0	0	0	0

Both formulations 50Curc-NLC and 100Curc-NLC showed to have the highest %EE, for the last formulation the concentration of Curc encapsulated was low when compared to the total amount of Curc in solution upon the formation of the nanoparticles. As such the formulation with $[Curc]_{Total}$ = 50 µg/mL was chosen to proceed with the adsorption of HAEye (0.04 %) and CZ as well as further tests.

3.2.2 Ceftazidime Adsorption

3.2.2.1 Characterization of CZ-loaded HyLNP

The adsorption of 0.04 % (w/v) of HAEye containing CZ in two different concentrations (5 and 2.5 mg/mL) was evaluated. Data from the properties of Curc-loaded and empty NLCs are shown in figure 3.11.

ζP changes to negative values in the presence of HAEye and the presence of CZ did not significantly change ($p \geq 0.05$) the surface charge of the hyLNPs in all tested formulations.

The addition of CZ in both concentrations did not significantly change ($p \geq 0.05$) the size when compared with empty hyLNPs. However, the size is significantly ($0.01 < p < 0.05$) different when HAEye and CZ were adsorbed to Curc-loaded nanoparticles with mean sizes of 524.0 ± 117.9 nm and 537.1 ± 38.8 nm for the formulations 50Curc-5Ceftz-hyLNP and 50Curc-2.5Ceftz-hyLNP, respectively.

It can be observed for the concentration of CZ at 5 mg/ml both CZ-Curc-loaded and CZ-loaded hyLNPs' size distribution showed no significant changes ($p \geq 0.05$) when compared with empty hyLNPs.

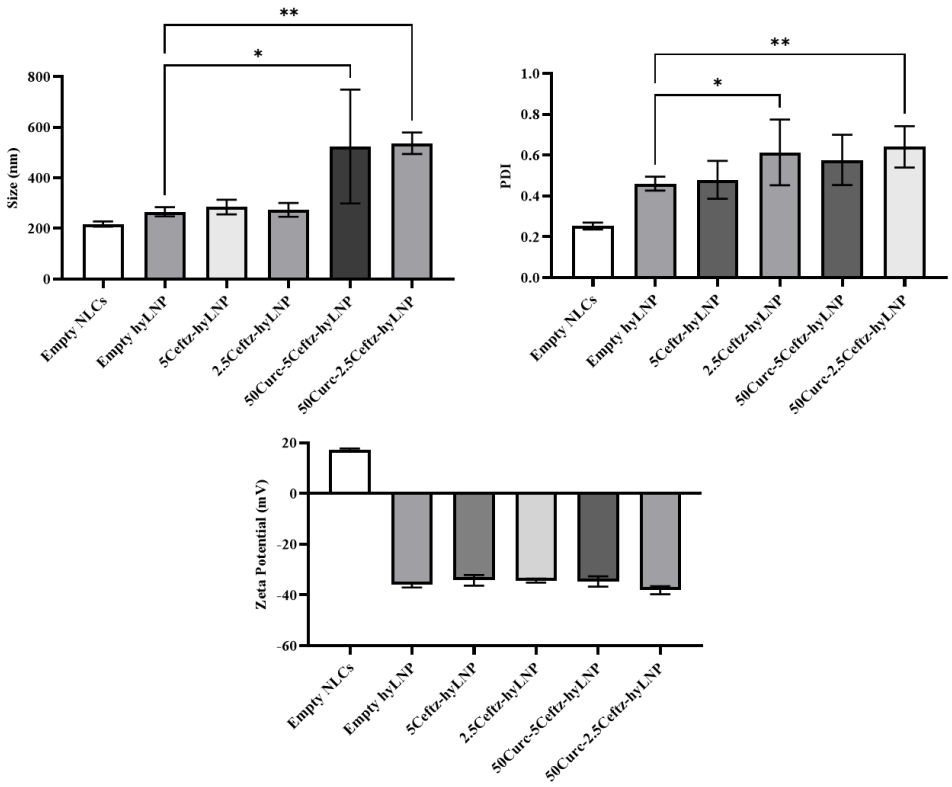

Figure 3.11: Effect of CZ adsorption at with the concentrations of 5 and 2.5 mg/mL in the physicochemical characteristics of Curc-loaded and empty hyLNPs. Results in terms of size (nm), PDI and ζP (mV) (mean ±SD, n = 9), (* $0.01 < p < 0.05$, ** $0.001 < p < 0.01$).

As such a secondary formulation was produced using the same batch of HAEye and the same methods with CZ adsorbed at 5 mg/mL (Figure 3.12). This secondary formulation showed to produce hyLNPs with significantly smaller sizes ($p < 0.0001$) when compared with the empty formulations (256.2 ± 6.0 nm) without significant ($p \geq 0.05$) difference in the surface charge or the size distribution of the hyLNPs. As such this formulation was used for further tests.

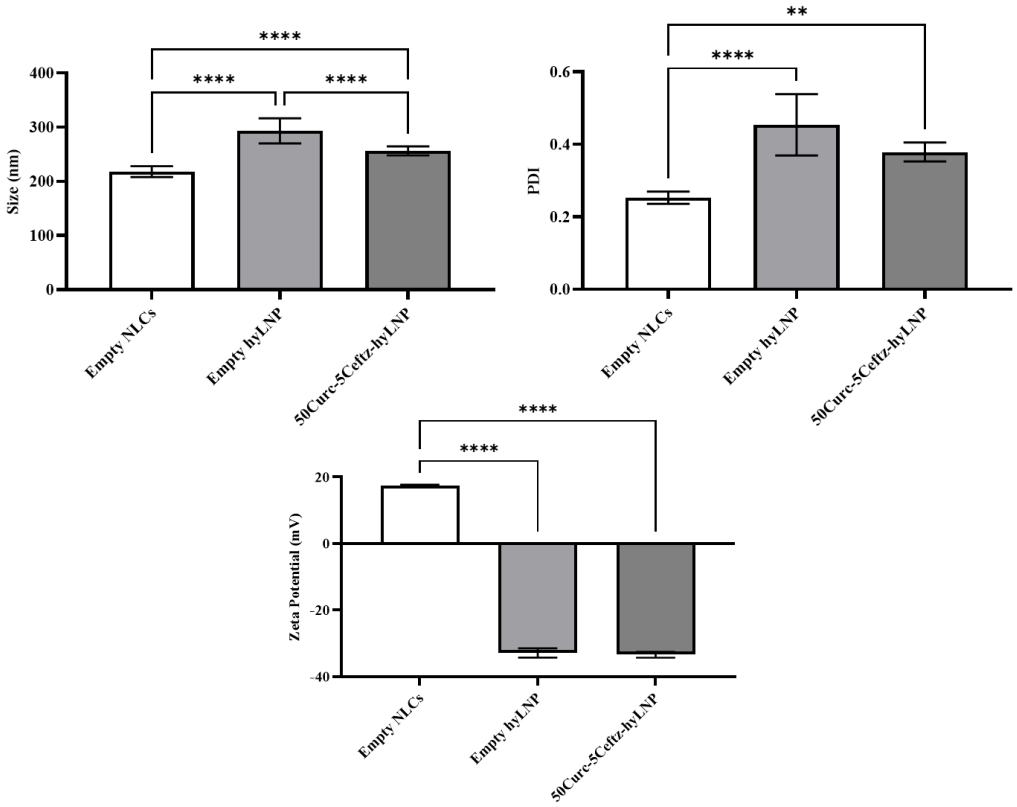

Figure 3.12: Effect of CZ adsorption at with the concentrations of 5 mg/mL in the physicochemical characteristics of Curc-loaded hyLNPs. Results in terms of size (nm), PDI and ζP (mV) (mean ±SD, n = 9), (** 0.001 < p < 0.01, **** p < 0.0001).

The preparation of CZ-loaded hyLNPs has successfully produced nanoparticles with the targeted characteristics for topical eye administration, successfully adsorbing HAEye at 0.04 % (w/v) without much variation in the size and PDI and maintaining the stability of the colloidal solution.

3.2.2.2 Adsorption Efficiency and Drug Loading of CZ

In order to determine the %AE and %DL of CZ in the different formulations, a calibration curve (Figure 3.13) for the CZ in an aqueous solution was determined at λ_{CZ} = 310 nm and used to determine the concentration of adsorbed CZ in the hyLNPs. The UV-Vis spectrum of CZ is also shown in figure 3.13.

To determine CZ's %AE and %DL, empty and loaded hyLNPs were subjected to ultrafiltration using membranes with a cut-off of 300 kDa which allowed the separation of CZ free in solution from the CZ adsorbed to hyLNPs' surface and the determination of %AE without the interference of the empty hyLNP.

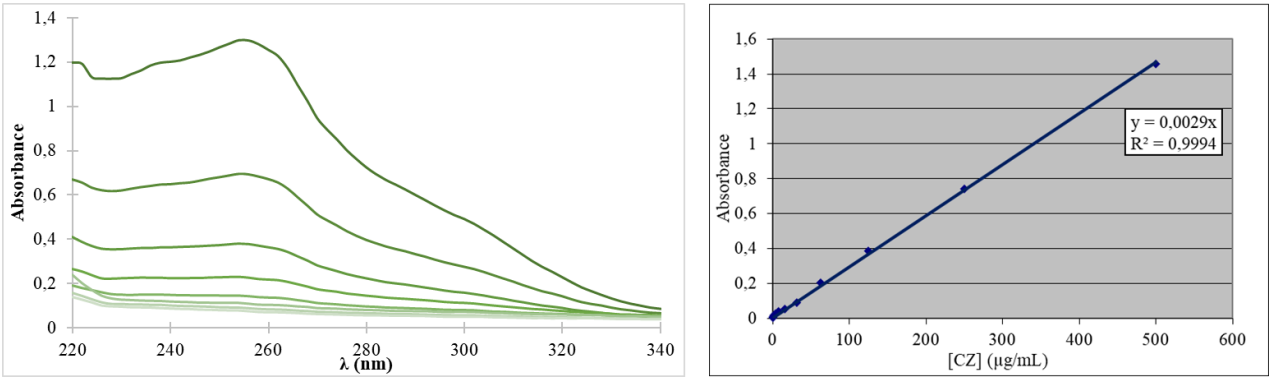

Figure 3.13: CZ's UV-Vis spectrum in aqueous solution (left) and calibration curve for CZ in aqueous solution (right), in descending concentrations of 125.0, 62.5, 31.3, 15.6, 7.8, 3.9, 2.0, 1.0 mg/mL

The concentration of Curc encapsulated, the concentration of CZ adsorbed, the adsorption efficiency (%AE) and drug loading (%DL) of CZ in the surface of hyLNPs are presented in table 3.5.

Table 3.5: Amount of CZ adsorbed at 5 mg/mL, the adsorption efficiency and drug loading in the hyLNPs (mean ±SD, n = 3).

$[Curc]_{Total}$ (µg/mL)	$[CZ]_{Total}$ (mg/mL)	$[CZ]_{adsorbed}$ (µg/mL)	$\%AE_{CZ}$	$\%DL_{CZ}$
50	**5**	**201.8 ± 47.0**	**48.4 ± 7.9**	**2.0 ± 0.3**
0	5	253.6 ± 8.0	58.5 ± 1.3	2.4 ± 0.1

It was observed that at 5 mg/mL CZ can be found to efficiently adsorb to the hyLNPs' surface with an efficiency above 50 % and a drug loading of ≥ 2.0 %. For the formulations with CZ at 2.5 mg/mL, the absorbance measurements were inconclusive due to the lack of adequate replicates of this formulation to determine the $[CZ]_{adsorbed}$ even after several ultrafiltration and ultracentrifugation cycles and considering λ^{CZ}_{max} = 256 nm.

It can be concluded that the adsorption of CZ to Cur-loaded hyLNPs was successful for the formulation with the higher CZ concentration. As such this formulation was chosen for the following *in vitro* studies.

3.3 *In Vitro* Studies

3.3.1 Mucoadhesion Studies

The mucoadhesive characteristics of HAEye and CS were tested through the changes in electrophoretic mobility of the hyLNPs due to the interaction of the polymers with mucins found in the tear fluid. In this work mucin type II from the porcine stomach was used as a model of the mucins.

In an aqueous solution (Figure 3.14) mucin-type II presented anionic behaviour with a mean ζP of -15.8 ± 0.8 mV. As expected, in an aqueous solution the incorporation of CS in the lipidic core subverts

the anionic charge of the lipids used, and the following adsorption of HAEye returns the anionic characteristics of the hyLNPs.

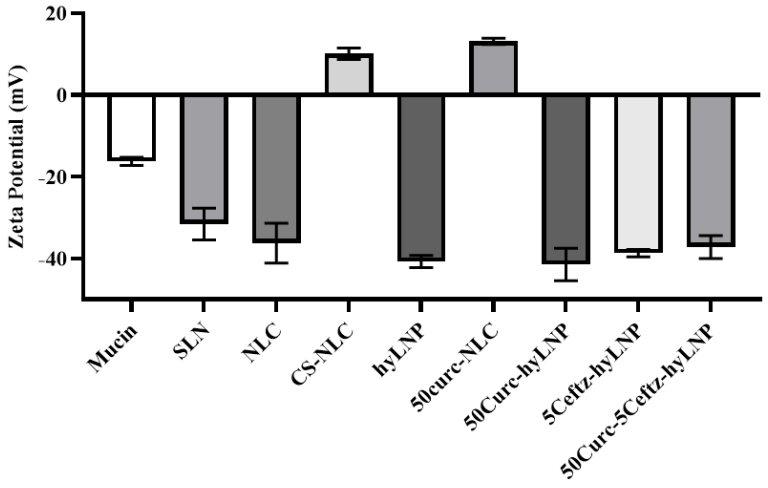

Figure 3.14: Surface charge of the several formulations produced in this work in aqueous solution. Mucin type II at 2 mg /mL in aqueous solution was used as the control solution (Mucin), in a 1:1 volume ratio.

The ζP of NPs mixed with mucin-type II solution (Figure 3.15) was significantly different ($p < 0.0001$) from nanoparticles without mucin for the 50Curc-NLC formulation.

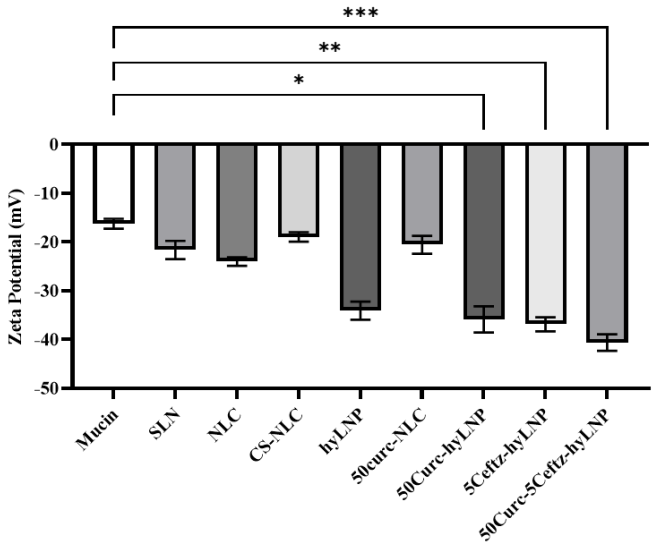

Figure 3.15: Surface charge of different formulations mixed with mucin type II at 2 mg/mL, (* $0.01 < p < 0.05$, ** $0.001 < p < 0.01$, *** $0.0001 < p < 0.001$).

No significant differences in ζP ($p \geq 0.05$) were observed between the CZ-Curc-loaded hyLNP in water and when incubated with mucin (Figure 3.16).

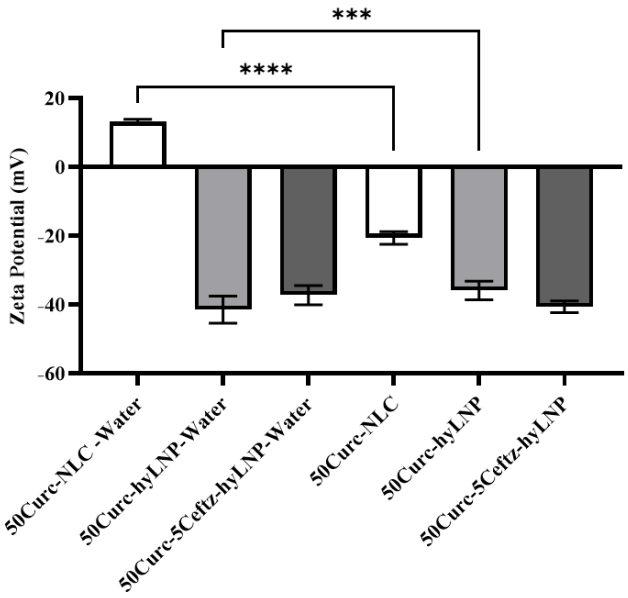

Figure 3.16: Surface charge changes between the several hyLNPs produced in aqueous solution (X-Water) and when incubated with Mucin, (*** 0.0001 < p < 0.001, **** p < 0.0001).

3.3.2 Drug Permeation Studies

The permeation of Curc and CZ from the formulations was evaluated using Franz-type diffusion cells with polyvinylidene difluoride (PVDF) membranes. Data from the permeation through membranes over time is presented in Figure 3.17 for the 50Curc-5CZ-hyLNP formulation, with approximately 60 % of CZ permeating in the first hour and completely permeated within the 2 hours of the study. Curc on the other hand presented a more sustained permeation with 40 % permeating within the first hour and complete permeation was reached in the second hour.

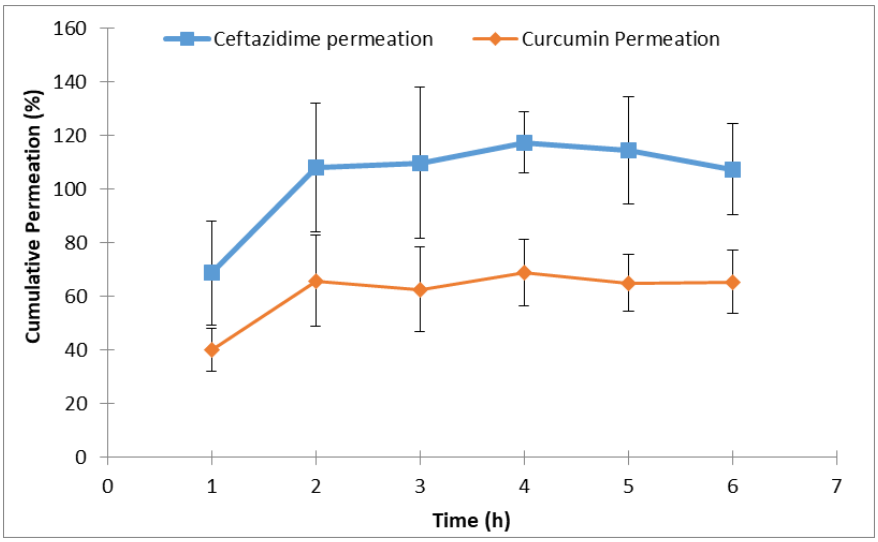

Figure 3.17: Cumulative permeation profile of CZ (□) adsorbed on to hyLNPs' surface and encapsulated Curc (◊) in 10 mM PBS pH 7.4 in a 1:1 ratio with EtOH through PVDF membranes at 37 ºC (mean ± SD, n=8).

3.3.3 Cell Uptake of HyLNP

The cellular uptake of Curc-loaded NLCs, Curc-loaded hyLNPs and Curc-CZ-hyLNPs by the ARPE-19 cell line was observed by fluorescence microscopy. For that cells were stained with different fluorophores for nuclei (DAPI-blue), plasma membrane (Phalloidin-red) and Curcumin (Nanoparticles-green), the results are shown in Figure 3.18.

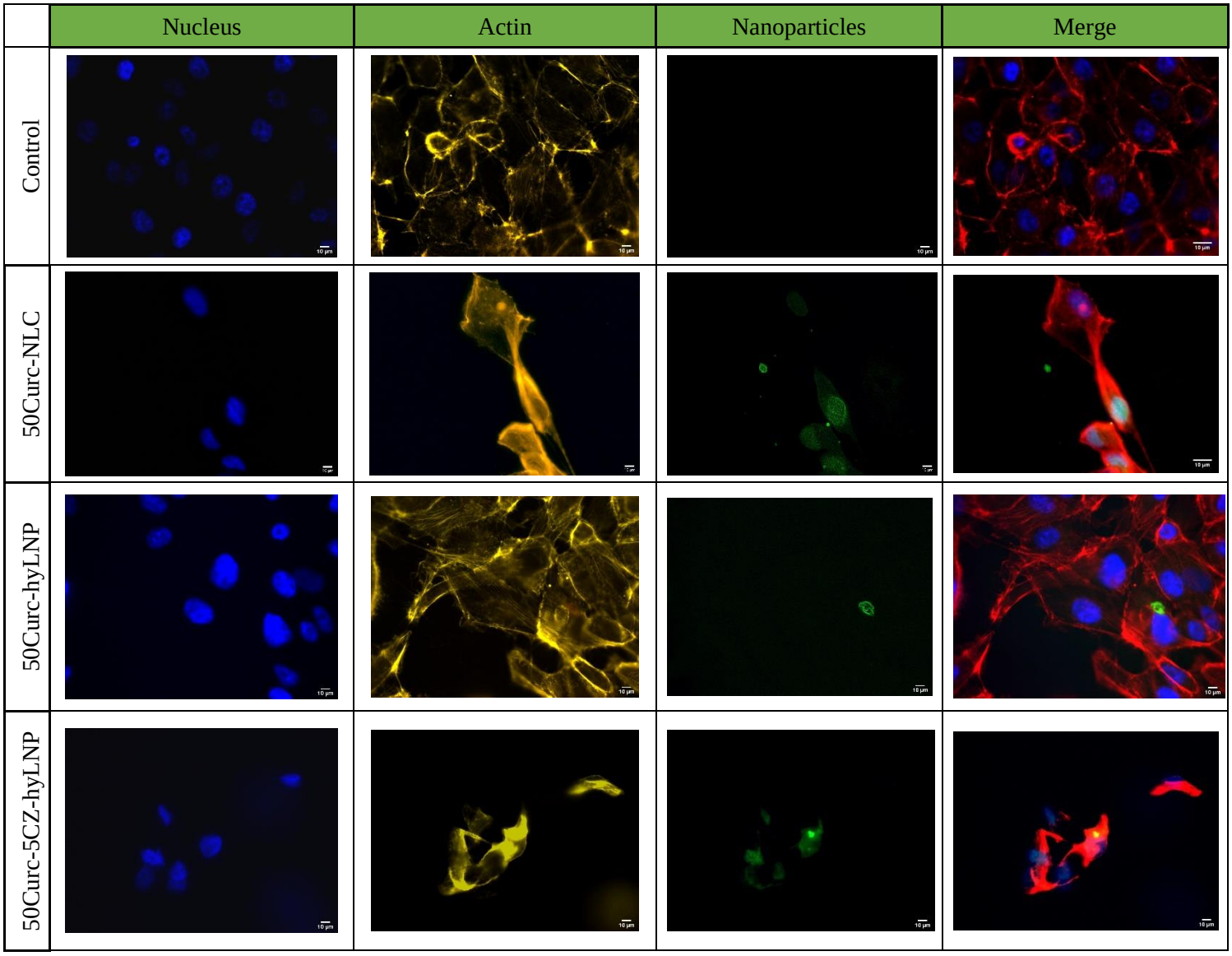

Figure 3.18: Drug loaded NLC and hyLNPs' cellular uptake in ARPE-19 cell line observed under confocal microscopy. Fluorescence microscopy images using 100x amplification. The blue and yellow stains represent the nuclei and plasma membranes of the cells, respectively. Curcumin loaded nanoparticles are represented in green. In the last column a merge of the images is presented.

All formulations, as shown from pictures in figure 3.18, with nanoparticles loaded with either Curc and CZ or just Curc were able to be internalized by ARPE-19 cells.

A further quantitative uptake assay was done using four different concentrations of the 3 formulations tested in the fluorescence microscopy (Figure 3.19). It can be observed that the association of the nanoparticles to the cells is concentration dependent, however, no significant differences ($p \geq 0.05$) were found between the different formulations tested at the same concentrations except at 100 µg/mL of the total amount of nanoparticles in which very significant differences ($0.001 < p < 0.01$) were observed upon the addition of HA of 300 kDa to the formulations with a higher amount of nanoparticles associated to the cells for the formulations 50Curc-hyLNPs and 50Curc-5CZ-hyLNPs.

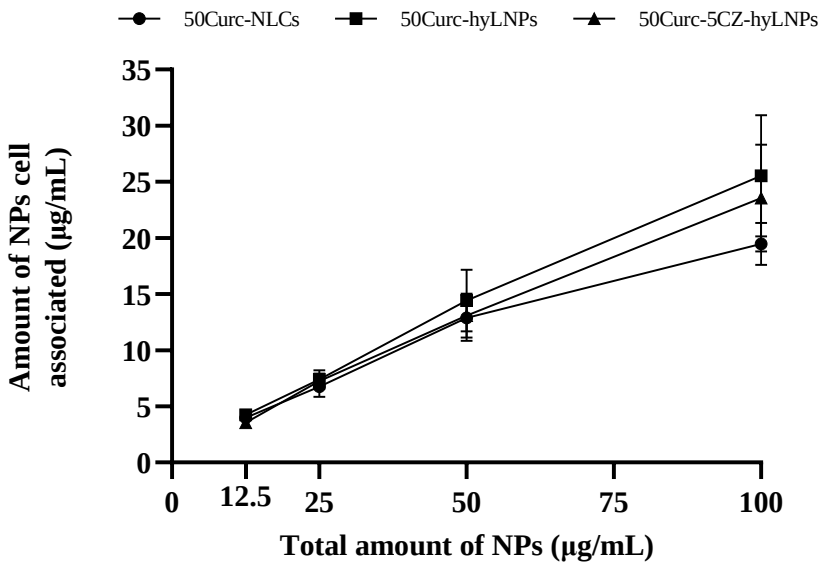

Figure 3.19: Quantification of nanoparticle uptake by fluorescence. The cells were exposed to Curc loaded nanoparticles and to hyLNPs with and without being loaded with CZ. The nanoparticles' concentrations tested were of 12.5, 25, 50 and 100 µg/mL (mean ±SD, n = 8).

3.3.4 Cell Viability Studies

The potential cytotoxicity of both empty hyLNPs and drug loaded hyLNPs was assessed using the MTT reduction assay to evaluate the cell viability of the ARPE-19 cell line, after the incubation of the different formulations at 500 µg/mL (Figure 3.20).

Results show that, although a significant ($0.01 < p < 0.05$) decrease in cell viability was observed for some of the formulations differing in Curc concentration (Figure 3.20, A), for the final chosen Curc concentration of 50 µg/mL, no significant ($p \geq 0.05$) cytotoxicity (61.4 ± 6.8 % of cell viability) was observed when compared with the culture's medium.

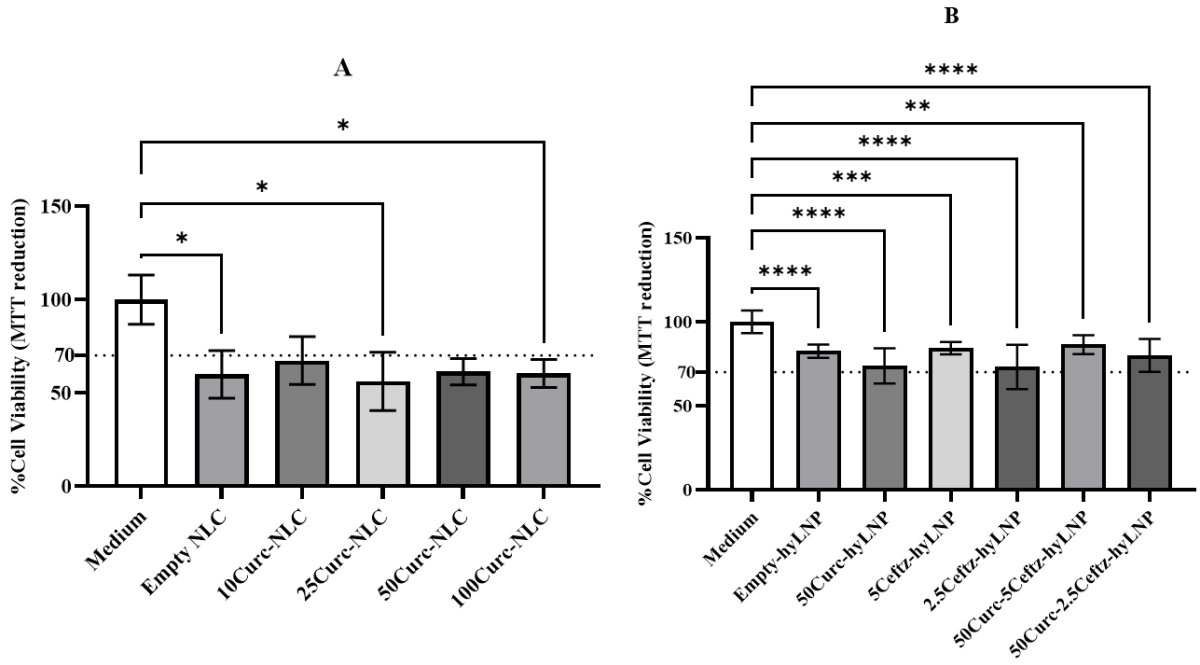

Figure 3.20: Cell viability of ARPE-19 cell line after exposed for 24h (mean ± SD, n=6) to 500 µg/mL of Curc-loaded NLCs **(A)** and hyLNPs **(B)**. Dashed lines represent a cell viability of 70%. (* $0.01 < p < 0.05$, ** $0.001 < p < 0.01$, *** $0.0001 < p < 0.001$, **** $p < 0.0001$).

It was observed that upon HA adsorption the formulations showed a very significant difference in cell viability ($0.001 < p < 0.01$) when compared to the culture medium.

3.3.5 Activity Assays

3.3.5.1 Antioxidant Activity of Curc-Loaded NPs

The ability of Cur-loaded NLCs to reduce the intracellular oxidative stress in ARPE-19 cells was followed using H2DCFDA fluorescence. The results showed (Figure 3.21) that all Curc concentrations tested, present a significant reduction in the %ROS ($0.01 < p < 0.05$) after 24 h of exposure when compared with the control culture medium.

The highest % ROS reduction was obtained in the 50Curc-NLC and 100Curc-NLC formulations at 60.4 ± 2.6 % and 58.4 ± 4.8 %, respectively, when compared with the negative control culture medium.

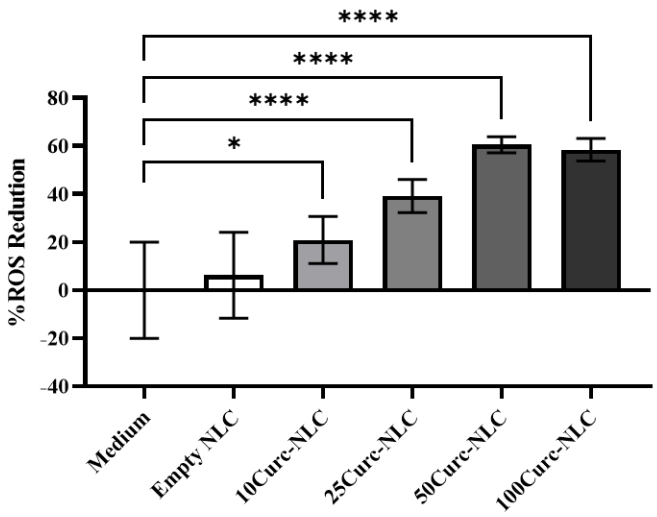

Figure 3.21: Percentage of the reduction in production of reactive oxygen species. ARPE-19 cells were exposed for 24h to Curc-loaded NLCs with differing concentrations of the antioxidant (10, 25, 50 and 100 µg/mL) (mean ± SD, n= 18), (* $0.01 < p < 0.05$, **** $p < 0.0001$). Oxidative stress was induced by adding 500 µM of H_2O_2 and it was used as the negative control (Medium).

3.3.5.2 Determination of Antimicrobial Activity of CZ

The susceptibility of *P. aeruginosa* to CZ free in solution or adsorbed to the hyLNPs was assessed by the microtiter plate antibacterial assay (Tabel 3.7). The minimum inhibitory concentration determined for CZ-loaded hyLNPs was found to be a lower concentration of 1.42 µg/mL for both tested formulations with and without Curc.

Table 3.6: Antimicrobial activity of free CZ, Curc-CZ loaded hyLNPs, and CZ loaded hyLNPs (*P. aeruginosa*) (Mean ± SD, n=4).

Formulation	Minimum inhibitory Concentration (MIC) (µg/mL)
Free CZ	1.95
Curc-CZ loaded hyLNPs	1.42
CZ loaded hyLNPs	1.42

4. Discussion

The design and development of a novel lipid core/polymer shell hybrid nanoparticle system with dual mucoadhesive and permeation enhancing properties aiming to interact with the mucosal barrier in the ocular tissues is described in the present work. Lipid-polymer hybrid nanoparticles, a merge of advantages of a lipidic core and polymeric shell, are becoming promising carriers for the delivery of drugs by topical application as they encapsulate drug molecules with a high encapsulation efficiency and the low cytotoxicity provided by the lipids and the mucoadhesive properties of polymers combined with their inherent small particle size can increase ocular bioavailability and permeation of the drugs in ocular tissue.

4.1 Formulation and Physicochemical Characteristics of HyLNPs

The chosen lipids and surfactants used in the formulation of SLNs and NLCs can alter their physicochemical properties, as such, the optimization of the formulation of the SLNs and NLCs is important for drug delivery.

Solid lipid nanoparticles (SLNs) and nanostructured lipid carriers (NLCs) provide several advantages to drug delivery to ocular tissues, including good biocompatibility, low cost of production and easy scale up and high drug loading efficiency [53,122]. The selection of PF68 as a surfactant and Precirol® as the lipid phase, in previous studies [123], showed to produce nanoparticles with adequate size, PDI and zeta potential for ocular delivery.

Alongside the selection of its constituents, lipidic nanoparticles can be produced using different formulation techniques such as sonification, solvent evaporation and hot high-shear homogenization which have a direct effect on the nanoparticles' size and PDI [124], with higher rotations producing smaller size particles and smaller PDI [123]. In the present work, all hyLNPs formulations were prepared by HHSH, as it allowed the production of nanoparticles with both size and polydispersity index in the range adequate for its application [36], the modulation of these parameters can be done by changing the rate and the time of homogenization. Furthermore, this method is free of organic solvent which allows for improved production and safety in the development of hyLNPs. As such, HHSH was the preferred method in hyLNPs' production in this work [123].

4.1.1 Formulation of HyLNPs

4.1.1.1 The Effect of Polymers

The addition of natural polymers such as CS, ALG and HA to the lipidic core, incorporated in the surfactant solution or adsorbed at its surface is a promising strategy for ocular drug delivery as they can enhance ocular penetration and drug bioavailability through their mucoadhesive characteristics [27,56].

Chitosan is a biodegradable polymer which presents strong mucoadhesive properties due to its polycationic nature that allows it to interact with the mostly anionic ocular surface through hydrogen and ionic bonding [37]. Additionally, CS is a permeation enhancer being able to transiently open the tight junctions between epithelial cells [125].

The incorporation of this polymer into the lipidic core showed that the modulation of the nanoparticle's size is concentration dependent with up to 0.05 mg/mL CS in the aqueous phase (Figure 3.1). With this concentration and using the HHSH method for the production of the nanoparticles, it allows for the production of a suitable nanoparticulate system with size and PDI for ocular drug delivery in line with data presented previously in the literature [17,126]. LMW CS helped to reduce the size and PDI of the nanoparticles when compared with CS with a higher molecular weight [127].

At a lower concentration, the addition of CS led to an apparent aggregation that can be justified by the low ζP in these formulations (Figure 3.1), the values in the range of - 20 mV to + 20 mV considered those which provide stable colloidal formulations [115]. With the incorporation by adsorption (Figure 3.2) of CS in the formulation, it is also observed that size is a function of the polymer concentration dependency but resulting in higher values (> 190 nm) than those obtained by the incorporation of 0.05 mg/mL of chitosan in the aqueous phase.

As such the best compromise was observed when the chitosan at 0.05 mg/mL is integrated into the aqueous phase with the surfactant PF68 at 0.1 % during the production step of the lipidic cores.

The biocompatible HA is a promising excipient for ocular delivery due to the mucoadhesive properties of the D-glucuronic acid monomers which bind to the sialic acid present in the mucins of the eye. Furthermore, the specific and reversible binding to cellular receptors in the corneal epithelium such as the CD44 receptor would allow nanoparticles, with HA adsorbed in their surface, to be internalized via endocytosis [64]. These properties depend, among other factors, on the molecular weight of HA and of pH of the solutions [73]. In this work, the size and PDI characteristics of the NPs did not seem to be influenced by the tested HA's molecular weights (50 and 300 kDa) when compared with the control formulations ($p \geq 0.05$) (Figure 3.3). These results are corroborated with previous studies as Silva et al. 2020 [36] found that the molecular weight of HA in EPOβ loaded CS/HA nanoparticles did not seem to increase or decrease the size of the PDI of the nanoparticles.

The choice of ophthalmologic grade hyaluronic acid with the molecular weight of 300 kDa over the 50 kDa was therefore made due to the increase in the number of binding moieties to the CD44 receptors with the increase of the MW of the polymer [73], in turn, increasing the internalization of HA coated nanoparticles in the cells of the cornea epithelium.

The sodium salt of alginic acid is a biocompatible and bioadhesive co-polymer whose adhesive properties vary depending on the M/G ratio of its residues in which the α-1, 4-L-guluronic acid residues provide this characteristic through weak electrostatic interactions with calcium ions present in the tear solution [38,75].

In this work, it was observed that at lower concentrations the different M/G composition of ALG in the aqueous solution did not show to influence the nanoparticle's size and PDI (Figure 3.4) when compared with the stearylamine-SLNs ($p \geq 0.05$) producing nanoparticles with good characteristics (164.3 ± 3.1 nm, 0.314 ± 0.011).

The higher size and PDI observed in the formulation with ALG 60%M|40%G at 0.1 % (w/v) can be explained by the high content of the α-1,4-L-guluronic acid (G) residue, this is known to result in particles with larger size and PDI [128], however, including the ratio, molecular weight of the polymer also affects the nanoparticles' size which could explain the bigger nanoparticles produced with a higher M/G ratio of the formulation 60%M|40%G at 0.1% (w/v).

4.1.1.2 The Effect of Permeation Enhancers

Although mucoadhesive polymers such as chitosan, hyaluronic acid and alginic acid enhance the retention time of the drug carrier in the cornea epithelium and conjunctiva, a second alternative to enhance the bioavailability is the use of permeation enhancers (PE) [92]. Bile salts are known to increase drug permeability by disrupting cell-cell junction and allowing the permeability of drugs via the paracellular route [129]. In this work, the bile salts SC and SD were tested for their influence on the lipid cores' physicochemical characteristics as sole surfactants and co-surfactants with PF68.

In this work SC at 1.0 % (w/v) and SD at 0.5 % (w/v) as sole surfactants were unable to provide enough stabilization for the lipid cores leading to the formation of higher sized nanoparticles (Figure 3.5). This could be due to the small-sized polar carboxylate anion (COO^-) and hydroxyl (OH) groups found in bile salts' chemical structure (Figure 3.6) which although give them amphiphilic propriety shown to be ineffective as sole stabilizer agents for lipidic nanoparticles formulation [130, 131]. Previous studies made by Talele, Sahu, and Mishra 2018 [132] using the same bile salts, found that the variation in concentration can yield SLNs with the particle size of 200 – 800 nm range with an increase in bile salt concentration leading to an increase in SLNs' size due to intermolecular interaction of the hydroxyl groups of the bile salts on to the SLNs' surface causing their coalescence.

Interestingly SC at 0.5 % (w/v) as the sole surfactant on the other hand was in line with previous studies [132] producing SLNs with appropriated sizes intended for nanoparticular systems (Figure 3.5) and, presenting no significant differences ($p \geq 0.05$) in size when compared with SLNs within the suitable range of 50 – 400 nm for topical ocular delivery [29,36].

When added with PF68, bile salts showed no significant changes to the mean size of the produced nanoparticles ($p \geq 0.05$) with the formulations presenting the sizes of 351.5 ± 7.8, 149.7 ± 4.3 and 325.2 ± 29.8 nm for SD 0.5 % (w/v), SC 0.5 % (w/v) and SC 1.0 % (w/v) respectively (Figure 3.5). It can be observed that similarly with formulations with SC as the sole surfactant as a co-surfactant, nanoparticles' size seems to be dependent on the bile salt's concentration, furthermore, comparing SD and SC at 0.5 % (w/v), the latter when in combination with PF68 showed to produce similar sized nanoparticles as the control formulations. As such this formulation was chosen for further studies, with SC as the permeation enhancer for the SLNs produced in this work.

4.1.2 Formulation Optimization

Having tested the components for their individual influence on SLNs' physicochemical characteristics the proceeding optimization steps were taken to efficiently encapsulate Curc in the SLNs' cores and adsorb CZ onto the polymeric shell while maintaining the hyLNPs' size, PDI and ζP appropriated to ocular drug delivery [29,132] as well as their mucoadhesive and permeation enhancing properties.

Firstly, the solubility of Curc in the lipidic core was tested. Since Curc's water solubility under acidic and neutral pH conditions is relatively low (0.6 μg/mL) [133], it can be a limiting factor for this molecule's therapeutic potential. As such, its encapsulation into lipidic cores would further aid in its bioavailability and allow Curc to become a viable therapeutic agent for the treatment of ocular diseases. Since the size of the lipidic cores is dependent on the lipid concentration in the organic phase [134] it is of interest that Curc can be easily dissolved in the least lipid concentration.

Curc demonstrated low solubility in all the different solid lipids tested except Imwitor® 988, a partial ester of caprylic acid and glycerol used in topical preparations [135], however, the high amount of lipid required to solubilize Curc would lead to nanoparticles with bigger sizes [134] and was, therefore, improper for topical eye delivery and, as such, this lipid was discarded alongside all solid lipids.

The results (Table 3.1) show that Curc has low solubility in most of the solid lipids and high solubility in the liquid lipids, with Trascutol® P being chosen due to it being able to solubilize the highest amount of Curcumin with the lowest amount of lipid needed.

The resulting NLCs were able to maintain physicochemical characteristics (Table 3.2) similar to those found in SLNs appropriated for ocular drug delivery [132].

Upon the addition of chitosan in the aqueous solution with the bile salt, NLCs showed to precipitate in solution even with the formulations showing high anionic ζP which would indicate a stable colloidal solution (Figure 3.7). Therefore, the formation of the precipitates couldn't be due to low electrostatic interaction between the nanoparticles in solution nor the critical micellar concentration of SC was reached, a value which is around 11–18 mM [136] in aqueous solution, as such, the precipitates could have appeared due to the possible excess of SC interacting with CS forming and CS-SC complexes [137] during the cooling step of the HHSH method through the electrostatic interaction of the carboxyl group of the bile salt and the primary amine group (pKa 6,5) present in the polymer [138,139]. Successful integration of bile salts in CS nanoparticles has been previously described by Hashem et al. 2019 [137] developing gene-loaded CS-SD nanoparticles with mean particle sizes from 96.5 ± 11.3 to 405.0 ± 46.4 nm.

As such, and since CS has itself been described to present permeation enhancing characteristics by, opening tight junctions between epithelial cells [70], the further use of bile salts as permeation enhancers was discarded in this work.

The final optimized formulations, therefore, were formed with a lipidic core with an irregular matrix able to encapsulate lipophilic drug molecules such as Cur and a polymeric permeation enhancer incorporated in the nanoparticles, these NLCs presented small mean size of 217.8 ± 5.4 nm and a small PDI of 0.251 ± 0.014 and a mean positive surface charge of + 17.1 ± 0.4 mV (Table 3.3) originating from the cationic amine groups of CS [18,66,67]. Despite formulating SLN and not NLCs, Sandri et al. 2010 [140] presented similar results in CS-Precirol® SNLs produced by high shear homogenization, showing sizes between 200 to 290 nm and higher PDI while using higher concentrations of CS than those presented in this work although with a higher PDI than that achieved in this work.

The subsequent adsorption of HAEye (300 kDa) to the lipidic cores slightly increased the size from 217.8 ± 5.4 nm to 241.4 ± 3.3 nm and an expected negative surface charge of - 26.6 ± 1.2 mV (Table 3.3), the adsorption of HA to the NLCs' surface can be mainly attributed to the hydrogen bonds and electrostatic interactions between the oppositely charged CS and HA.

Although using a strictly polymeric nanoparticulate system of CS/TPP/HA, B. Silva et al. 2020 [36] demonstrated similar results in the size and PDI characteristics in formulations with a 1:1 ratio of LMW CS/HAEye, however, in this work a shift in ζP from positive to negative upon the addition of the anionic polymer was observed which was not observed by B. Silva et al. 2020 [36], this shift is important as it can be an indicator of successful adsorption of HAEye to the NLCs' surface.

4.2 Encapsulation/Adsorption Efficiency and Drug Loading

4.2.1 Curcumin Encapsulation

Due to its lipophilic nature, Curc was chosen to be the model lipophilic drug to be encapsulated inside the lipidic matrix. As such, in this work, the molecule was added to the lipidic phase in several different concentrations in order to test their potential to alter the physicochemical characteristics of the NLCs. It was observed that the encapsulation of Curc in NLCs did not significantly impact the size at the smaller Curc concentrations maintaining it between 200 – 270 nm nor it had a significant impact on the PDI of the lipid cores (Figure 3.8). These results are in line with previous reports by, Sun et al. 2013 [117], reporting the successful formulation of Curc-loaded NLCs presenting small particle sizes and a narrow particle size distribution.

On dilution in DMSO, Curc presented an absorbance peak at 435 nm (Figure 3.9), comparable with previous values reported [141]. Spectroscopic determination of Curc concentration was done initially by UV-Vis spectroscopy and fluorescence spectroscopy, however, owing to the latter's increased sensibility and specificity as well as due to the low concentrations of Curc used in this work, fluorescence measurements were used to determine Curc concentration in solution for the determination of the %EE and %DL. The direct method of ultracentrifugation showed to be suitable as it provided a fast way to measure the concentration of Curc encapsulated in the lipid cores while avoiding the interference presented by the excess Curc and empty NLCs suspended in solution.

It was observed that in all concentrations, NLCs can efficiently encapsulate Curc with percentages above 85 % and a high drug loading (Table 3.4). These percentages are justified due to the presence of the liquid lipid Transcutol® P which readily solubilizes Curc in the irregular matrix formed by the lipid phase. It was further observed that there is a limit to the amount of Curc able to be encapsulated in the lipid matrix as with the highest Curc concentration, 100Curc-NLC, although a high %EE was obtained, the total amount of drug encapsulated was 27.52 ± 2.76 µg/mL out of the total 100 µg/mL dissolved in the lipid phase. Sun et al. 2013 [117] also reported similar high encapsulation efficiencies, of > 90 %, and high drug loading percentages of Curc in their Curc-loaded NLCs formulations.

These results are in line with other studies which reported NLCs to be carriers able to encapsulate high amounts of lipophilic drugs. This high encapsulation found in NLCs, similarly to the SLNs, is mainly due to the degree of crystallization of the lipid core, on the length of the chains of the fatty acid glycerides, and the addition of liquid lipids which increases the imperfections better accommodating the encapsulated drug molecules in the crystal matrixes [34,53-55]. These characteristics allow the accommodation of Curc in the lipid cores of the NLCs with a high encapsulation efficiency and drug loading.

4.2.2 Ceftazidime Adsorption

The cephalosporin ceftazidime prevents the synthesis of a cell wall on the part of gram-positive and gram-negative bacteria this is of interest for the treatment of ocular pathologies with a bacterial origin, however, its high instability in aqueous solution is its main drawback with previous studies showing a maximum storage period of 5 days at 7 ºC before degrading to pyridine [142], as such this instability inhibits its use in ocular delivery.

The adsorption mechanisms of CZ onto nanoparticles' surface are not yet known, however, it's a structure (Figure 4.1) containing double bounded carbon atoms as well as the carbonyl and amino groups these groups may participate in π binding complexes and hydrogen bonding respectively [143], which in turn may provide enough stabilization for the antibiotic to be viable for topical ocular delivery. This adsorption to nanoparticulate systems and combined with the use of mucoadhesive polymers such as CS and HA which allows the interaction with the mucus layer could allow the increase in bioavailability of this antibiotic in the ocular tissue and improve its stability under storage conditions.

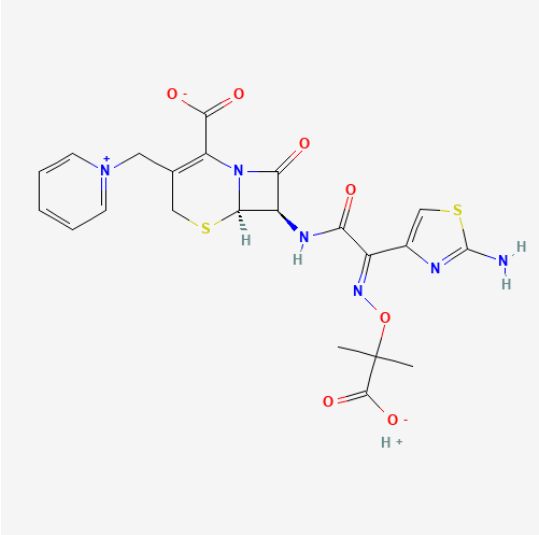

Figure 4.1: Chemical structure the antibiotic ceftazidime. Publicly available at Pubchem [144].

As with Curc-loaded NLCs the adsorption of CZ to hyLNPs' surface was evaluated in terms of the effect on the size, PDI and ζP characteristics. It was observed that the adsorption of the antibiotic CZ at a concentration of 5 mg/mL to the empty hyLNPs' surface did not show significant ($p \geq 0.05$) differences in the size and nanoparticles' size distribution of the HA/CS-lipid hybrid nanoparticles (Figure 3.11). Upon the addition of Curc, however, hyLNPs of higher sizes (Figure 3.11) were formed upon the simultaneous adsorption of HA and CZ to the lipid cores, this could be due to the hydration of hyaluronic acid in the batch used, leading to the crosslink between the chains of the polymer and its swelling, this, in turn, could have increased the size of the nanoparticles upon the adsorption step [145,146].

Upon production of a second formulation with a batch of HAEye of equal molecular weight and using the same methods of production this second formulations showed the adequate characteristics for ocular delivery [132]: high negative ζP of - 33.3 ± 0.5 mV that provides electrostatic stabilization [115], a size of 256.2 ± 6.0 nm, within the dimensions of 50 - 400 nm [29,36] and a narrow size dispersity of 0.386 ± 0.013 (Figure 3.12).

The adsorption efficiency of CZ-Curc-loaded hyLNPs, determined as described in section 2.2.2, as shown a median AE % slightly above the 50 % for the maximum concentration tested, this is not as those results found by B. Silva et al. 2020 [36], which efficiently encapsulated CZ in CS/TPP/HA polymeric nanoparticles with an EE% of 78.4 ± 1.0 % (Table 3.5). The median AE % found can be due to electrostatic repulsion between CZ and the exposed CS chains at the NLCs' surface, since both CZ and LMW CS are positively charged owned to a quaternary ammonium (pKa 4.02) and primary amine groups (pKa 6,5) respectively. These characteristics could in turn provoke some electrostatic repulsion negatively impacting the AE % of CZ onto the hyLNPs, however, this repulsion in turn is addressed through the presence of the anionic charge presented at the surface of the hyLNPs by the HAEye allowing the adsorption of some of the CZ to the surface of the nanoparticulate system. As such the pH of the aqueous solution in which the nanoparticulate system is in suspension is of extreme importance to guarantee the efficient encapsulation and/or adsorption.

As such, in this work CZ-Cur-loaded hyLNPs were successfully obtained with adequate characteristics to ocular administration in eye drops being, a size which allows for ease of transportation through the several biological barriers present in the eye, a narrow size distribution indicating a relative homogeneous dispersion, a high negative ζP which provides stability to the colloidal dispersion through electrostatic repulsion [115] and promotes the adsorption of positively charged drug molecules. Furthermore, the drug-loaded formulations showed to encapsulate successfully and efficiently lipophilic drugs and adsorb hydrophilic molecules with pharmaceutical interest without provoking aggregation of the nanoparticulate system.

4.3 *In Vitro* Studies

4.3.1 Mucoadhesion Studies

The interaction to mucin of each change in the complexion of the formulations produced, from SLN to CZ-Curc-loaded hyLNPs, was tested in the presence of mucin by the measurement of the changes in ζP of a mucin dispersion before and after its incubation with each of the formulations. The changes in ζP of the formulations containing only CS (both CS-NLCs and 50curc-NLCs) from a mean positive charge in aqueous solution to a mean negative charge (Figure 3.14) when the nanoparticles were incubated with mucin denotes that the interaction between the amine groups of CS and the carboxylic acid groups of the sialic acid residues present in the mucin [147] happens in solution. These findings are in line with previous studies made by de Campos et al. 2004 [148] and their work with CS nanoparticles.

When mucin is incubated with hyLNPs (Figure 3.14) the increase in surface charge is to be expected as both molecules present negatively charged groups which induced an increase in the measured surface charge, however, the significant changes ($0.0001 < p < 0.001$) observed between the 50Curc-hyLNPs, in the aqueous solution and incubated with mucin, indicate a successful interaction of the HAEye (300 kDa) with the sialic acids residues of the mucins. However, in this work HA was chosen due to its targeting capabilities of HA, which stems from its binding to the CD44 receptors expressed in the cells of the corneal epithelium and endothelium, and not from its interaction with the mucins in the tear fluid [73], the determination of this interaction is secondary, but it did provide confirmation that HAEye successfully covered most of the lipid core's surface.

As such in this work, we were able to produce hyLNPs capable of binding to the mucin produced in the ocular tissue through the electrostatic interactions between the cationic chitosan and the sialic acids present in the mucin.

4.3.2 Drug Permeation Studies

In the assay of permeation using Franz-type diffusion cells, PVDF membranes were used instead of cellulose-based membranes as usual [36], as it was observed strong, irreversible adsorption of Curc was to the cellulose membranes.

As expected, the CZ permeated rapidly through the membranes and completely permeated within 2 h of the studies (Figure 3.17), since the molecules are presented at the surface of the hyLNPs through weak electrostatic interactions it is therefore readily released from the nanoparticles. This rapid but sustainable permeation is desirable for an antibiotic such as CZ allowing the immediate treatment of bacterial infections in the ocular tissues. These results are in part, in line with previous studies done by the group [36] in which an initial burst phase of CZ permeation was attributed to CZ adsorbed in the surface.

For the entrapped Curc, it was observed an initial burst release of 40 % followed by a more controlled permeation until 60 % of the Curc was permeated within the second hour (Figure 3.17) in which no further increased permeation was observed, suggesting a controlled permeation of the antioxidant from the irregular lipidic matrixes through the membranes.

These results can lead to the conclusion that hyLNPs enable the co-permeation of the two drugs enabling the quick delivery of hydrophilic antibiotics and a posterior controlled release of an anti-inflammatory and antioxidant which could be an advantage in long-term treatments.

However, to further determine the permeation enhancing capabilities of CS, *ex vivo* and *in vivo* studies using conjunctivas and corneas from fresh pig eyes could be undertaken to determine a more precise permeation of both drugs since the *in vitro* studies used in this work do not consider the biological barrier presented by the cornea [7, 10-12], furthermore, NLCs enhance permeation either by phagocytosis/endocytosis dissociation of the drug from the NLCs, further aided by the CD44 mediated internalization, or collision-mediated transfer of the drug from NLCs to the cornea [149,150], therefore, a biological model could be used to further assess the permeation provided by the mucoadhesive hyLNPs.

4.3.3 Cell Uptake of HyLNP

In this work, it was observed, by optical analysis, that, although at a low number, all drug loaded formulations were able to be internalized by the ARPE-19 cell line. The observed low number of internalized nanoparticles was most likely due to the low number of cells analysed; this in turn could be attributed as a consequence of the harsh fixating and washing steps of the multi-staining process. However, it can be observed that the Curc-loaded lipid cores seem to be more readily internalized or bounded to the cells' surface than hyLNPs coated by HAEye (Figure 3.18), this could be due to the internalization method differing from uncoated NLCs and hyLNPs whereas the latter is a receptor-mediated uptake through the CD44 receptor which means the uptake must happen at specific sites and with a smaller number of binding sites readily available at the cells' surface, therefore, limiting the amount of hyLNPs being internalized [73], on the other hand, the lipid cores making up the NLCs are readily internalized into the ARPE-19 cell lines due to being prepared using endogenous lipids such as glyceryl distearate present in the cell membrane [46].

The quantitative uptake (Figure 3.19) at different concentrations gave a better insight into the uptake of the hyLNPs, as it was observed a concentration dependency for the association of both Cur-loaded lipid cores and HA coated hyLNPs to the cells with the highest concentration of the tested HAEye showing a higher amount of hyLNPs associated to the cells with or without being loaded with 5 mg/mL of CZ.

These results show that the adsorption of the HAEye (300 kDa) polymer enhances the association of the nanoparticles that it coats to the ARPE-19 human retinal cell line at higher concentrations of the hyLNPs. It must be noted that, contrary to fluorescence microscopy, the quantitative data here presented does not necessarily correspond only to the amount of internalized hyLNPs by the cell line, since the used method does not allow the differentiation of intracellular and surface-bound nanoparticles.

The quantitative results are in line with previous studies being documented which found that SLN and NLC are promptly internalised by a wide variety of cell lines [151] including the human retinal cell line by either phagocytosis or endocytosis [149]. On the other hand, nanoparticles coated by CS or HA have also been shown to be easily internalized in cultures of the ARPE-19 cell line [152], with Zaki, Nasti, and Tirelli 2011 [153] finding a similar decrease in HA-coated CS/TPP nanoparticles' internalization in phagocytic cell models and a concentration dependency on NPs' internalization.

4.3.4 Cell Viability Studies

Although most of the constituents used for the production of the hyLNPs, both lipids and polymers have been described to produce no cytotoxicity either owning to them being endogenous to the ocular tissue such as HA or being biocompatible compounds such as CS [18,64,72], the cytotoxicity of these components needs to be determined.

In this work, within the levels proposed by the International Organization for Standardization (ISO 10993-5:2009) [154], a slight decrease in metabolic activity was observed after the culture medium was incubated with Curc-loaded CS-NLCs and empty NLCs at concentrations of 500 µg/mL (Figure 3.20). These results go against previous studies. Lakhani et al. 2018 [150] using an *in vitro* corneal hydration study observed no adverse effects in the corneal integrity upon contact with Curc-loaded NLCs for 3h with further corneal histology studies also showing no insult to the corneal epithelium or the stroma for both empty NLCs and Curc-loaded NLCs.

The concept of SLNs and NLCs being well tolerated carriers in, *in vitro* studies, is well documented [151], and therefore, we could conclude that the lipids composing the cores may not be the origin for the decrease in cell viability observed in this study, and since no scalable decrease in cell viability with the rise in encapsulated Curc concentration was observed in this work and previous works [150], the most likely cause of the cytotoxicity can be attributed to the presence of the cationic CS in the formulation. Previous studies show that this polymer is capable to induce cytotoxicity depending on its MW and degree of deacetylation (DD), with H.-S. Huang and Schoenwald 2004 [155] observing a CS dose-dependent cytotoxicity in A549 cell line (MTT reduction assay) in polymer concentrations higher than 0.741 mg/mL. This toxicity was also observed to depend more on the DD than the MW with a decrease of DD from 88% to 61% showing to attenuate the cytotoxicity of CS nanoparticles.

With these two characteristics, MW and DD, being critical in both physical and biological properties as well as for the NPs' formulation, studies are required, in the formulation of nanocarriers, to determine the possible cytotoxicity provoked by the inclusion of mucoadhesive polymers such as CS of a cationic nature for topical administration to the eye, even if such compounds are widely considered to be biocompatible [65].

Upon the adsorption of HA and CZ, although a decrease (Figure 3.20) in cell viability was observed, it was within the limits required by the ISO 10993-5:2009 and both molecules were therefore considered to be non-cytotoxic, indeed the observed decrease above the 70 % limit when compared to culture medium could be attributed to the possible presence of uncoated CS-NLCs mixed the colloidal solutions provoking the observed cytotoxicity as aforementioned in this section. These results are in line with previous studies, with de la Fuente, Seijo, and Alonso 2008 [127] and B. Silva et. al 2020 [36] observing no significant decrease in cell viability for CS-HA polymeric nanoparticles and CZ-loaded CS/HA nanoparticles respectively.

As such even with the slight cytotoxicity provoked by CS the polymer/lipid hybrid nanoparticles developed in this work showed to have no cytotoxic effect in the ARPE-19 cell line when these nanoparticles are coated with the naturally occurring HA and when loaded with the antioxidant Curc and antibiotic CZ.

4.3.5 Activity Assays

4.3.5.1 Antioxidant Activity of Curc-Loaded NPs

In this work, Curc-loaded NLCs showed to maintain the antioxidant effect of Curc encapsulated in the lipidic matrix of the NLCs. Furthermore, at 50 µg/mL the percentage in ROS reduction showed to be the maximum among the tested Curc concentrations with a 60.4 ± 2.6 % reduction on H_2O_2 induced ROS production. Similar ROS reduction has been observed in previous studies, Fan et al. 2018 [156] observed a cellular antioxidant activity higher when Curc at 5 µg/ml was encapsulated in BSA-dextran nanoparticles when compared with free curcumin.

These results show that the antioxidant properties of Curcumin are maintained after encapsulation in the irregular lipidic matrix of the NLCs and that this antioxidant activity is dependent on the concentration of Curc until the 50 µg/mL with the higher concentration of 100 µg/mL showing no significant ($p \geq 0.05$) reduction of the production of ROS when compared with the 50Curc-NLC formulations.

As such, the nanostructured lipid carriers made up of precirol® and transcutol® P can be used as delivery systems for Curc and other hydrophobic drug molecules to improve their bioavailability in ocular tissues.

4.3.5.2 Determination of Antimicrobial Activity of CZ

The results of the microtiter plate antibacterial assay show that the adsorption of CZ to the hyLNPs' surface nor the presence of Curc interfered with the antimicrobial activity of CZ against *P. aeruginosa* both adsorbed and free CZ showing very similar MICs. These results also confirm the successful adsorption of the antibiotic in the hyLNPs' surface. Furthermore, the lower MIC for both formulations is indicative of a rise in the efficiency of the antimicrobial activity of CZ in comparison with the antibiotic in free solution. This enhanced efficiency can be due to the ready association of the hyLNPs to the cell wall bacteria acting as a drug reservoir [149,150,157].

The MIC obtained in this work for an aqueous solution of CZ-Curc-loaded hyLNPs is similar to that observed by previous works of the investigation group [158] with CZ-loaded CS/TPP/HA nanoparticles in a gel solution showing a MIC of 1.56 µg/mL, although a lower than that of the antibiotic in free solution which was explained by the association of the NPs with an HMPC gel which led to slower diffusion of the drug molecule and lower efficiency observed.

As such, the prepared mucoadhesive nano-formulations preserved and enhanced the antibacterial effects of CZ and could therefore be used to treat ocular infectious diseases.

5. Conclusion & Future Work

The main objective of this work was the development of a nanoparticulate system composed of biocompatible mucoadhesive polymers capable of increasing the bioavailability of both lipophilic and hydrophilic drugs when topically applied to the ocular tissue in order to act as future nanocarriers for the treatment of ocular pathologies.

Both CS and HA are well-known polymers that demonstrate mucoadhesive properties being able to maintain their presence in the ocular tissues through different mechanisms, with the cationic CS weakly binding through electrostatic interactions to the terminal sialic acid residues of the glycoproteins and glycolipids present in the ocular mucin in the mucus layer and HA through specific binding to expressed HA-binding receptors found at the surface of the ocular epithelium improving the residence time of drugs in these tissues. CZ is a powerful antimicrobial agent against a wide variety of pathologies with bacterial origin such as *P. aeruginosa*, responsible for common eye infections. Curc has shown powerful therapeutical potential owing to its antioxidant and anti-inflammatory properties but presents low bioavailability when applied in topical administration to the eye.

After the optimization process, the final CZ-Cur-loaded hyLNP formulations produced in this work showed appropriate physicochemical properties for topical ocular applications such as a median size of 256.2 ± 6.0 nm, a narrow size distribution of 0.386 ± 0.013 and ζP of - 33.3 ± 0.5 mV with the presence of the drugs having no significant impact on these properties. Cur was successfully encapsulated to the hyLNPs' lipidic core with an efficiency of 86.5 ± 0.9 % at an initial concentration of 50 µg/mL. Similarly, CZ was efficiently adsorbed to the HA present at the surface of the nanoparticles with an efficiency of 48.4 ± 7.9 %.

In vitro, mucoadhesive studies confirmed that the formulations containing CS and HA showed increased interaction with ocular mucin potentially prolonging the residence time of Curc and CZ in the eye. Permeation studies successfully demonstrated that both drugs are released from the hyLNPs allowing their permeation through synthetic membranes. Cellular uptake studies reveal that both NLCs and hyLNPs are successfully internalized or associated with the ARPE-19 cell line, a model of the human retinal cells.

Cell viability studies demonstrated that all of the nanoparticulate components except the polymer chitosan are not cytotoxic for the ARPE-19 cell line. The results of the *in vitro* activity assays demonstrate that the encapsulation and adsorption of the drugs to the hyLNPs do not affect their antimicrobial and antioxidant activities maintaining their efficiency to decrease ROS generation and maintain bacterial growth inhibition for Curc and CZ, respectively, and may in fact enhance their therapeutic properties.

To summarize, the developed lipid/polymer hybrid nanoparticles loaded with both hydrophilic and lipophilic drugs seem capable to deliver their therapeutic cargo while maintaining it at a prolonged residence time in the eye due to their mucoadhesive properties thus increasing the bioavailability of the loaded drugs maintaining their efficacy. For future work other biological and pharmaceutical properties need to be studied: the viscosity of the produced hyLNP solution is essential to be determined so as to avoid damage to the corneal epithelium, to determine if the nanoparticulate system is capable of sustainably releasing the drug load and further evaluation of hyLNPs' short- and long-term stability under storage conditions needs to be assessed so as to determine their viability as a topical drug delivery system to the eye.

6. Bibliography

[1]: “Programa Nacional Para a Saúde Da Visão- Revisão e Extensão.” 2015. Www.Insa.Min-Saude.Pt. Serviço Nacional de Saúde. 2015. https://www.insa.min-saude.pt/plano-nacional-de-saude-aprovada-a-revisao-e-extensao-ate-2020/.

[2]: Magalhães, Augusto, Manuel Falcão, Nuno Campos, Manuel Monteiro Grillo, Joaquim Neto Murta, Jorge Breda, Pedro Menéres, and Maria João Quadrado. 2018. “Estratégia Nacional Para a Saúde Da Visão.” Revista Sociedade Portuguesa de Oftalmologia, November, Vol. 42 N.o 3 (2018): Estratégia Nacional para a Saúde da Visão. https://doi.org/10.48560/RSPO.15414.

[3]: “World Health Organization (WHO).” n.d. World Health Organization (WHO). Accessed December 4, 2022. http://www.who.int.

[4]: Gaudana, Ripal, J. Jwala, Sai H. S. Boddu, and Ashim K. Mitra. 2008. “Recent Perspectives in Ocular Drug Delivery.” Pharmaceutical Research, no. 5 (August). https://doi.org/10.1007/s11095-008-9694-0.

[5]: Awwad, Sahar, Abeer H A Mohamed Ahmed, Garima Sharma, Jacob S Heng, Peng T Khaw, Steve Brocchini, and Alastair Lockwood. 2017. “Principles of Pharmacology in the Eye.” British Journal of Pharmacology, no. 23 (October): 4205–23. https://doi.org/10.1111/bph.14024.

[6]: Patel, Ashaben. 2013. “Ocular Drug Delivery Systems: An Overview.” World Journal of Pharmacology, no. 2: 47. https://doi.org/10.5497/wjp.v2.i2.47.

[7]: Janagam, Dileep R., Linfeng Wu, and Tao L. Lowe. 2017. “Nanoparticles for Drug Delivery to the Anterior Segment of the Eye.” Advanced Drug Delivery Reviews, December 31–64. https://doi.org/10.1016/j.addr.2017.04.001.

[8]: Adapted from “Anatomy of the Human Eye”, by BioRender.com (2021). “BioRender App.” n.d. BioRender App. Accessed December 4, 2022. https://app.biorender.com/biorender-templates.

[9]: Wang, Yanyan, Xiaoyue Xu, Yan Gu, Yanju Cheng, and Feng Cao. 2018. “Recent Advance of Nanoparticle-Based Topical Drug Delivery to the Posterior Segment of the Eye.” Expert Opinion on Drug Delivery, no. 7 (July): 687–701. https://doi.org/10.1080/17425247.2018.1496080.

[10]: Gulsen, Derya, and Anuj Chauhan. 2004. “Ophthalmic Drug Delivery through Contact Lenses.” Investigative Opthalmology & Visual Science, no. 7 (July): 2342. https://doi.org/10.1167/iovs.03-0959.

[11]: Shastri, DH, PK Shelat, AK Shukla, and PB Patel. 2010. “Ophthalmic Drug Delivery System: Challenges and Approaches.” Systematic Reviews in Pharmacy, no. 2: 113. https://doi.org/10.4103/0975-8453.75042.

[12]: Chaurasia, Shyam, Rayne Lim, Rajamani Lakshminarayanan, and Rajiv Mohan. 2015. “Nanomedicine Approaches for Corneal Diseases.” Journal of Functional Biomaterials, no. 2 (April): 277–98. https://doi.org/10.3390/jfb6020277.

[13]: Zimmerman, Thom J., Jeffrey D. Baumann, and John Hetherington. 1983. “Side Effects of Timolol.” Survey of Ophthalmology, December, 243–49. https://doi.org/10.1016/0039-6257(83)90140-6.

[14]: Mun, Ellina A., Peter W. J. Morrison, Adrian C. Williams, and Vitaliy V. Khutoryanskiy. 2014. “On the Barrier Properties of the Cornea: A Microscopy Study of the Penetration of Fluorescently Labeled Nanoparticles, Polymers, and Sodium Fluorescein.” Molecular Pharmaceutics, no. 10 (August): 3556–64. https://doi.org/10.1021/mp500332m.

[15]: Huang, Hong-Shian, and Ronald D. Schoenwald. 1983. “Corneal Penetration Behavior of β-Blocking Agents I: Physicochemical Factors.” Journal of Pharmaceutical Sciences, no. 11 (November): 1266–72. https://doi.org/10.1002/jps.2600721108.

[16]: Rowsey, Tyler G., and Dimitrios Karamichos. 2017. “The Role of Lipids in Corneal Diseases and Dystrophies: A Systematic Review.” Clinical and Translational Medicine, no. 1 (September). https://doi.org/10.1186/s40169-017-0158-1.

[17]: Silva, Mariana, Raquel Calado, Joana Marto, Ana Bettencourt, António Almeida, and Lídia Gonçalves. 2017. “Chitosan Nanoparticles as a Mucoadhesive Drug Delivery System for Ocular Administration.” Marine Drugs, no. 12 (December): 370. https://doi.org/10.3390/md15120370.

[18]: Dubashynskaya, Natallia, Daria Poshina, Sergei Raik, Arto Urtti, and Yury A. Skorik. 2019. “Polysaccharides in Ocular Drug Delivery.” Pharmaceutics, no. 1 (December): 22. https://doi.org/10.3390/pharmaceutics12010022.

[19]: Waite, David, Yujing Wang, David Jones, Alan Stitt, and Thakur Raghu Raj Singh. 2017. “Posterior Drug Delivery via Periocular Route: Challenges and Opportunities.” Therapeutic Delivery, no. 8 (July): 685–99. https://doi.org/10.4155/tde-2017-0097.

[20]: PEYMAN, GHOLAM A., ELEONORA M. LAD, and DARIUS M. MOSHFEGHI. 2009. “INTRAVITREAL INJECTION OF THERAPEUTIC AGENTS.” Retina, no. 7 (July): 875–912. https://doi.org/10.1097/iae.0b013e3181a94f01.

[21]: Nayak, Kritika, and Manju Misra. 2018. “A Review on Recent Drug Delivery Systems for Posterior Segment of Eye.” Biomedicine & Pharmacotherapy, November 1564–82. https://doi.org/10.1016/j.biopha.2018.08.138.

[22]: Achouri, Djamila, Kamel Alhanout, Philippe Piccerelle, and Véronique Andrieu. 2012. “Recent Advances in Ocular Drug Delivery.” Drug Development and Industrial Pharmacy, no. 11 (November): 1599–1617. https://doi.org/10.3109/03639045.2012.736515.

[23]: Djebli, Nassim, Sonia Khier, Florence Griguer, Anne-Laure Coutant, Alexandra Tavernier, Gerard Fabre, Caroline Leriche, and David Fabre. 2016. “Ocular Drug Distribution After Topical Administration: Population Pharmacokinetic Model in Rabbits.” European Journal of Drug Metabolism and Pharmacokinetics, no. 1 (January): 59–68. https://doi.org/10.1007/s13318-016-0319-4.

[24]: Popov, Alexey, Elizabeth Enlow, James Bourassa, and Hongming Chen. 2016. “Mucus-Penetrating Nanoparticles Made with ‘Mucoadhesive’ Poly(Vinyl Alcohol).” Nanomedicine: Nanotechnology, Biology and Medicine, no. 7 (October): 1863–71. https://doi.org/10.1016/j.nano.2016.04.006.

[25]: Mukherjee, Anubhab, Ariana K Waters, Pranav Kalyan, Achal Singh Achrol, Santosh Kesari, and Venkata Mahidhar Yenugonda. 2019. “<P>Lipid&Ndash;Polymer Hybrid Nanoparticles as a next-Generation Drug Delivery Platform: State of the Art, Emerging Technologies, and Perspectives</P>” International Journal of Nanomedicine, March, 1937–52. https://doi.org/10.2147/ijn.s198353.

[26]: Bharali, Dhruba J., Donald Armstrong, and Shaker A. Mousa. 2013. “Hybrid Polymeric Nanoparticles: Potential Candidate for Ophthalmic Delivery.” In Oxidative Stress and Nanotechnology, 279–86. Humana Press. http://dx.doi.org/10.1007/978-1-62703-475-3_18.

[27]: Nagarwal, Ramesh C., Shri Kant, P.N. Singh, P. Maiti, and J.K. Pandit. 2009. “Polymeric Nanoparticulate System: A Potential Approach for Ocular Drug Delivery.” Journal of Controlled Release, no. 1 (May): 2–13. https://doi.org/10.1016/j.jconrel.2008.12.018.

[28]: Farokhzad, Omid C., and Robert Langer. 2009. “Impact of Nanotechnology on Drug Delivery.” ACS Nano, no. 1 (January): 16–20. https://doi.org/10.1021/nn900002m.

[29]: Bachu, Rinda, Pallabitha Chowdhury, Zahraa Al-Saedi, Pradeep Karla, and Sai Boddu. 2018. “Ocular Drug Delivery Barriers—Role of Nanocarriers in the Treatment of Anterior Segment Ocular Diseases.” Pharmaceutics, no. 1 (February): 28. https://doi.org/10.3390/pharmaceutics10010028.

[30]: Jain, RoonalL, and JP Shastri. 2011. “Study of Ocular Drug Delivery System Using Drug-Loaded Liposomes.” International Journal of Pharmaceutical Investigation, no. 1: 35. https://doi.org/10.4103/2230-973x.76727.

[31]: Huang, Yi, Qi Tao, Dongzhi Hou, Sheng Hu, Shuangyan Tian, Yanzhong Chen, Ruyi Gui, Lingling Yang, and Yao Wang. 2017. “A Novel Ion-Exchange Carrier Based upon Liposome-Encapsulated Montmorillonite for Ophthalmic Delivery of Betaxolol Hydrochloride.” International Journal of Nanomedicine, March 1731–45. https://doi.org/10.2147/ijn.s122747.

[32]: Fahmy, Heba Mohamed, Engy Abd El-Malek Saeed Saad, Neveen Moustafa Sabra, Amal Ahmed El-Gohary, Faten Fathy Mohamed, and Mohamed Hassaneen Gaber. 2018. “Treatment Merits of Latanoprost/Thymoquinone – Encapsulated Liposome for Glaucomatus Rabbits.” International Journal of Pharmaceutics, no. 1 (September): 597–608. https://doi.org/10.1016/j.ijpharm.2018.07.012.

[33]: Mühlen, Annette zur, Cora Schwarz, and Wolfgang Mehnert. 1998. “Solid Lipid Nanoparticles (SLN) for Controlled Drug Delivery – Drug Release and Release Mechanism.” European Journal of Pharmaceutics and Biopharmaceutics, no. 2 (March): 149–55. https://doi.org/10.1016/s0939-6411(97)00150-1.

[34]: Attama, Anthony A., Stephan Reichl, and Christel C. Müller-Goymann. 2008. “Diclofenac Sodium Delivery to the Eye: In Vitro Evaluation of Novel Solid Lipid Nanoparticle Formulation Using Human Cornea Construct.” International Journal of Pharmaceutics, no. 1–2 (May): 307–13. https://doi.org/10.1016/j.ijpharm.2007.12.007.

[35]: Başaran, Ebru, Müzeyyen Demirel, Başar Sırmagül, and Yasemin Yazan. 2010. “Cyclosporine-A Incorporated Cationic Solid Lipid Nanoparticles for Ocular Delivery.” Journal of Microencapsulation, no. 1 (January): 37–47. https://doi.org/10.3109/02652040902846883.

[36]: Silva, Beatriz, Joana Marto, Berta São Braz, Esmeralda Delgado, António José Almeida, and Lídia Gonçalves. 2020. “New Nanoparticles for Topical Ocular Delivery of Erythropoietin.” International Journal of Pharmaceutics, February, 119020. https://doi.org/10.1016/j.ijpharm.2020.119020.

[37]: Wadhwa, Sheetu, Rishi Paliwal, Shivani R. Paliwal, and S. P. Vyas. 2009. “Hyaluronic Acid Modified Chitosan Nanoparticles for Effective Management of Glaucoma: Development, Characterization, and Evaluation.” Journal of Drug Targeting, no. 4 (November): 292–302. https://doi.org/10.3109/10611860903450023.

[38]: Thomas, Deepa, Neethu Mathew, and Megha S. Nath. 2021. “Starch Modified Alginate Nanoparticles for Drug Delivery Application.” International Journal of Biological Macromolecules, March, 277–84. https://doi.org/10.1016/j.ijbiomac.2020.12.227.

[39]: Costa, J. R., N. C. Silva, B. Sarmento, and M. Pintado. 2015. “Potential Chitosan-Coated Alginate Nanoparticles for Ocular Delivery of Daptomycin.” European Journal of Clinical Microbiology & Infectious Diseases, no. 6 (March): 1255–62. https://doi.org/10.1007/s10096-015-2344-7.

[40]: Ibrahim, Howida Kamal, Iman Sadar El-Leithy, and Amna Awad Makky. 2010. “Mucoadhesive Nanoparticles as Carrier Systems for Prolonged Ocular Delivery of Gatifloxacin/Prednisolone Bitherapy.” Molecular Pharmaceutics, no. 2 (March): 576–85. https://doi.org/10.1021/mp900279c.

[41]: MOTWANI, S, S CHOPRA, S TALEGAONKAR, K KOHLI, F AHMAD, and R KHAR. 2007. "Chitosan–Sodium Alginate Nanoparticles as Submicroscopic Reservoirs for Ocular Delivery: Formulation, Optimisation and in Vitro Characterisation." European Journal of Pharmaceutics and Biopharmaceutics, September. https://doi.org/10.1016/j.ejpb.2007.09.009.

[42]: Aryal, Santosh, Che-Ming Jack Hu, Victoria Fu, and Liangfang Zhang. 2012. "Nanoparticledrug Delivery Enhances the Cytotoxicity of Hydrophobic–Hydrophilic Drug Conjugates." J. Mater. Chem., no. 3: 994–99. https://doi.org/10.1039/c1jm13834k.

[43]: Liu, Dan, Yunfei Lian, Qiuyu Fang, Lu Liu, Jundong Zhang, and Juan Li. 2018. "Hyaluronic-Acid-Modified Lipid-Polymer Hybrid Nanoparticles as an Efficient Ocular Delivery Platform for Moxifloxacin Hydrochloride." International Journal of Biological Macromolecules, September 1026–36. https://doi.org/10.1016/j.ijbiomac.2018.05.113.

[44]: Qamar, Zufika, Farheen Fatima Qizilbash, Mohammad Kashif Iqubal, Asgar Ali, Jasjeet Kaur Narang, Javed Ali, and Sanjula Baboota. 2020. "Nano-Based Drug Delivery System: Recent Strategies for the Treatment of Ocular Disease and Future Perspective." Recent Patents on Drug Delivery & Formulation, no. 4 (April): 246–54. https://doi.org/10.2174/1872211314666191224115211.

[45]: Yadav, Khushwant S., Rahul Rajpurohit, and Sushmita Sharma. 2019. "Glaucoma: Current Treatment and Impact of Advanced Drug Delivery Systems." Life Sciences, March, 362–76. https://doi.org/10.1016/j.lfs.2019.02.029.

[46]: Hadinoto, Kunn, Ajitha Sundaresan, and Wean Sin Cheow. 2013. "Lipid–Polymer Hybrid Nanoparticles as a New Generation Therapeutic Delivery Platform: A Review." European Journal of Pharmaceutics and Biopharmaceutics, no. 3 (November): 427–43. https://doi.org/10.1016/j.ejpb.2013.07.002.

[47]: Law, S.L, K.J Huang, and C.H Chiang. 2000. "Acyclovir-Containing Liposomes for Potential Ocular Delivery." Journal of Controlled Release, no. 1–2 (January): 135–40. https://doi.org/10.1016/s0168-3659(99)00192-3.

[48]: Agarwal, Renu, Igor Iezhitsa, Puneet Agarwal, Nurul Alimah Abdul Nasir, Norhafiza Razali, Renad Alyautdin, and Nafeeza Mohd Ismail. 2014. "Liposomes in Topical Ophthalmic Drug Delivery: An Update." Drug Delivery, no. 4 (August): 1075–91. https://doi.org/10.3109/10717544.2014.943336.

[49]: Mehnert, W. 2001. "Solid Lipid Nanoparticles Production, Characterization and Applications." Advanced Drug Delivery Reviews, no. 2–3 (April): 165–96. https://doi.org/10.1016/s0169-409x(01)00105-3.

[50]: Muchow, Marc, Philippe Maincent, and Rainer H. Müller. 2008. "Lipid Nanoparticles with a Solid Matrix (SLN®, NLC®, LDC®) for Oral Drug Delivery." Drug Development and Industrial Pharmacy, no. 12 (January): 1394–1405. https://doi.org/10.1080/03639040802130061.

[51]: Mohammadi-Samani, Soliman, and Parisa Ghasemiyeh. 2018. "Solid Lipid Nanoparticles and Nanostructured Lipid Carriers as Novel Drug Delivery Systems: Applications, Advantages and Disadvantages." Research in Pharmaceutical Sciences, no. 4: 288. https://doi.org/10.4103/1735-5362.235156.

[52]: Naseri, Neda, Hadi Valizadeh, and Parvin Zakeri-Milani. 2015. "Solid Lipid Nanoparticles and Nanostructured Lipid Carriers: Structure, Preparation and Application." Advanced Pharmaceutical Bulletin, no. 3 (September): 305–13. https://doi.org/10.15171/apb.2015.043.

[53]: Seyfoddin, Ali, John Shaw, and Raida Al-Kassas. 2010. "Solid Lipid Nanoparticles for Ocular Drug Delivery." Drug Delivery, no. 7 (May): 467–89. https://doi.org/10.3109/10717544.2010.483257.

[54]: Müller, R.H, M Radtke, and S.A Wissing. 2002. “Nanostructured Lipid Matrices for Improved Microencapsulation of Drugs.” International Journal of Pharmaceutics, no. 1–2 (August): 121–28. https://doi.org/10.1016/s0378-5173(02)00180-1.

[55]: Li, Xiang, Shu-fang Nie, Jun Kong, Ning Li, Cheng-yi Ju, and Wei-san Pan. 2008. “A Controlled-Release Ocular Delivery System for Ibuprofen Based on Nanostructured Lipid Carriers.” International Journal of Pharmaceutics, no. 1–2 (November): 177–82. https://doi.org/10.1016/j.ijpharm.2008.07.017.

[56]: ZHANG, LI, and LIANGFANG ZHANG. 2010. “LIPID–POLYMER HYBRID NANOPARTICLES: SYNTHESIS, CHARACTERIZATION AND APPLICATIONS.” Nano LIFE, no. 01n02 (March): 163–73. https://doi.org/10.1142/s179398441000016x.

[57]: Lee, Jin Whan, Jae Han Park, and Joseph R. Robinson. 2000. “Bioadhesive-Based Dosage Forms: The Next Generation.” Journal of Pharmaceutical Sciences, no. 7 (July): 850–66. https://doi.org/10.1002/1520-6017(200007)89:7<850::aid-jps2>3.0.co;2-g.

[58]: Gholizadeh, Shima, Ziqing Wang, Xi Chen, Reza Dana, and Nasim Annabi. 2021. “Advanced Nanodelivery Platforms for Topical Ophthalmic Drug Delivery.” Drug Discovery Today, no. 6 (June): 1437–49. https://doi.org/10.1016/j.drudis.2021.02.027.

[59]: LUDWIG, A. 2005. “The Use of Mucoadhesive Polymers in Ocular Drug Delivery.” Advanced Drug Delivery Reviews, no. 11 (November): 1595–1639. https://doi.org/10.1016/j.addr.2005.07.005.

[60]: Barbu, Eugen, Liliana Verestiuc, Thomas G. Nevell, and John Tsibouklis. 2006. “Polymeric Materials for Ophthalmic Drug Delivery: Trends and Perspectives.” Journal of Materials Chemistry, no. 34: 3439. https://doi.org/10.1039/b605640g.

[61]: Uccello-Barretta, Gloria, Samuele Nazzi, Ylenia Zambito, Giacomo Di Colo, Federica Balzano, and Marco Sansò. 2010. “Synergistic Interaction between TS-Polysaccharide and Hyaluronic Acid: Implications in the Formulation of Eye Drops.” International Journal of Pharmaceutics, no. 1–2 (August): 122–31. https://doi.org/10.1016/j.ijpharm.2010.05.031.

[62]: Weng, Yuhua, Juan Liu, Shubin Jin, Weisheng Guo, Xingjie Liang, and Zhongbo Hu. 2017. “Nanotechnology-Based Strategies for Treatment of Ocular Disease.” Acta Pharmaceutica Sinica B, no. 3 (May): 281–91. https://doi.org/10.1016/j.apsb.2016.09.001.

[63]: Patil, Sanjay & Rayasa, Murthy & Mahajan, Hitendra & Wagh, Rajendra & Gattani, Surendra. 2006. “Mucoadhesive polymers: Means of improving drug delivery.” Pharma Times. 38. 25-28.

[64]: Guter, Michaela, and Miriam Breunig. 2017. “Hyaluronan as a Promising Excipient for Ocular Drug Delivery.” European Journal of Pharmaceutics and Biopharmaceutics, April, 34–49. https://doi.org/10.1016/j.ejpb.2016.11.035.

[65]: Ren, Dongwen, Hongfu Yi, Wei Wang, and Xiaojun Ma. 2005. “The Enzymatic Degradation and Swelling Properties of Chitosan Matrices with Different Degrees of N-Acetylation.” Carbohydrate Research, no. 15 (October): 2403–10. https://doi.org/10.1016/j.carres.2005.07.022.

[66]: Chhonker, Yashpal S., Yarra Durga Prasad, Hardik Chandasana, Akhilesh Vishvkarma, Kalyan Mitra, Praveen K. Shukla, and Rabi S. Bhatta. 2015. “Amphotericin-B Entrapped Lecithin/Chitosan Nanoparticles for Prolonged Ocular Application.” International Journal of Biological Macromolecules, January 1451–58. https://doi.org/10.1016/j.ijbiomac.2014.10.014.

[67]: TAKEUCHI, H, J THONGBORISUTE, Y MATSUI, H SUGIHARA, H YAMAMOTO, and Y KAWASHIMA. 2005. “Novel Mucoadhesion Tests for Polymers and Polymer-Coated Particles to Design Optimal Mucoadhesive Drug Delivery Systems.” Advanced Drug Delivery Reviews, no. 11 (November): 1583–94. https://doi.org/10.1016/j.addr.2005.07.008.

[68]: Sonaje, Kiran, Yu-Hsin Lin, Jyuhn-Huarng Juang, Shiaw-Pyng Wey, Chiung-Tong Chen, and Hsing-Wen Sung. 2009. “In Vivo Evaluation of Safety and Efficacy of Self-Assembled Nanoparticles for Oral Insulin Delivery.” Biomaterials, no. 12 (April): 2329–39. https://doi.org/10.1016/j.biomaterials.2008.12.066.

[69]: Zamboulis, Alexandra, Stavroula Nanaki, Georgia Michailidou, Ioanna Koumentakou, Maria Lazaridou, Nina Maria Ainali, Eleftheria Xanthopoulou, and Dimitrios N. Bikiaris. 2020. “Chitosan and Its Derivatives for Ocular Delivery Formulations: Recent Advances and Developments.” Polymers, no. 7 (July): 1519. https://doi.org/10.3390/polym12071519.

[70]: Sonaje, Kiran, Er-Yuan Chuang, Kun-Ju Lin, Tzu-Chen Yen, Fang-Yi Su, Michael T. Tseng, and Hsing-Wen Sung. 2012. “Opening of Epithelial Tight Junctions and Enhancement of Paracellular Permeation by Chitosan: Microscopic, Ultrastructural, and Computed-Tomographic Observations.” Molecular Pharmaceutics, no. 5 (April): 1271–79. https://doi.org/10.1021/mp200572t.

[71]: Hsu, Li-Wen, Pei-Ling Lee, Chiung-Tong Chen, Fwu-Long Mi, Jyuhn-Huarng Juang, Shiaw-Min Hwang, Yi-Cheng Ho, and Hsing-Wen Sung. 2012. “Elucidating the Signaling Mechanism of an Epithelial Tight-Junction Opening Induced by Chitosan.” Biomaterials, no. 26 (September): 6254–63. https://doi.org/10.1016/j.biomaterials.2012.05.013.

[72]: Sudha, Prasad N., and Maximas H. Rose. 2014. “Beneficial Effects of Hyaluronic Acid.” In Advances in Food and Nutrition Research, 137–76. Elsevier. http://dx.doi.org/10.1016/B978-0-12-800269-8.00009-9.

[73]: Zhang, Xiaodan, Danyi Wei, Yang Xu, and Qiang Zhu. 2021. “Hyaluronic Acid in Ocular Drug Delivery.” Carbohydrate Polymers, July, 118006. https://doi.org/10.1016/j.carbpol.2021.118006.

[74]: Severino, Patricia, Classius F. da Silva, Luciana N. Andrade, Daniele de Lima Oliveira, Joana Campos, and Eliana B. Souto. 2019. “Alginate Nanoparticles for Drug Delivery and Targeting.” Current Pharmaceutical Design, no. 11 (August): 1312–34. https://doi.org/10.2174/1381612825666190425163424.

[75]: Noreen, Sobia, Shazia Akram Ghumman, Fozia Batool, Bushra Ijaz, Maryam Basharat, Shazia Noureen, Tusneem Kausar, and Shahid Iqbal. 2020. “Terminalia Arjuna Gum/Alginate in Situ Gel System with Prolonged Retention Time for Ophthalmic Drug Delivery.” International Journal of Biological Macromolecules, June 1056–67. https://doi.org/10.1016/j.ijbiomac.2019.10.193.

[76]: Rajaonarivony, M., C. Vauthier, G. Couarraze, F. Puisieux, and P. Couvreur. 1993. “Development of a New Drug Carrier Made from Alginate.” Journal of Pharmaceutical Sciences, no. 9 (September): 912–17. https://doi.org/10.1002/jps.2600820909.

[77]: Mandal, Bivash, Himanshu Bhattacharjee, Nivesh Mittal, Hongkee Sah, Pavan Balabathula, Laura A. Thoma, and George C. Wood. 2013. “Core–Shell-Type Lipid–Polymer Hybrid Nanoparticles as a Drug Delivery Platform.” Nanomedicine: Nanotechnology, Biology and Medicine, no. 4 (May): 474–91. https://doi.org/10.1016/j.nano.2012.11.010.

[78]: Bou, Sophie, Xinyue Wang, Nicolas Anton, Redouane Bouchaala, Andrey S. Klymchenko, and Mayeul Collot. 2020. “Lipid-Core/Polymer-Shell Hybrid Nanoparticles: Synthesis and Characterization by Fluorescence Labeling and Electrophoresis.” Soft Matter, no. 17: 4173–81. https://doi.org/10.1039/d0sm00077a.

[79]: Huynh, N.T., C. Passirani, P. Saulnier, and J.P. Benoit. 2009. “Lipid Nanocapsules: A New Platform for Nanomedicine.” International Journal of Pharmaceutics, no. 2 (September): 201–9. https://doi.org/10.1016/j.ijpharm.2009.04.026.

[80]: Oh, Keun Sang, Kyung Eun Lee, Sung Sik Han, Sun Hang Cho, Dongmin Kim, and Soon Hong Yuk. 2005. “Formation of Core/Shell Nanoparticles with a Lipid Core and Their Application as a Drug Delivery System.” Biomacromolecules, no. 2 (February): 1062–67. https://doi.org/10.1021/bm049234r.

[81]: Estella-Hermoso de Mendoza, Ander, Miguel A Campanero, Hugo Lana, Janny A Villa-Pulgarin, Janis de la Iglesia-Vicente, Faustino Mollinedo, and María J Blanco-Prieto. 2012. “Complete Inhibition of Extranodal Dissemination of Lymphoma by Edelfosine-Loaded Lipid Nanoparticles.” Nanomedicine, no. 5 (May): 679–90. https://doi.org/10.2217/nnm.11.134.

[82]: Li, Jian, Ying-zi He, Wen Li, Yun-zhen Shen, Yu-ru Li, and Yun-feng Wang. 2010. “A Novel Polymer-Lipid Hybrid Nanoparticle for Efficient Nonviral Gene Delivery.” Acta Pharmacologica Sinica, no. 4 (March): 509–14. https://doi.org/10.1038/aps.2010.15.

[83]: Park, Jason, Stephen H. Wrzesinski, Eric Stern, Michael Look, Jason Criscione, Ragy Ragheb, Steven M. Jay, et al. 2012. “Combination Delivery of TGF-β Inhibitor and IL-2 by Nanoscale Liposomal Polymeric Gels Enhances Tumour Immunotherapy.” Nature Materials, no. 10 (July): 895–905. https://doi.org/10.1038/nmat3355.

[84]: Mieszawska, Aneta J., Anita Gianella, David P. Cormode, Yiming Zhao, Andries Meijerink, Robert Langer, Omid C. Farokhzad, Zahi A. Fayad, and Willem J. M. Mulder. 2012. “Engineering of Lipid-Coated PLGA Nanoparticles with a Tunable Payload of Diagnostically Active Nanocrystals for Medical Imaging.” Chemical Communications, no. 47: 5835. https://doi.org/10.1039/c2cc32149a.

[85]: Khabaz, Fardin, and Rajesh Khare. 2014. “Effect of Chain Architecture on the Size, Shape, and Intrinsic Viscosity of Chains in Polymer Solutions: A Molecular Simulation Study.” The Journal of Chemical Physics, no. 21 (December): 214904. https://doi.org/10.1063/1.4902052.

[86]: Madsen, Claus G., Anders Skov, Stefania Baldursdottir, Thomas Rades, Lene Jorgensen, and Natalie J. Medlicott. 2015. “Simple Measurements for Prediction of Drug Release from Polymer Matrices – Solubility Parameters and Intrinsic Viscosity.” European Journal of Pharmaceutics and Biopharmaceutics, May 1–7. https://doi.org/10.1016/j.ejpb.2015.02.001.

[87]: Graessley, W. 1980. “Polymer Chain Dimensions and the Dependence of Viscoelastic Properties on Concentration, Molecular Weight and Solvent Power.” Polymer, no. 3 (March): 258–62. https://doi.org/10.1016/0032-3861(80)90266-9.

[88]: Dubald, Marion, Sandrine Bourgeois, Véronique Andrieu, and Hatem Fessi. 2018. “Ophthalmic Drug Delivery Systems for Antibiotherapy—A Review.” Pharmaceutics, no. 1 (January): 10. https://doi.org/10.3390/pharmaceutics10010010.

[89]: Aktaş, Yeşim, Nurşen Ünlü, Mehmet Orhan, Murat İrkeç, and A. Atilla Hıncal. 2003. “Influence of Hydroxypropyl β-Cyclodextrin on the Corneal Permeation of Pilocarpine.” Drug Development and Industrial Pharmacy, no. 2 (January): 223–30. https://doi.org/10.1081/ddc-120016730.

[90]: Morrison, Peter W.J., and Vitaliy V. Khutoryanskiy. 2014. “Enhancement in Corneal Permeability of Riboflavin Using Calcium Sequestering Compounds.” International Journal of Pharmaceutics, no. 1–2 (September): 56–64. https://doi.org/10.1016/j.ijpharm.2014.06.007.

[91]: Morrison, Peter W. J., Natalia N. Porfiryeva, Sukhmanpreet Chahal, Ilgiz A. Salakhov, Charlène Lacourt, Irina I. Semina, Rouslan I. Moustafine, and Vitaliy V. Khutoryanskiy. 2017. “Crown Ethers: Novel Permeability Enhancers for Ocular Drug Delivery?” Molecular Pharmaceutics, no. 10 (August): 3528–38. https://doi.org/10.1021/acs.molpharmaceut.7b00556.

[92]: Mahaling, Binapani, and Dhirendra S. Katti. 2016. “Understanding the Influence of Surface Properties of Nanoparticles and Penetration Enhancers for Improving Bioavailability in Eye Tissues in Vivo.” International Journal of Pharmaceutics, no. 1–2 (March): 1–9. https://doi.org/10.1016/j.ijpharm.2016.01.053.

[93]: Saettone, M.Fabrizio, Patrizia Chetoni, Riccardo Cerbai, Gabriela Mazzanti, and Laura Braghiroli. 1996. “Evaluation of Ocular Permeation Enhancers: In Vitro Effects on Corneal Transport of Four β-Blockers, and in Vitro/in Vivo Toxic Activity.” International Journal of Pharmaceutics, no. 1 (September): 103–13. https://doi.org/10.1016/0378-5173(96)04663-7.

[94]: Burgalassi, Susi, Daniela Monti, Annalisa Brignoccoli, Ortenzio Fabiani, Carla Lenzi, Andrea Pirone, and Patrizia Chetoni. 2004. “Development of Cultured Rabbit Corneal Epithelium for Drug Permeation Studies: A Comparison with Excised Rabbit Cornea.” Journal of Ocular Pharmacology and Therapeutics, no. 6 (December): 518–32. https://doi.org/10.1089/jop.2004.20.518.

[95]: Bijl, Pieter van der, Armorél D. van Eyk, and David Meyer. 2001. “Effects of Three Penetration Enhancers on Transcorneal Permeation of Cyclosporine.” Cornea, no. 5 (July): 505–8. https://doi.org/10.1097/00003226-200107000-00013.

[96]: Godbey, Renee E.W., Keith Green, and David S. Hull. 1979. “Influence of Cetylpyridinium Chloride on Corneal Permeability to Penicillin.” Journal of Pharmaceutical Sciences, no. 9 (September): 1176–78. https://doi.org/10.1002/jps.2600680932.

[97]: Arai, Shoko, Naoki Yamamoto, Masakazu Katoh, and Hajime Kojima. 2008. “An in Vitro Evaluation Method to Test Ocular Irritation Using a Human Corneal Epithelium Model.” Alternatives to Animal Testing and Experimentation, 83–90. https://doi.org/10.11232/aatex.13.83.

[98]: Ostacolo, Carmine, Ciro Caruso, Diana Tronino, Salvatore Troisi, Sonia Laneri, Luigi Pacente, Antonio Del Prete, and Antonia Sacchi. 2013. “Enhancement of Corneal Permeation of Riboflavin-5′-Phosphate through Vitamin E TPGS: A Promising Approach in Corneal Trans-Epithelial Cross Linking Treatment.” International Journal of Pharmaceutics, no. 2 (January): 148–53. https://doi.org/10.1016/j.ijpharm.2012.09.051.

[99]: Burgalassi, Susi, Patrizia Chetoni, Daniela Monti, and M.Fabrizio Saettone. 2001. “Cytotoxicity of Potential Ocular Permeation Enhancers Evaluated on Rabbit and Human Corneal Epithelial Cell Lines.” Toxicology Letters, no. 1 (May): 1–8. https://doi.org/10.1016/s0378-4274(01)00261-2.

[100]: Liu, Chang, Lingyu Tai, Wenjian Zhang, Gang Wei, Weisan Pan, and Weiyue Lu. 2014. “Penetratin, a Potentially Powerful Absorption Enhancer for Noninvasive Intraocular Drug Delivery.” Molecular Pharmaceutics, no. 4 (February): 1218–27. https://doi.org/10.1021/mp400681n.

[101]: Urošević, Maja, Ljubiša Nikolić, Ivana Gajić, Vesna Nikolić, Ana Dinić, and Vojkan Miljković. 2022. “Curcumin: Biological Activities and Modern Pharmaceutical Forms.” Antibiotics, no. 2 (January): 135. https://doi.org/10.3390/antibiotics11020135.

[102]: Radomska-Leśniewska, Dorota M., Anna Osiecka-Iwan, Anna Hyc, Agata Góźdź, Anna M. Dąbrowska, and Piotr Skopiński. 2019. “Therapeutic Potential of Curcumin in Eye Diseases.” Central European Journal of Immunology, no. 2: 181–89. https://doi.org/10.5114/ceji.2019.87070.

[103]: Chrysostomou, Vicki, Fatemeh Rezania, Ian A Trounce, and Jonathan G Crowston. 2013. “Oxidative Stress and Mitochondrial Dysfunction in Glaucoma.” Current Opinion in Pharmacology, no. 1 (February): 12–15. https://doi.org/10.1016/j.coph.2012.09.008.

[104]: Christian Maihöfner, Ursula Schlötzer-Schrehardt, Hans Gühring, Hanns Ulrich Zeilhofer, Gottfried O. H. Naumann, Andreas Pahl, Christian Mardin, Ernst R. Tamm, Kay Brune. 2001. "Expression of Cyclooxygenase-1 and -2 in Normal and Glaucomatous Human Eyes". Invest. Ophthalmol. Vis. Sci. 42(11):2616-2624. https://doi.org/10.5167/uzh-5516

[105]: Menon, Venugopal P., and Adluri Ram Sudheer. n.d. "ANTIOXIDANT AND ANTI-INFLAMMATORY PROPERTIES OF CURCUMIN." In ADVANCES IN EXPERIMENTAL MEDICINE AND BIOLOGY, 105–25. Springer US. http://dx.doi.org/10.1007/978-0-387-46401-5_3.

[106]: Trujillo, Joyce, Luis Fernando Granados-Castro, Cecilia Zazueta, Ana Cristina Andérica-Romero, Yolanda Irasema Chirino, and José Pedraza-Chaverrí. 2014. "Mitochondria as a Target in the Therapeutic Properties of Curcumin." Archiv Der Pharmazie, no. 12 (September): 873–84. https://doi.org/10.1002/ardp.201400266.

[107]: Mou-Tuan Huang, Thomas Lysz, Thomas Ferraro, Tanveer F. Abidi, Jeffrey D. Laskin, Allan H. Conney. 1991. "Inhibitory Effects of Curcumin on in Vitro Lipoxygenase and Cyclooxygenase Activities in Mouse Epidermis". Cancer Res, 1 February: 813–819.

[108]: Lin, Yvonne G., Ajaikumar B. Kunnumakkara, Asha Nair, William M. Merritt, Liz Y. Han, Guillermo N. Armaiz-Pena, Aparna A. Kamat, et al. 2007. "Curcumin Inhibits Tumor Growth and Angiogenesis in Ovarian Carcinoma by Targeting the Nuclear Factor-KB Pathway." Clinical Cancer Research, no. 11 (June): 3423–30. https://doi.org/10.1158/1078-0432.ccr-06-3072.

[109]: Tønnesen, Hanne Hjorth, and Jan Karlsen. 1985. "Studies on Curcumin and Curcuminoids." Zeitschrift For Lebensmittel-Untersuchung Und -Forschung, no. 5 (May): 402–4. https://doi.org/10.1007/bf01027775.

[110]: Bouattour, Yassine, Florent Neflot-Bissuel, Mounir Traïkia, Anne-Sophie Biesse-Martin, Robin Frederic, Mouloud Yessaad, Mireille Jouannet, Mathieu Wasiak, Philip Chennell, and Valerie Sautou. 2021. "Cyclodextrins Allow the Combination of Incompatible Vancomycin and Ceftazidime into an Ophthalmic Formulation for the Treatment of Bacterial Keratitis." International Journal of Molecular Sciences, no. 19 (September): 10538. https://doi.org/10.3390/ijms221910538.

[111]: Subedi, Dinesh, Ajay Kumar Vijay, and Mark Willcox. 2018. "Overview of Mechanisms of Antibiotic Resistance in Pseudomonas Aeruginosa: An Ocular Perspective." Clinical and Experimental Optometry, no. 2 (March): 162–71. https://doi.org/10.1111/cxo.12621.

[112]: Das, Samayitree, Sharon D'Souza, Bhavya Gorimanipalli, Rohit Shetty, Arkasubhra Ghosh, and Vrushali Deshpande. 2022. "Ocular Surface Infection Mediated Molecular Stress Responses: A Review." International Journal of Molecular Sciences, no. 6 (March): 3111. https://doi.org/10.3390/ijms23063111.

[113]: Budai, Marianna, Lívia Budai, MagdolnaE Szilasi, Ilona Petrikovics, and Chamari Wijesooriya. 2013. "Optimization of Liposomal Encapsulation for Ceftazidime for Developing a Potential Eye Drop Formulation." Journal of Basic and Clinical Pharmacy, no. 3: 73. https://doi.org/10.4103/0976-0105.118810.

[114]: Gaspar, Diana P., Vasco Faria, Lídia M.D. Gonçalves, Pablo Taboada, Carmen Remuñán-López, and António J. Almeida. 2016. "Rifabutin-Loaded Solid Lipid Nanoparticles for Inhaled Antitubercular Therapy: Physicochemical and in Vitro Studies." International Journal of Pharmaceutics, no. 1–2 (January): 199–209. https://doi.org/10.1016/j.ijpharm.2015.11.050.

[115]: Zetasizer Nano Series User Manual. (2013).

[116]: Liu, Dandan, Jinyu Li, Hao Pan, Fengwei He, Zhidong Liu, Qingyin Wu, Chunping Bai, Shihui Yu, and Xinggang Yang. 2016. “Potential Advantages of a Novel Chitosan-N-Acetylcysteine Surface Modified Nanostructured Lipid Carrier on the Performance of Ophthalmic Delivery of Curcumin.” Scientific Reports, no. 1 (June). https://doi.org/10.1038/srep28796.

[117]: Sun, Jiabei, Chao Bi, Hok Man Chan, Shaoping Sun, Qingwen Zhang, and Ying Zheng. 2013. “Curcumin-Loaded Solid Lipid Nanoparticles Have Prolonged in Vitro Antitumour Activity, Cellular Uptake and Improved in Vivo Bioavailability.” Colloids and Surfaces B: Biointerfaces, November, 367–75. https://doi.org/10.1016/j.colsurfb.2013.06.032.

[118]: Lopes, R., C.V. Eleutério, L.M.D. Gonçalves, M.E.M. Cruz, and A.J. Almeida. 2012. “Lipid Nanoparticles Containing Oryzalin for the Treatment of Leishmaniasis.” European Journal of Pharmaceutical Sciences, no. 4 (March): 442–50. https://doi.org/10.1016/j.ejps.2011.09.017.

[119]: Sarker, Satyajit D., Lutfun Nahar, and Yashodharan Kumarasamy. 2007. “Microtitre Plate-Based Antibacterial Assay Incorporating Resazurin as an Indicator of Cell Growth, and Its Application in the in Vitro Antibacterial Screening of Phytochemicals.” Methods, no. 4 (August): 321–24. https://doi.org/10.1016/j.ymeth.2007.01.006.

[120]: Cockerill, F.R.; Wikler, M.A.; Alder, J.; Dudley, M.N.; Eliopoulos, G.M.; Ferraro, M.J.; Hardy, D.J.; Hecht, D.; Hindler, J.; Patel, J.; et al. “Methods for Dilution Antimicrobial Susceptibility Tests for Bacteria That Grow Aerobically” Approved Standard, 9th ed.; Clinical and Laboratory Standards Institute: Wayne, PA, USA, 2012; Volume 32.

[121]: PD-10 Desalting Columns, GE Healthcare. Instructions manual 52-1308-00 BB.

[122]: Bonilla, Lorena, Marta Espina, Patricia Severino, Amanda Cano, Miren Ettcheto, Antoni Camins, Maria Luisa García, Eliana B. Souto, and Elena Sánchez-López. 2021. “Lipid Nanoparticles for the Posterior Eye Segment.” Pharmaceutics, no. 1 (December): 90. https://doi.org/10.3390/pharmaceutics14010090.

[123]: Souto, Eliana B., Slavomira Doktorovova, Aleksandra Zielinska, and Amélia M. Silva. 2019. “Key Production Parameters for the Development of Solid Lipid Nanoparticles by High Shear Homogenization.” Pharmaceutical Development and Technology, no. 9 (August): 1181–85. https://doi.org/10.1080/10837450.2019.1647235.

[124]: Souto, Eliana B., Slavomira Doktorovova, Aleksandra Zielinska, and Amélia M. Silva. 2019. “Key Production Parameters for the Development of Solid Lipid Nanoparticles by High Shear Homogenization.” Pharmaceutical Development and Technology, no. 9 (August): 1181–85. https://doi.org/10.1080/10837450.2019.1647235.

[125]: Yeh, Tzyy-Harn, Li-Wen Hsu, Michael T. Tseng, Pei-Ling Lee, Kiran Sonjae, Yi-Cheng Ho, and Hsing-Wen Sung. 2011. “Mechanism and Consequence of Chitosan-Mediated Reversible Epithelial Tight Junction Opening.” Biomaterials, no. 26 (September): 6164–73. https://doi.org/10.1016/j.biomaterials.2011.03.056.

[126]: Luo, Qiuhua, Junming Zhao, Xiangrong Zhang, and Weisan Pan. 2011. “Nanostructured Lipid Carrier (NLC) Coated with Chitosan Oligosaccharides and Its Potential Use in Ocular Drug Delivery System.” International Journal of Pharmaceutics, no. 1–2 (January): 185–91. https://doi.org/10.1016/j.ijpharm.2010.10.013.

[127]: Fuente, Maria de la, Begon~a Seijo, and Maria J. Alonso. 2008. “Novel Hyaluronic Acid-Chitosan Nanoparticles for Ocular Gene Therapy.” Investigative Opthalmology & Visual Science, no. 5 (May): 2016. https://doi.org/10.1167/iovs.07-1077.

[128]: Stender, Emil G.P., Sanaullah Khan, Richard Ipsen, Finn Madsen, Per Hägglund, Maher Abou Hachem, Kristoffer Almdal, Peter Westh, and Birte Svensson. 2018. "Effect of Alginate Size, Mannuronic/Guluronic Acid Content and PH on Particle Size, Thermodynamics and Composition of Complexes with β-Lactoglobulin." Food Hydrocolloids, February, 157–63. https://doi.org/10.1016/j.foodhyd.2017.09.001.

[129]: Mikov, M., J. P. Fawcett, K. Kuhajda, and S. Kevresan. 2006. "Pharmacology of Bile Acids and Their Derivatives: Absorption Promoters and Therapeutic Agents." European Journal of Drug Metabolism and Pharmacokinetics, no. 3 (September): 237–51. https://doi.org/10.1007/bf03190714.

[130]: Salminen, Hanna, Thrandur Helgason, Susanne Aulbach, Bjarki Kristinsson, Kristberg Kristbergsson, and Jochen Weiss. 2014. "Influence of Co-Surfactants on Crystallization and Stability of Solid Lipid Nanoparticles." Journal of Colloid and Interface Science, July, 256–63. https://doi.org/10.1016/j.jcis.2014.04.009.

[131]: Westesen, Kirsten, and Britta Siekmann. 1997. "Investigation of the Gel Formation of Phospholipid-Stabilized Solid Lipid Nanoparticles." International Journal of Pharmaceutics, no. 1 (May): 35–45. https://doi.org/10.1016/s0378-5173(97)04890-4.

[132]: Talele, Paurnima, Saugata Sahu, and Ashok Kumar Mishra. 2018. "Physicochemical Characterization of Solid Lipid Nanoparticles Comprised of Glycerol Monostearate and Bile Salts." Colloids and Surfaces B: Biointerfaces, December, 517–25. https://doi.org/10.1016/j.colsurfb.2018.08.067.

[133]: Kurien, Biji T., Anil Singh, Hiroyuki Matsumoto, and R. Hal Scofield. 2007. "Improving the Solubility and Pharmacological Efficacy of Curcumin by Heat Treatment." ASSAY and Drug Development Technologies, no. 4 (August): 567–76. https://doi.org/10.1089/adt.2007.064.

[134]: Vitorino, Carla, Filomena A. Carvalho, António J. Almeida, João J. Sousa, and Alberto A.C.C. Pais. 2011. "The Size of Solid Lipid Nanoparticles: An Interpretation from Experimental Design." Colloids and Surfaces B: Biointerfaces, no. 1 (May): 117–30. https://doi.org/10.1016/j.colsurfb.2010.12.024.

[135]: Inwitor 988, Technical data sheet, IOI Oleochemical.

[136]: Zhang, Xichen, John K. Jackson, and Helen M. Burt. 1996. "Determination of Surfactant Critical Micelle Concentration by a Novel Fluorescence Depolarization Technique." Journal of Biochemical and Biophysical Methods, no. 3–4 (February): 145–50. https://doi.org/10.1016/0165-022x(95)00032-m.

[137]: Hashem, Fahima M., Mohamed Nasr, Ahmed Khairy, and Abdulmalik Alqurshi. 2019. "<P>In Vitro Cytotoxicity and Transfection Efficiency of PDNA Encoded P53 Gene-Loaded Chitosan-Sodium Deoxycholate Nanoparticles</P>" International Journal of Nanomedicine, June, 4123–31. https://doi.org/10.2147/ijn.s205324.

[138]: Chen, Mei-Chin, Fwu-Long Mi, Zi-Xian Liao, Chun-Wen Hsiao, Kiran Sonaje, Min-Fan Chung, Li-Wen Hsu, and Hsing-Wen Sung. 2013. "Recent Advances in Chitosan-Based Nanoparticles for Oral Delivery of Macromolecules." Advanced Drug Delivery Reviews, no. 6 (June): 865–79. https://doi.org/10.1016/j.addr.2012.10.010.

[139]: Panith, Nootchanartch, Jetsada Wichaphon, Sittiwat Lertsiri, and Nuttawee Niamsiri. 2016. "Effect of Physical and Physicochemical Characteristics of Chitosan on Fat-Binding Capacities under in Vitro Gastrointestinal Conditions." LWT - Food Science and Technology, September, 25–32. https://doi.org/10.1016/j.lwt.2016.03.013.

[140]: Sandri, Giuseppina, Maria Cristina Bonferoni, Evren Homan Gökçe, Franca Ferrari, Silvia Rossi, Maddalena Patrini, and Carla Caramella. 2010. "Chitosan-Associated SLN: In VitroandEx VivoCharacterization of Cyclosporine A Loaded Ophthalmic Systems." Journal of Microencapsulation, no. 8 (November): 735–46. https://doi.org/10.3109/02652048.2010.517854.

[141]: Priyadarsini, Kavirayani. 2014. "The Chemistry of Curcumin: From Extraction to Therapeutic Agent." Molecules, no. 12 (December): 20091–112. https://doi.org/10.3390/molecules191220091.

[142]: Barnes, A. R., and S. Nash. 1999. "Stability of Ceftazidime in a Viscous Eye Drop Formulation." Journal of Clinical Pharmacy and Therapeutics, no. 4 (August): 299–302. https://doi.org/10.1046/j.1365-2710.1999.00230.x.

[143]: Biernat, Paweł, Beata Borak, Jan Meler, and Bożena Karolewicz. 2018. "THE STUDY OF ADSORPTION AND DESORPTION OF ANTIBIOTICS ON THE SURFACE OF NANOPARTICLES." Acta Poloniae Pharmaceutica - Drug Research, no. 5 (October): 1215–22. https://doi.org/10.32383/appdr/86212.

[144]: PubChem. n.d. "PubChem." PubChem. Accessed March 20, 2022. https://pubchem.ncbi.nlm.nih.gov.

[145]: Shimojo, Andréa Arruda Martins, Aline Mara Barbosa Pires, Rafael Lichy, Ana Amélia Rodrigues, and Maria Helena Andrade Santana. 2014. "The Crosslinking Degree Controls the Mechanical, Rheological, and Swelling Properties of Hyaluronic Acid Microparticles." Journal of Biomedical Materials Research Part A, no. 2 (May): 730–37. https://doi.org/10.1002/jbm.a.35225.

[146]: Milas, Michel, Marguerite Rinaudo, Isabelle Roure, Saphwan Al-Assaf, Glyn O. Phillips, and Peter A. Williams. 2001. "Comparative Rheological Behavior of Hyaluronan from Bacterial and Animal Sources with Cross-Linked Hyaluronan (Hylan) in Aqueous Solution." Biopolymers, no. 4: 191–204. https://doi.org/10.1002/1097-0282(20011005)59:4<191::aid-bip1018>3.0.co;2-m.

[147]: Argüeso, Pablo, José M. Herreras, Margarita Calonge, Lucía Citores, José C. Pastor, and Tomás Girbés. 1998. "Analysis of Human Ocular Mucus." Cornea, no. 2 (March): 200–207. https://doi.org/10.1097/00003226-199803000-00015.

[148]: Campos, Angela M. de, Yolanda Diebold, Edison L. S. Carvalho, Alejandro Sánchez, and Maria José Alonso. 2004. "Chitosan Nanoparticles as New Ocular Drug Delivery Systems: In Vitro Stability, in Vivo Fate, and Cellular Toxicity." Pharmaceutical Research, no. 5 (May): 803–10. https://doi.org/10.1023/b:pham.0000026432.75781.cb.

[149]: Kumari, Preeti, Muddineti Omkara Swami, Sravan Kumar Nadipalli, Srividya Myneni, Balaram Ghosh, and Swati Biswas. 2015. "Curcumin Delivery by Poly(Lactide)-Based Co-Polymeric Micelles: An In Vitro Anticancer Study." Pharmaceutical Research, no. 4 (November): 826–41. https://doi.org/10.1007/s11095-015-1830-z.

[150]: Lakhani, Prit, Akash Patil, Pranjal Taskar, Eman Ashour, and Soumyajit Majumdar. 2018. "Curcumin-Loaded Nanostructured Lipid Carriers for Ocular Drug Delivery: Design Optimization and Characterization." Journal of Drug Delivery Science and Technology, October, 159–66. https://doi.org/10.1016/j.jddst.2018.07.010.

[151]: Doktorovova, Slavomira, Eliana B. Souto, and Amélia M. Silva. 2014. "Nanotoxicology Applied to Solid Lipid Nanoparticles and Nanostructured Lipid Carriers – A Systematic Review of in Vitro Data." European Journal of Pharmaceutics and Biopharmaceutics, no. 1 (May): 1–18. https://doi.org/10.1016/j.ejpb.2014.02.005.

[152]: Martens, Thomas F, Karen Peynshaert, Thaís Leite Nascimento, Elias Fattal, Marcus Karlstetter, Thomas Langmann, Serge Picaud, et al. 2017. "Effect of Hyaluronic Acid-Binding to Lipoplexes on Intravitreal Drug Delivery for Retinal Gene Therapy." European Journal of Pharmaceutical Sciences, May, 27–35. https://doi.org/10.1016/j.ejps.2017.02.027.

[153]: Zaki, Noha M., Alessandro Nasti, and Nicola Tirelli. 2011. "Nanocarriers for Cytoplasmic Delivery: Cellular Uptake and Intracellular Fate of Chitosan and Hyaluronic Acid-Coated Chitosan Nanoparticles in a Phagocytic Cell Model." Macromolecular Bioscience, no. 12 (September): 1747–60. https://doi.org/10.1002/mabi.201100156.

[154]: ISO/EN10993-5. Int. Stand. ISO 10993-5 Biol. Eval. Med. devices - Part 5 Tests Cytotox. Vitr. Methods 3rd Ed, 42 (2009).

[155]: Huang, Min, Eugene Khor, and Lee-Yong Lim. 2004. "Uptake and Cytotoxicity of Chitosan Molecules and Nanoparticles: Effects of Molecular Weight and Degree of Deacetylation." Pharmaceutical Research, no. 2 (February): 344–53. https://doi.org/10.1023/b:pham.0000016249.52831.a5.

[156]: Fan, Yuting, Jiang Yi, Yuzhu Zhang, and Wallace Yokoyama. 2018. "Fabrication of Curcumin-Loaded Bovine Serum Albumin (BSA)-Dextran Nanoparticles and the Cellular Antioxidant Activity." Food Chemistry, January, 1210–18. https://doi.org/10.1016/j.foodchem.2017.07.075.

[157]: Zhang, L., D. Pornpattananangkul, C.-M. Hu, and C.-M. Huang. 2010. "Development of Nanoparticles for Antimicrobial Drug Delivery." Current Medicinal Chemistry, no. 6 (February): 585–94. https://doi.org/10.2174/092986710790416290.

[158]: Calado, Raquel Sofia D´Abreu. 2017 "Development of a topical mucoadhesive ocular delivery system for ceftazidime.".